

**SECONDARY METABOLITES FROM MARINE
DERIVED ACTINOBACTERIA AND THEIR
BIOACTIVITIES**

**A thesis submitted to
the Graduate School of Engineering and Sciences of
İzmir Institute of Technology
in Partial Fulfillment of the Requirements for the Degree of**

MASTER OF SCIENCE

in Bioengineering

by

Özge CAN

July 2024

İZMİR

We approve the thesis of **Özge CAN**

Examining Committee Members:

Prof. Dr. Erdal BEDİR

Department of Bioengineering, İzmir Institute of Technology

Prof. Dr. Ataç UZEL

Department of Biology, Ege University

Assist. Prof. Hümevra TAŞKENT SEZGİN

Department of Bioengineering, İzmir Institute of Technology

26 June 2024

Prof. Dr. Erdal BEDİR

Supervisor, Department of Bioengineering
İzmir Institute of Technology

Assoc. Prof. Dr. Ceyda ÖKSEL KARAKUŞ

Head of the Department of Bioengineering

Prof. Dr. Mehtap EANES

Dean of the Graduate School of
Engineering and Sciences

ACKNOWLEDGEMENT

I am genuinely grateful to my supervisor, Prof. Dr. Erdal BEDİR, for his precious guidance, immense knowledge, patience and motivation throughout my thesis studies.

I would like to express my gratitude to Mustafa Ünver KURT and Dr. Melis KÜÇÜKSOLAK for sharing their knowledge and experience during my research and giving me their full support, caring and patience,

I would like to express my gratitude to the jury members of my thesis, Prof. Dr. Ataç UZEL and Assist. Prof. Hümeýra TAŞKENT SEZGİN for giving valuable time and comments,

I would like to thank to Prof. Dr. Ataç UZEL for his full support and monitoring,

I want to express my thanks to Mert SUDAĞIDAN for sharing his bacterial stock collection and supporting me with his knowledge,

I kindly thank Assoc. Prof. Nur Başak SÜRMEĪ and all Sürmeli Lab Group for providing their laboratory equipment to use,

I am thankful to all Bedir Group members, especially Göklem ÜNER and Gamze DOĞAN, for supporting me with their experiences and for their valuable friendship,

I appreciate Lecturers Evrim PAŞIK and Dane RUSCUKLU and the management of the Biotechnology and Bioengineering Research Center (Izmir Institute of Technology) for equipment and technical support,

Last but not least, I am deeply grateful to my mother, Yasemin CAN, my father, Abdalbaki CAN, and my brother, Mehmet CAN, for their full support and unconditional love.

This thesis was supported by the Scientific and Technological Research Council of Turkey (TUBITAK) 1001 Project (Grant Number: 122R077) and TUBITAK 2210-A (Scholarship number: 1649B022104315).

ABSTRACT

SECONDARY METABOLITES FROM MARINE DERIVED ACTINOBACTERIA AND THEIR BIOACTIVITIES

Actinobacteria is noteworthy for producing numerous bioactive secondary metabolites, including antibacterial and anticancer compounds. Within the scope of this thesis, Actinobacteria were isolated from Ilica Bay of Izmir (Turkey) to reveal their antimicrobial potential. Fermentation broths of twelve isolates were extracted with ethyl acetate and screened versus selected pathogens (*Staphylococcus aureus*, *Escherichia coli* and *Candida albicans*) via disc diffusion assay. Most isolates exhibited antimicrobial activity against at least one pathogen. The isolates were suggested to be *Streptomyces* members based on their morphological characteristics. Based on its antimicrobial potency and secondary metabolite profile, isolate (35M1) was selected for further studies. A whole genome sequence (WGS) analysis of the isolate clarified its identity as *Streptomyces* sp. 35M1, deposited in DDBJ/ENA/GenBank (Accession number: JBCLWP010000000).

A preparative scale fermentation followed by a bioactivity-guided isolation study resulted in the purification and characterization of five compounds, which were identified as Actinomycin D (ActD), Actinomycin X2 (ActX2), Actinomycin XO β (ActXO β), Collismycin A (ColA) and Collismycin C (ColC). Further, antibiofilm effects were investigated, revealing that ActD and ActX2 had biofilm inhibitory effects against methicillin-resistant *Staphylococcus aureus*, *Listeria monocytogenes* and *Staphylococcus epidermidis*. Lastly, a synergism study was conducted with the compounds in good quantity (ActD, ActX2, and ActXO β). ActD with Nalidixic acid and ActX2 with Ampicillin, Nalidixic acid, and Rifampicin demonstrated synergistic effects against gram-negative *E. coli*, being reported first time in the literature.

Keywords: *Streptomyces*, Actinomycin, Collismycin, Antibacterial, Antibiofilm, Synergism

ÖZET

DENİZEL KAYNAKLI AKTİNOBAKTERİLERİN SEKONDER METABOLİTLERİ VE BUNLARIN BİYOAKTİVİTELERİ

Aktinobakteriler, antibakteriyel ve antikanser bileşikler dahil olmak üzere birçok biyoaktif ikincil metabolit üretebilmesi açısından dikkat çekmektedir. Bu tez kapsamında, İzmir (Türkiye) Ilıca Körfezi'nden Aktinobakteri olduğu öngörülen bakteriler izole edilerek antimikrobiyal potansiyelleri ortaya konmuştur. On iki izolata fermentasyon sıvıları etil asetat ile ekstre edilerek, disk difüzyon testi ile seçilen patojenlere karşı (*Staphylococcus aureus*, *Escherichia coli* ve *Candida albicans*) taranmıştır. İzolatların çoğunluğu en az bir patojene karşı antimikrobiyal aktivite göstermiştir. Elde edilen izolatların morfolojik özelliklerine dayanarak *Streptomyces* üyeleri oldukları düşünülmüştür. Antimikrobiyal potansiyel ve ikincil metabolit profillerine dayanarak, 35M1 izolatu ileri çalışmalar için seçilmiştir. İlgili izolata tüm genom dizilim (WGS) analizi sonucu türü *Streptomyces* sp. 35M1 olarak netleştirilmiş ve DDBJ/ENA/GenBank sistemine kaydedilmiştir (Erişim numarası: JBCLWP010000000).

Preparatif ölçekli fermentasyonu takiben biyoaktivite rehberli izolasyon çalışmaları gerçekleştirilmiş, beş bileşik saflaştırılarak karakterize edilmiştir. Bu bileşikler; Actinomycin D (ActD), Actinomycin X2 (ActX2), Actinomycin XOβ (ActXOβ), Collismycin A (ColA) ve Collismycin C (ColC) olarak tanımlanmıştır. Sonrasında, ilgili moleküllerin antibiyofilm etkileri araştırılmış ve ActD ile ActX2'nin Metisiline dirençli *Staphylococcus aureus*, *Listeria monocytogenes* ve *Staphylococcus epidermidis* 'e karşı biyofilm inhibitör etkileri olduğu ortaya konmuştur. Son olarak, yeterli miktarda bulunan bileşikler ile (ActD, ActX2 ve ActXOβ) bir sinerjizm çalışması yapılmıştır. ActD ile Nalidiksik asit ve ActX2 ile Ampisilin, Nalidiksik asit ve Rifampisin kombinasyonları, gram-negatif *E. coli* 'ye karşı sinerjik etki göstermiş ve bu durum literatürde ilk kez rapor edilmiştir.

Anahtar Kelimeler: *Streptomyces*, Actinomycin, Collismycin, Antibakteriyel, Antibiofilm, Sinerjizm

TABLE OF CONTENTS

LIST OF FIGURES	viii
LIST OF TABLES.....	xi
CHAPTER 1	1
1.1. Actinobacteria	2
1.1.2. Natural Products (NPs) from Actinobacteria	3
1.2. Biosynthesis of Secondary Metabolites	5
1.3. Strategies Against Pathogenic Bacteria	8
1.4. Objectives of The Thesis.....	15
CHAPTER 2	16
2.1. Materials.....	16
2.1.1. Microorganisms	16
2.1.2. Culture Media.....	16
2.1.3. Chemicals	18
2.1.4. Instruments	18
2.2. Methods.....	19
2.2.1. Sample Collection	19
2.2.2. Isolation Studies of <i>Streptomyces</i> Species	19
2.2.3. Analytical-Scale Fermentation	20
2.2.4. Further Studies with 35M1	22
2.2.5. Preparative-Scale Fermentation.....	24
2.2.6. Bioactivity-Guided Isolation	25
2.2.7. Bioactivity Analyses.....	30
2.2.8. Data Analysis.....	33
CHAPTER 3	35
3.1. Isolation and Characterization of Isolates	35
3.2. Analytical-Scale Fermentation.....	38
3.2.1. Antimicrobial Activity of Isolates	40
3.2.2. Selection of an Isolate	42
3.3. Successive Studies with 35M1	43
3.3.1. WGS Analysis	43

3.3.2. Determination of Growth Curve.....	52
3.4. Preparative-Scale Studies.....	54
3.4.1. Structure Elucidation of Isolated Compounds.....	58
3.4.2. LC-MS/MS Analysis.....	74
3.5. Bioactivity Analyses.....	83
3.5.1. MIC Test.....	84
3.5.2. Antibiofilm Activity.....	89
3.5.3. Synergistic Activity.....	94
CHAPTER 4.....	98
REFERENCES.....	101

LIST OF FIGURES

<u>Figure</u>	<u>Page</u>
Figure 1.1. Primary and secondary metabolite production during microbial growth.....	1
Figure 1.2. The life cycle of Actinobacteria	3
Figure 1.3. Summarized microbial biosynthesis pathways.....	6
Figure 1.4. Common antibiotic targets and resistance mechanisms of bacteria	9
Figure 1.5. Biofilm formation steps, created with BioRender.com.	13
Figure 2.1. Overall preparative-scale fermentation and SPE processes	24
Figure 2.2. The evaporation process of D101-Ace fraction	26
Figure 2.3. Images of the fractionation step	26
Figure 2.4. SG-01 precipitate and its TLC profile.....	27
Figure 2.5. Isolation scheme (Part 1).....	28
Figure 2.6. Isolation scheme (Part 2).....	29
Figure 3.1. Examples of spread plate technique incubation results.....	36
Figure 3.2. Examples of the isolated <i>Streptomyces</i> suspected cultures on SFM agar	37
Figure 3.3. Microscope images of the selected isolates.....	37
Figure 3.4. Fermentation broths after the incubation.....	39
Figure 3.5. TLC profiles of the isolates with 90:10 (CHCl ₃ :MeOH) system.	39
Figure 3.6. TLC profiles of the isolates with 80:20 (MeOH:H ₂ O) system.....	40
Figure 3.7. The colony morphology of 35M1 on M1 agar	43
Figure 3.8. The phylogeny tree of 35M1.	45
Figure 3.9. The chemical structures of selected compounds from AntiSmash results ...	51
Figure 3.10. The growth curve of <i>Streptomyces</i> sp. 35M1.....	52
Figure 3.11. Antimicrobial disc diffusion results of <i>Streptomyces</i> sp. 35M1 extract concerning incubation times	53
Figure 3.12. EtOAc extract TLC profiles of daily fermentation samples.....	54
Figure 3.13. Depiction of the preparative-scale fermentation endpoint and TLC profiles of specific days for comparison with the analytical scale.	55
Figure 3.14. Depiction of dry forms of fractions	57
Figure 3.15. The chemical structure of SG-01	58

<u>Figure</u>	<u>Page</u>
Figure 3.16. The ¹ H NMR spectrum of SG-01	62
Figure 3.17. The ¹³ C NMR spectrum of SG-01	62
Figure 3.18. The HMBC spectrum of SG-01	63
Figure 3.19. The COSY spectrum of SG-01	63
Figure 3.20. The HSQC spectrum of SG-01	64
Figure 3.21. The chemical structure of SG-02	64
Figure 3.22. The ¹ H NMR spectrum of SG-02	67
Figure 3.23. The chemical structure of SG-03	67
Figure 3.24. The ¹ H NMR spectrum of SG-03	69
Figure 3.25. The chemical structure of SG-04	70
Figure 3.26. The ¹ H NMR spectrum of SG-04	71
Figure 3.27. The chemical structure of SG-05	72
Figure 3.28. The ¹ H NMR spectrum of SG-05	73
Figure 3.29. The ¹³ C NMR spectrum of SG-05	74
Figure 3.30. RT means vs Parent mass heat map.	75
Figure 3.31. ESI- full MS spectrum belonging to the 35M1 extract	77
Figure 3.32. ESI-MS of <i>m/z</i> 1255.5961 base peak (SG-01)	78
Figure 3.33. ESI-MS of <i>m/z</i> 1269.6156 base peak (SG-02)	78
Figure 3.34. ESI-MS of <i>m/z</i> 1271.5922 base peak (SG-03).....	79
Figure 3.35. ESI-MS of <i>m/z</i> 269.0917 base peak (SG-04).....	79
Figure 3.36. ESI-MS of <i>m/z</i> 275.0848 base peak (SG-05).....	80
Figure 3.37. <i>S. epidermidis</i> growth percentages with respect to varied concentrations of agents.....	85
Figure 3.38. MRSA growth percentages with respect to varied concentrations of agents.	86
Figure 3.39. <i>L. monocytogenes</i> growth percentages with respect to varied concentrations of agents.....	87
Figure 3.40. MRSA biofilm growth curve (%) with respect to varied concentrations of agents in 10 % TSB + 0.1 % glucose.	90
Figure 3.41. <i>L. monocytogenes</i> biofilm growth curve (%) with respect to varied concentrations of agents in 10 % TSB + 0.1 % glucose.....	91

<u>Figure</u>	<u>Page</u>
Figure 3.42. Biofilm eradication assay results as biofilm (%) vs concentration of compounds in 10 % TSB + 0.1 % glucose medium.	92
Figure 3.43. Images of wells belonging to biofilm eradication assay before the solubilization step of CV under a light microscope at 5x magnification. .	93
Figure 3.44. Dose-Effect curve and median-effect plot of single compounds, plotted using CompuSyn.	95
Figure 3.45. Combination index plots created with CompuSyn.	97
Figure 3.46. Synergy results obtained from growth percentages of E. coli with respect to combinations and FICI calculations	96

LIST OF TABLES

<u>Table</u>	<u>Page</u>
Table 1.1. Some of bioactive compounds isolated from Actinobacteria are shown.....	4
Table 2.1. Utilized nutrient media	16
Table 2.2. Utilized chemicals	18
Table 2.3. Utilized equipment.....	19
Table 2.4 Chromatographic analysis method	23
Table 3.1. Results of disc diffusion test together with dry weights of extracts from analytical-scale fermentation study.....	41
Table 3.2. NCBI Blast results.	44
Table 3.3. DSMZ Type (Strain) Genome Server Results	44
Table 3.4. AntiSmash results	47
Table 3.5. Disc diffusion results of fractions from SPE. *Control 1 describes LLE extraction of fermentation broth with EtOAc.	56
Table 3.6. It shows the zone of inhibition (mm) from disc diffusion tests of the main column (<i>ACT-RP2111</i>) fractions against <i>S. aureus</i> , <i>E. coli</i> and <i>C. albicans</i> . Standard: D101-Ace extract, Positive Control: Kanamycin for bacteria and Nystatin for yeast.	57
Table 3.7. ¹ H and ¹³ C NMR spectroscopic data of SG-01 (ActD) ^a (CDCl ₃ , ¹ H: 400 MHz, ¹³ C:100 MHz).....	59
Table 3.8. ¹ H spectroscopic data of SG-02 (ActX2) ^a (CDCl ₃ , ¹ H: 400 MHz)	65
Table 3.9. ¹ H NMR spectroscopic data of SG-03 (ActXoβ) ^a (CDCl ₃ , ¹ H: 400 MHz) ...	68
Table 3.10. ¹ H and ¹³ C NMR spectroscopic data of SG-04 (CoIA) ^a (d6-DMSO, ¹ H: 400 MHz, ¹³ C:100 MHz)	70
Table 3.11. ¹ H and ¹³ C NMR spectroscopic data of SG-05 (CoIC) ^a (¹ H: 400 MHz in d6- DMSO, ¹³ C:100 MHz in CDCl ₃)	72
Table 3.12. GNPS metabolomics results related to Actinomycin derivatives.....	80
Table 3.13. Five unknown compounds found by GNPS analysis	803
Table 3.14. MIC values of isolated compounds	88
Table 3.15. MBIC values of isolated compounds.....	89

ABBREVIATIONS

$^1\text{D-NMR}$	One-Dimensional Nuclear Magnetic Resonance
$^2\text{D-NMR}$	Two-Dimensional Nuclear Magnetic Resonance
$^1\text{H-NMR}$	Proton Nuclear Magnetic Resonance
$^{13}\text{CNMR}$	Carbon Nuclear Magnetic Resonance
Ace	Acetone
I	Acetonitrile
ActD	Actinomycin D
ActX2	Actinomycin X2
ActXO β	Actinomycin Xo β
ANOVA	Analysis of Variance
CD_3OD	Deuterated Methanol
CDCl_3	Deuterated Chloroform
CFU	Colony Forming Unit
CH_2Cl_2	Dichloromethane
CHCl_3	Chloroform
CLSI	Clinical and Laboratory Standards Institute
ColA	Collismycin A
ColC	Collismycin C
COSY	Correlation Spectroscopy
CV	Crystal Violet
<i>d</i>	Doublet
DCM	Dichloromethane
<i>dd</i>	Doublet-doublet
DMSO	Dimethyl Sulfoxide
DNA	Deoxyribonucleic Acid
dsDNA	Double-Stranded DNA
EPS	Extracellular Polymeric Substances
EtOAc	Ethyl Acetate
EtOH	Ethanol
FAS	Fatty Acid Synthesis

FDA	Food and Drug Administration
FIC	Fractional Inhibitory Concentration
FICI	Fractional Inhibitory Concentration Index
Fr	Fraction
H ₂ O	Water
H ₂ SO ₄	Sulfuric Acid
HMBC	Heteronuclear Multiple Bond Coherence
HSQC	Heteronuclear Single Quantum Coherence
IPA	Isopropyl Alcohol
<i>m</i>	Multiplet
MeOH	Methanol
MDR	Multidrug Resistance
MHA	Mueller Hinton Agar
MHB	Mueller Hinton Broth
NaCl	Sodium Chloride
<i>n</i> -Hex	<i>n</i> -Hexane
NMR	Nuclear Magnetic Resonance
NRPS	Non-Ribosomal Peptide Synthase
Prep-TLC	Preparative-Thin Layer Chromatography
QQ	Quorum Quencher
QS	Quorum Sensing
QSI	Quorum Sensing Inhibitors
RNA	Ribonucleic Acid
RP	Reverse Phase
<i>s</i>	Singlet
SAR	Structure-Activity Relationship
<i>t</i>	Triplet
T1PKS	Type-1 Polyketide synthase
T2PKS	Type-2 Polyketide synthase
T3PKS	Type-3 Polyketide synthase
TLC	Thin Layer Chromatography
TLC	Thin Layer Chromatography
TSA	Tryptic Soy Agar

TSB	Tryptic Soy Broth
TTC	2,3,5-Triphenyl-tetrazolium chloride Solution
UV	Ultraviolet

CHAPTER 1

INTRODUCTION

Microorganisms play a key role in the environment by recycling and maintaining nutrient chain balance, supporting vital physiological functions in plants and animals. They possess a remarkable chemical and molecular diversity to serve dynamic interactions among themselves and with higher organisms. To maintain metabolic functions, development and growth (**Figure 1.1**), they need primary metabolites, which are known as central metabolites, such as lactic acid, ethanol, and vitamins. On the other hand, secondary metabolites, produced under stress conditions, are not essential for growth and development. These compounds fulfill various roles for the producer microorganisms, such as defense, competition for resources, and communication. With the purpose of defense and thriving in competition, some microorganisms can produce metabolites with antioxidant, antimicrobial, and cytotoxic properties.¹⁻⁵

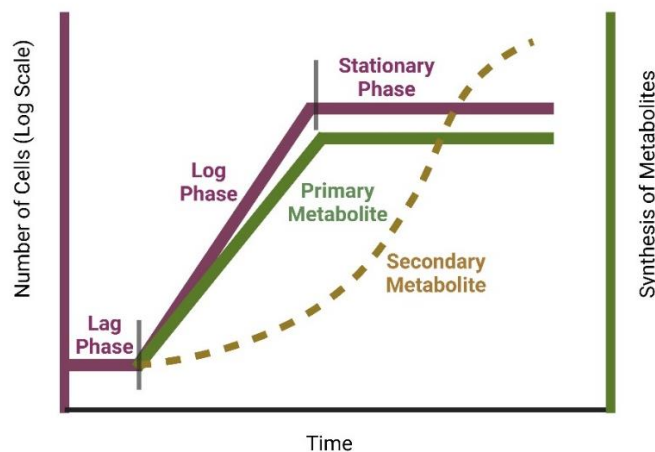


Figure 1.1. Primary and secondary metabolite production during microbial growth, created with Biorender.com

As pharmaceuticals, microbial natural products have been widely used to treat infections, starting with the discovery of penicillin. However, after the 1970s, a discovery void was the case, leaving humankind vulnerable to newly emerging drug-resistant pathogens.⁶

Thus, the discovery of novel antimicrobial compounds or new therapeutic approaches has been a must. However, the re-discovery of the same compounds led scientists to investigate the microorganisms in previously overlooked or less studied habitats, like marine environments. Marine-specific ecosystems have distinct environmental conditions that differ from the soil, like variations in salinity, pressure, and temperature. These unique ecological factors shape the adaptation of species and the synthesis of specific compounds.⁷⁻⁹ Consequently, the marine ecosystem has become a focal source for discovering novel molecules.

1.1. Actinobacteria

Actinobacteria are one of the largest phyla in the bacteria domain. They are gram-positive, filamentous, and spore-forming bacteria. They have a high proportion of guanine and cytosine in their genome. Most Actinobacteria are primarily soil-dwelling organisms as semi-dormant spores, mainly when nutrients are scarce. Nevertheless, this phylum has evolved to inhabit various ecological niches. They are particularly prevalent in soils, especially alkaline and organic-rich ones. Actinobacteria are found on the surface and at depths exceeding two meters below ground level. Most Actinobacteria are aerobic and mesophilic, mainly thriving in the pH range of 6 to 9.^{10, 11}

Actinobacteria have complex life cycles (**Figure 1.2**) compared to bacteria and undergo growth by developing hyphae that give rise to a vegetative mycelium. Simultaneously, they disperse through spores formed on specific reproductive structures known as aerial hyphae. Consequently, their life cycle bears many similarities to that of filamentous fungi, although due to their genome, they are under the bacteria kingdom.^{10,}

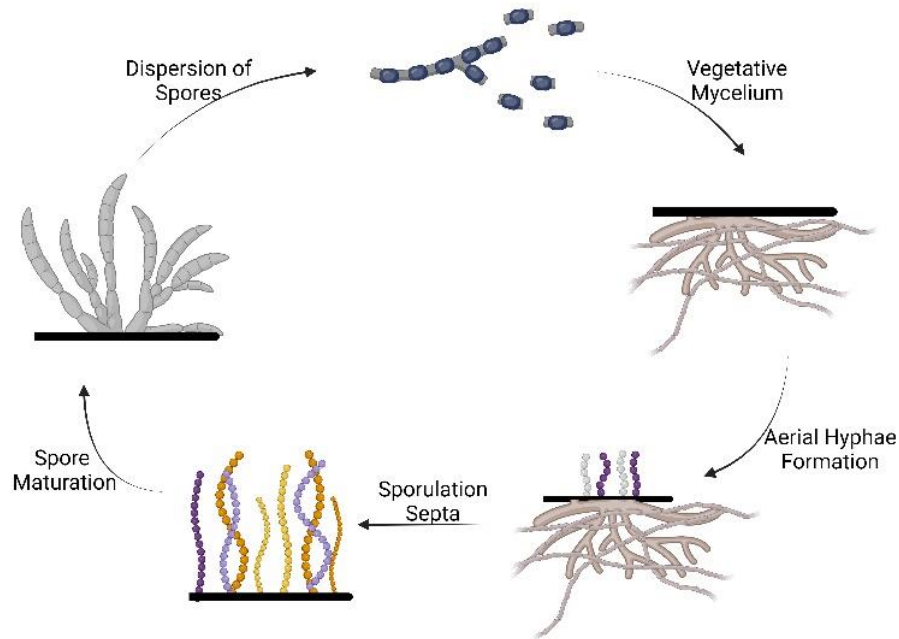


Figure 1.2. The life cycle of Actinobacteria, created with BioRender.com.

Streptomyces is the representative genus within the Streptomycetaceae family, situated in the *Actinomycetales* order of the *Schizomycetes* class.¹¹ Early genetic investigations in the 1950s led to the mapping of the chromosome of *Streptomyces coelicolor* as a model organism and so to the identification of the genes responsible for producing bioactive secondary metabolites.¹² Currently, there is a focus on manipulating biosynthetic gene clusters (BGCs), aiming to find more potential from cryptic sequences to produce novel compounds. The *Streptomyces* genus is of commercial interest for varied industries.¹³

1.1.2. Natural Products (NPs) from Actinobacteria

Actinobacteria, as mentioned, are a great source as they have been found to produce approximately 10,000 secondary metabolites, and at least 45 % of them are found to be biologically active. Actinobacteria involve the members of the genera *Salinispora*, *Micromonospora*, *Streptomyces*, and *Nocardia*, which are found to be the primary

producers of such compounds (*see Table 1.1*).¹¹ One remarkable example of the compounds is Salinosporamide A, which is extracted from *Salinispora tropica*, and its Phase III clinical trials have been completed for patients of Newly Diagnosed Glioblastoma (MIRAGE).¹⁴ However, among the genera, the genus *Streptomyces* is a prolific producer of bioactive secondary metabolites and is responsible for producing more than 50 % of clinically relevant antibiotics. They cover almost 80 % of marketed drugs obtained from microbial sources having varied modes of action.^{15, 16} For example, Streptomycin¹⁷ (from *Streptomyces griseus*) and Kanamycin¹⁸ (from *Streptomyces kanamyceticus*) can inhibit protein synthesis via binding to the 30S ribosomal subunit. At the same time, Erythromycin¹⁹ (from *Streptomyces erythraeus*) interferes with the DNA translation process of bacteria.

Table 1.1. Some of bioactive compounds isolated from Actinobacteria are shown.

COMPOUND	PRODUCER	BIOACTIVITY
Arenimycin ²⁰	<i>Salinispora arenicola</i>	Antibacterial, Cytotoxic
Carboxamycin ²¹	<i>Streptomyces</i> sp.	Antibacterial
Erythromycin ¹⁹	<i>Saccharopolyspora erythrae</i>	Antifungal
Fosfomycin ²²	<i>Streptomyces fradie</i>	Antibacterial
FK520 Ascomycin ²³	<i>Streptomyces</i> sp.	Antifungal, Immunosuppressive
Kanglemycin C ²⁴	<i>Nocardia</i> sp.	Immunosuppressive
Valinomycin ²⁵	<i>Streptomyces</i> sp.	Antibacterial
Zorbamycin ²⁶	<i>Streptomyces</i> sp.	Cytotoxic
Ivermectin ²⁷	<i>Streptomyces avermitilis</i>	Antiparasitic
Collismycin C ²⁸	<i>Streptomyces</i> sp. MC025	Antibiofilm, Neuroprotective
Granaticin ²⁹	<i>Streptomyces violaceoruber</i> Tü22	Antibiofilm

Meanwhile, the mode of action of Actinomycin D (from *Streptomyces sindanensis*) involves intercalation into DNA thus inhibiting RNA synthesis, leading to cell death.³⁰ Actinomycin D is utilized in clinical settings primarily as an anticancer drug and is available under the brand name Cosmegen. This drug is used to treat Wilms' tumor, rhabdomyosarcoma, Ewing's sarcoma, and certain types of testicular cancer.^{31, 32} Collismycin A is another natural compound produced by *Streptomyces* sp. that has antiproliferative activity against cancer cells and antimicrobial activity as iron chelator.^{33, 34} Recent studies have shown that iron can contribute to the initiation, progression, and metastasis of tumors.^{35, 36} At the biological level, bacteria utilize various uptake systems and produce siderophores to bind and sequester iron within the environment, as it is an essential component for their regulatory proteins and metabolic enzymes.³⁷ Therefore, the iron chelation strategy can provide new options against cancer and bacterial infections.

1.2. Biosynthesis of Secondary Metabolites

The genes responsible for facilitating the synthesis and production of the secondary metabolites in Actinobacteria are known as biosynthetic gene clusters (BGCs). BGCs include genes related to transcriptional control of secondary metabolites and a self-resistance gene that grants the producer organism immunity to its bioactive metabolites.^{13,}

38

The varied activities of the metabolites owe their action to their specified chemical structures, as the structures are key for their action mechanisms on a target. The structures of secondary metabolites derived chemically from primary metabolism pathways, including acetyl-CoA (via the acetate pathway), mevalonate (via the mevalonate pathway), shikimic acid (through the shikimate pathway), and methylerythritol phosphate (via the methylerythritol phosphate pathway). The acetate pathway is mainly responsible for producing phenols, prostaglandins, polyether, and macrolide antibiotics. Meanwhile, the shikimate pathway is used to synthesize alkaloids and some other phenolic compounds. The methylerythritol phosphate pathways contribute to the biosynthesis of a diverse array of terpenoids and steroids.^{4, 39, 40}

Bacterial secondary metabolite biosynthesis requires specific genes tightly organized in BGCs. Thus, two major pathways are polyketide biosynthesis (PKS) and

non-ribosomal peptide synthesis (NRPS) encoded in BGCs (**Figure 1.3**). Those pathways include synthetase enzymes, which have a role in folding protein domains independently, mediating the construction of polymer chains and tailoring them to be fully functional.⁴¹

42

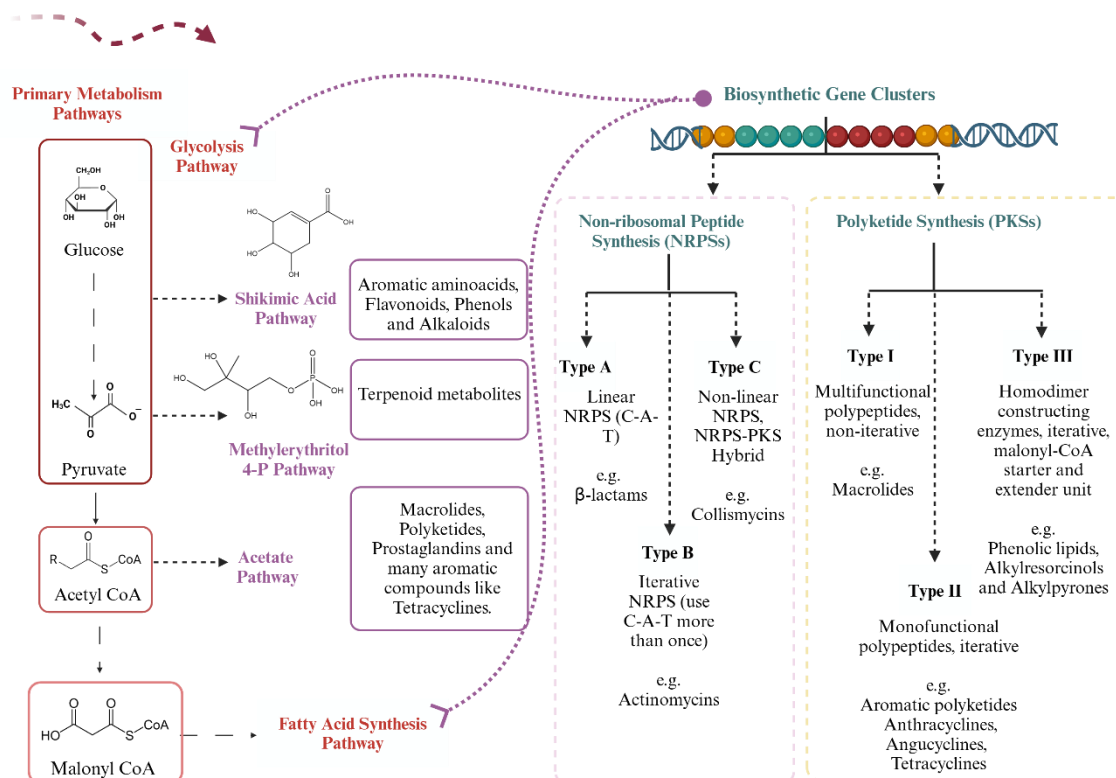


Figure 1.3. Summarized microbial biosynthesis pathways, created with BioRender.com

Starting from PKS, the biosynthesis of polyketides is highly complex as multifunctional enzymes are involved. Actinobacteria have specific PKSs as types I, II, and III. Firstly, type I PKSs (T1PKS) include multifunctional domain modules with specific enzymatic reactions. Each module, in a noniterative way, can create a condensation cycle. Macrolide compounds (e.g., Spiramycin, Pikromycin) have macrocyclic lactone rings and can be given as examples of molecules synthesized from T1PKS. Type II PKSs (T2PKS), on the other hand, can produce aromatic polyketides, which are classified into seven groups based on their polyphenolic ring system angucyclines, tetracyclines, anthracyclines and so on.^{43, 44} Type III PKSs (T3PKS)

include multiple enzymes that produce homodimers and catalyze certain reactions in a cascade way, including cyclization and extension. For example, the pathway is involved in Dihydroxyphenylglycine (3,5-DHPG) production, isolated from *Streptomyces violaceoruber*. The molecule includes a non-proteinogenic amino acid and is used to produce Kendomycin along with some other glycopeptide antibiotics like Vancomycin.⁴⁷

Thus, due to PKSs, varied bioactive compounds are produced. In addition, polyketide synthesis is connected to fatty acid synthesis at certain steps, which gives the organism the advantage of creating secondary metabolites with lipids in their structures.⁴³ ⁴⁴ Fatty acid synthesis (FAS), as in the case of glycolysis, is a primary metabolism pathway but also includes some precursors used in secondary metabolism. PKSs and FAS utilize homologous domains to carry the growing fatty acid or polyketide via a kind of pantetheine-linked thioester. The common chemistry of thioester, similar structural characteristics, and adaptable construction have led to the extensive presence of hybrid PKS-FAS pathways in the bacteria. Both systems use the precursors acetyl-CoA and malonyl-CoA, but they do not compete since fatty acid synthesis mainly occurs in growing cells. At the same time, polyketides, as secondary metabolites, are typically synthesized at early or mid-stationary phases.^{48, 49}

The second major pathway for producing secondary metabolites is NRPS, which involves enzymes used to synthesize peptide molecules with non-proteinogenic amino acids besides proteinogenic ones. NRPS system has modules named epimerization, methylation, cyclization, formylation, reduction, oxidation and other domains for additional modifications. The enzymes can recruit many more building blocks, like fatty acids and hydroxyl acids, to assemble them with peptide chains. Each module of enzymes comprises a catalytic domain that incorporates single residues. After the covalent attachment of amino acids is performed onto the integrated carrier protein domain, intermediates and substrates are transported to adjacent catalytic domains for further chemical modification or formation of the new bonds. In the last module, the terminal thioesterase domain finalizes the synthesis process to give the end product.^{45, 46} Daptomycin, an FDA-approved antibiotic drug, is produced through NRPSs by *Streptomyces roseosporus* NRRL1379.⁵⁰

Secondary metabolites isolated from Actinobacteria can play roles as antiviral, antibiofilm immunosuppressive, cytotoxic, antibacterial, plant growth-promoting, antihypertensive, insecticide, antioxidative, and herbicidal agents.^{15, 16}

1.3. Strategies Against Pathogenic Microorganisms

Bacteria are the most common type of microorganisms. Even though many bacteria benefit human health, some are pathogenic and can cause infections ranging from mild to severe. These pathogenic bacteria employ different mechanisms to evade the host's immune system and cause diseases. Bacterial pathogens can lead to morbidity and mortality, so threat to public health. Thus, in different areas of life, there is a constant need for agents to help us against pathogens, like antibiotics, quorum sensing inhibitors, and antibiofilm agents.⁵¹

On the other hand, fungi are eukaryotic microorganisms, found in almost everywhere and they can exist as yeasts, molds, or a combination of both forms. Yeasts, for example, are the single cell microorganisms that reproduce through budding. They can cause varied infections on humans, just as vaginal infections and so decrease well-being.¹⁶⁶

1.3.1. Antimicrobial Activity

Infectious diseases due to bacteria with virulence are a constant threat to human and animal health.

One of the pathogens that threaten human well-being is *S. epidermidis*, which is often regarded as a benign skin commensal and has significant clinical importance due to its role in healthcare-associated infections. This organism is a leading cause of nosocomial infections, particularly those related to indwelling medical devices such as catheters, prosthetic joints, and heart valves.⁵²

Another common pathogen is *L. monocytogenes*, which is a significant concern in the food industry due to its ability to thrive in refrigerated environments, which is uncommon among many pathogens. This bacterium can contaminate foods, including ready-to-eat meals, dairy products, seafood, and vegetables.⁵³

Thus, to combat such pathogens, antibiotics are used to treat infections. Most of the antibiotics used in clinics to combat such infections act by targeting vital cellular processes or synthesis. These targets typically involve (1) inhibiting the synthesis of DNA

or RNA, mediated by RNA polymerase or DNA topoisomerase, (2) disrupting protein synthesis through the ribosome, and (3) interfering with cell wall synthesis, especially peptidoglycan formation.⁵⁴

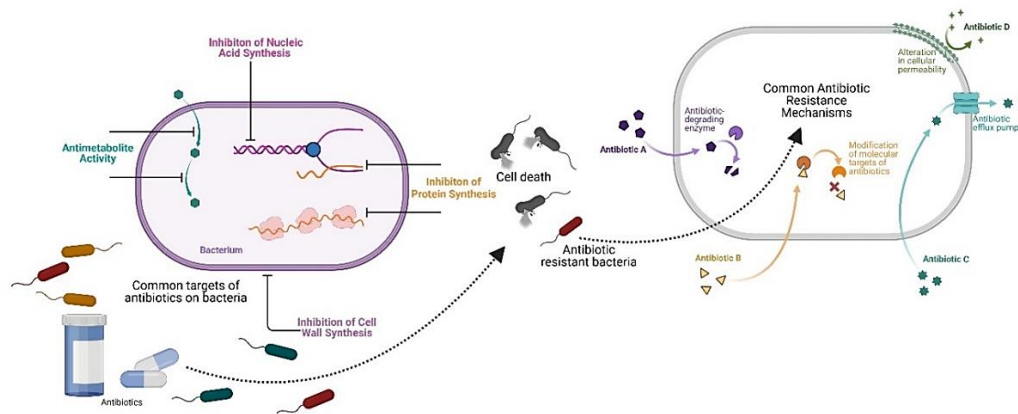


Figure 1.4. Common antibiotic targets and resistance mechanisms of bacteria, created with BioRender.com.

Antibiotics like Penicillin and Vancomycin⁵⁵ interfere with cell wall biosynthesis. Some antibiotics disrupt cell wall synthesis by targeting lipid II, a crucial intermediate in peptidoglycan biosynthesis. Certain peptides, such as lanthipeptides⁵⁶, bind to lipid II and create a polymerized complex that compromises cell membrane integrity, which leads to electrolyte leakage. Antibiotics like Linezolid and Tetracycline inhibit protein synthesis. Tetracycline binds to the smaller 30S subunit, interfering with translation processes.⁵⁷ Rifampicin, isolated from *Streptomyces mediterranei*, impedes DNA-dependent RNA polymerase.⁵⁸ As a result, antibiotics employ diverse mechanisms to disrupt crucial cellular processes (**Figure 1.4**), illustrating the varied strategies that could be used to combat bacterial infections.

Antibiotics were a significant breakthrough in healthcare as they drastically reduced mortality when first introduced. Nevertheless, over-prescription and unnecessary consumption of antibiotics cause antibiotic resistance among bacteria. This is one of the vital threats against humans, contributing to an estimated 4.95 million deaths globally in 2019. Examples of the so-called superbugs are *Escherichia coli* O157:H7, resistant to

carbapenems, and methicillin-resistant *Staphylococcus aureus* (MRSA), resistant to most prescribed beta-lactam antibiotics.⁵⁹

MRSA is resistant to several common antibiotics, making it a significant public health concern. As its infections range from mild to severe life-threatening conditions such as pneumonia, bloodstream infections (bacteremia), and surgical site infections. According to the Centers for Disease Control and Prevention (CDC), MRSA infections are estimated to cause over 10,000 deaths annually in the United States alone.⁶⁰ To combat the infection, Vancomycin (from *Streptomyces orientalis*) has been used to treat MRSA infections, but inevitable resistance started to emerge as Vancomycin-intermediate (VISA) and Vancomycin-resistant (VRSA) strains which made people helpless against the infections again. Alternative antibiotics, such as Daptomycin (from *Streptomyces roseosporus*), are often used for MRSA infections, but resistance to these antibiotics could also be acquired eventually.^{50, 61}

Hence, there is always an inevitable resistance against antibiotics, and there is a constant need for new therapeutic approaches or novel antimicrobial compounds. One of the approaches to combat such resistance is utilizing antibiofilm activities. The role of biofilms greatly contributes to resistance. Bacteria residing in a biofilm can demonstrate a 10 to 1,000-fold increase in antibiotic resistance compared to similar bacteria in a planktonic state.⁶²

Antifungals, on the other hand, are drugs that kill or inhibit the growth of fungi responsible for various infections. Especially, systemic fungal infections, including those caused by *C. albicans*, have become significant contributors to morbidity and mortality in immunocompromised patients.¹⁶⁶ In this respect, *Streptomyces* species are known to produce varied antifungal agents. For example, amphotericin B is one of the most well-known polyene macrolides, produced by *Streptomyces nodosus*.¹⁶⁷

1.3.2. Antibiofilm Activity

Bacterial biofilm formation is a complex process by which bacteria adhere to surfaces and become a multicellular community within a self-produced extracellular matrix (ECM). It has a sophisticated structure resulting from the interplay between bacteria and EPS. These polymers comprise extracellular polysaccharides, proteins,

DNA, and lipids. Therefore, understanding biofilm formation and dispersal is crucial for developing strategies to prevent and control biofilm-related infections and decrease their impact in various applications, like dental and bone implants.^{63, 64}

Biofilm formation is mainly triggered when there are stress factors in the environment, and it consists of four steps: aggregation, adhesion, development, and maturity. The first step includes reversible and irreversible adhesion phases. Reversible adhesion starts when microorganisms encounter the surface. During this timeframe, weak interactions like van der Waals and electrostatic forces occur with the surface. After that, irreversible adhesion occurs via covalent interactions and with the help of EPS production. Then, bacterial numbers increase significantly, making an overall filamentous-like colony structure. Bacterial cells adapt to live in such an environment, mainly in a dormant state. Lastly, the release of bacteria occurs to produce more biofilms on a larger surface^{63, 64}.

Thus, biofilms on the surface get larger, creating a much worse situation even though antibiotics are used at their therapeutic window. Hence, the antibiotic dose to be used to treat becomes much higher as the elimination of biofilm becomes difficult. However, increased doses are not applicable in clinics as dose toxicity becomes relevant. For that reason, there is a need for antibiofilm agents to target biofilm with low doses (**Figure 1.5**). One way to achieve this, could be persuading the biofilm's initial adhesion stage via adhesin and adhesion proteins. This way, compounds could not necessarily kill bacteria, only preventing them from being attached to the surface. For attachment to the surface, adhesins play a crucial role for bacteria as they act as bridges between bacteria and host cells or between bacteria themselves. For that reason, recent studies have shown that strategies targeting adhesins are unlikely to increase bacterial resistance or disrupt their life cycle. Instead, they interfere with the adhesion phase, hindering infection.⁶⁵

Secondly, there could be a focus on early formation stages, which include progressive formation of EPS and highly active communication between bacterial cells. In this stage, bacteria use quorum sensing (QS) molecules to coordinate their actions and evaluate the environment. Accordingly, QS directly influences bacterial behavior within biofilms. Against this, numerous studies have shown that certain compounds via quorum quenching can disrupt QS, thereby breaking down biofilms. These compounds are referred to as quorum-sensing inhibitors (QSIs). QSIs primarily function through two mechanisms: targeting QS synthetase to deactivate or degrade QS signal molecules and targeting QS receptors to either block the reception of QS molecules or compete with

them.^{63, 64, 66, 85} For example, Actinomycin D was found to exhibit significant anti-QS activity. At a concentration of 12.5 µg/mL, it notably inhibited violacein biosynthesis in *Chromobacterium violaceum* by 65 %, and at 25 µg/disc, it suppressed Prodigiosin production in *Serratia proteamaculans*, creating a pigment inhibition zone of 13.5 mm, without affecting bacterial growth. These results highlight that researchers are not only focused on discovering new compounds but also re-examining known antibiotics for potential bioactivities.⁶⁷

Thirdly, the maturation stage, which is typically characterized by a gradient chemical microenvironment and mature EPS, can be targeted. The microenvironment in such mature biofilms is hypoxic and has a low pH, creating a hostile environment for bacteria. Thus, to survive, bacteria differentiate into various subpopulations for protection, and some become persistent bacteria. Persistence is an epigenetic trait first identified in 1942, and it does not mean developing of drug resistance; instead, their slow metabolism or dormancy state allows them to evade the effects of drugs. Targeting dormant bacteria, or persister cells, can help remove biofilms and address chronic and recurrent infections more effectively. However, the challenge of disruption of the microenvironment at first could be difficult to simulate *in vivo*.^{63, 64, 68, 85} Dispersin B, a glycoside hydrolase, is produced by the periodontal pathogen *Aggregatibacter actinomycetemcomitans*. It can detach adherent cells from mature biofilm colonies by disrupting biofilm formation. The process is facilitated by catalyzing the hydrolysis of linear polymers of N-acetyl-D-glucosamines present in the biofilm matrices.⁶⁹

The dispersion stage is the final target where there is residual accumulation of biofilm. Numerous studies have identified active biofilm dispersal as a promising strategy for controlling and removing biofilms. D-type amino acids are critical compounds secreted by bacteria during the biofilm dispersal phase. Consequently, therapeutic approaches have been suggested that combinatorial therapy of D-type amino acids with drugs might help, as certain D-type amino acids can effectively break down the EPS in biofilms, and a second compound could act on vulnerable bacteria.^{63, 64, 70, 85}

Overall, an anti-biofilm agent could target any stage of the biofilm shown in **Figure 1.5**. However, targeting the biofilm needs to be strain-specific. Because components inside the biofilm differ from strain to strain.

For example, *L. monocytogenes* has flagella and irreversibly attaches to the surface and with that, its mobility and autolytic capacity decrease, aiding colonization. Its biofilm matrix primarily comprises of proteins, including teichoic acids, the main

polysaccharide components, and extracellular DNA (eDNA). Such components play a critical role in maintaining the structural integrity of its biofilm.⁷¹ *L. monocytogenes* is particularly problematic due to its ability to form biofilms on various surfaces within food processing environments, such as stainless steel, plastic, and rubber. Biofilms protect bacteria from environmental stresses and sanitizing agents, making them difficult to eradicate and posing a persistent risk of contamination.^{71, 72}

On the other hand, *S. aureus*, which does not have pilli or flagella, attaches to the surface with the aid of cell surface-associated adhesin proteins. The biofilm matrix of it is primarily composed of water and various organic elements as well as bacterial microcolonies and polysaccharide intercellular adhesins.⁷³ Biofilm-associated infections are notoriously difficult to treat and often require the removal of the infected device.⁷⁴

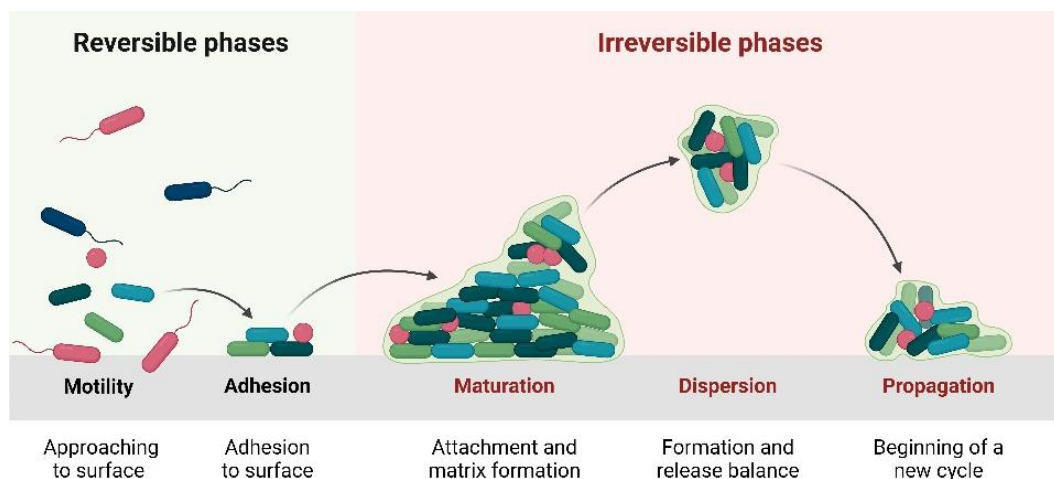


Figure 1.5. Biofilm formation steps, created with BioRender.com.

Several molecules isolated from *Streptomyces* sp. are known to have antibiofilm effects. An example is that a molecule named 5812-A/C isolated from *Streptomyces roseoflavus* INA-Ac-5812, exhibited a comparable inhibitory effect against Gram-positive bacteria compared to daptomycin.⁷³ This is significant as daptomycin stands out as the most potent antibiotic for combating Gram-positive bacteria within biofilms.¹⁷⁵ The mechanism of action of 5812-A/C involves disrupting membrane integrity, which differs

from daptomycin. Additionally, unlike daptomycin, 5812-A/C can penetrate mature biofilms and impede the metabolic activity of embedded *S. aureus*.⁷⁵

Another example of an antibiofilm agent is an angucycline-type antibiotic, 8-O-methyltetrangomycin, isolated from *Streptomyces* sp. SBRK2 demonstrated MIC of 2 µg/mL against MRSA. At sub-inhibition concentrations, it effectively decreased the formation of biofilms by *S. aureus* ATCC25923 and enhanced the cell surface hydrophobicity index. These results indicate that 8-O-methyltetrangomycin shows potential as a candidate for developing anti-biofilm agents aimed at combating drug-resistant pathogens.⁷⁶

1.3.3. Synergistic Activity

Synergism is an important phenomenon for developing combination therapeutics with varied health benefits. As novel drug candidate discovery has been becoming difficult, research groups make a lot of effort to combine different compounds to combat multi-drug resistant (MDR) pathogens.^{77, 78}

With this purpose, different combinations of compounds are used to enhance bioactivities. For example, Trimethoprim, a well-known dihydrofolate reductase inhibitor, enhances Sulfonamide activity that interrupt *p*-aminobenzoic acid conversion in cells. Thus, when combined, broad-spectrum bactericidal activity occurs, and it is currently used in clinics to treat common diseases like urinary tract infections.⁷⁹

Another example is a Dalfopristin-Quinupristin combination, which is FDA-approved and has activity against Gram-positive bacteria, including multidrug-resistant *Streptococcus* species.⁸⁰ Vancomycin is also found to have synergistic activity with Oxacillin, Cephalothin, Cefazolin, and Imipenem in vitro against MRSA.⁸¹ Streptomycin isolated from *Streptomyces griseus* acts synergistically with Tetracycline and Penicillin against *Brucella abortus* which is abortion causative for cattle.⁸² The combination of Ampicillin and Ceftriaxone has emerged as a leading treatment for severe *Enterococcus faecalis* infections, including endocarditis.⁸³ Amoxicillin/Clavulanic acid combination approved by FDA and used to counteract β-lactamase activity overcoming Beta-lactam resistance.⁸⁴

Hence, combination therapy has been used to manage infectious diseases and could have some other advantages such as reducing dose-dependent toxicity.

Overall, antimicrobial and antibiofilm activities together with synergism are crucial fields to focus on as there is a constant need for new therapeutics or different therapy approaches against pathogenic bacteria that gain resistance day by day.

1.4. Objectives of The Thesis

The main objectives of this thesis are:

Isolation of bioactive Actinobacteria, from Ilica Bay-Izmir as the region is lack of extensive screening study,

Morphological characterization of the isolates,

Determination of their antimicrobial activity and analysis of chemical profiles,

Selection of an isolate for preparative studies,

Identification of the selected species by WGS analysis,

Profiling of metabolites by LC-MS/MS analysis,

Purification, and structural elucidation of bioactive molecules via bioassay guided fractionation,

Assessment of pure compounds' antimicrobial, antibiofilm, and synergistic properties.

CHAPTER 2

MATERIALS AND METHODS

2.1. Materials

2.1.1. Microorganisms

For antimicrobial tests, *Staphylococcus aureus* ATCC 25923, methicillin-resistant *Staphylococcus aureus* ATCC 43300, *Escherichia coli* ATCC 25922, *Listeria monocytogenes* ATCC 19115, *Staphylococcus epidermidis* ATCC 14990, *Candida albicans* DSMZ 5817 and Fluconazole resistant *C. albicans* were used. Resistant *C. albicans* is a clinical isolate was obtained from Ege University/Izmir.

2.1.2. Culture Media

The media used in this study is shown in **Table 2.1**. They were used after sterilization with an autoclave for 15 min at 121 °C.

Table 2.1. Utilized nutrient media

Medium Name	Ingredients	Usage
Tryptic Soy Agar (TSA) (ThermoFisher Oxoid)	15 g pancreatic digest of casein, 5 g enzymatic digest of soybean, 5 g sodium chloride and 15 g agar dissolved in 1 L distilled water	Pathogenic bacteria enrichment

Cont. on next page

Table 2.1 (Cont.)

Medium Name	Ingredients	Usage
TSB (ThermoFisher Oxoid)	15 g pancreatic digest of casein, 5 g enzymatic digest of soybean and 5 g sodium chloride dissolved in 1 L distilled water	Pathogenic bacteria enrichment
TSB 10 % with Glucose ⁹⁶	1.5 g pancreatic digest of casein, 0.5 g enzymatic digest of soybean, 0.55 g sodium chloride dissolved in 1 L distilled water and 0.1 % glucose (w/v) was added	Activity studies
Mannitol Soy Flour (SFM) ⁸⁶	20 g mannitol, 15 g NaCl, 20 g soy flour, 15 g bacteriological agar dissolved in 1 L distilled water	Sporulation of <i>Streptomyces</i> strains
Muller-Hinton Agar (MHA) (ThermoFisher Oxoid)	3 g dehydrated infusion from beef, 17.5 g casein hydrolysate, starch 1.5 g and 17 g agar dissolved in 1 L distilled water	Activity studies
Muller-Hinton Broth (MHB) (ThermoFisher Oxoid)	3 g dehydrated infusion from beef, 17.5 g casein hydrolysate and starch 1.5 g dissolved in 1 L distilled water	Activity studies
M1 Agar ⁸⁷	15 g bacteriological agar, 10 g soluble starch, 4 g yeast extract, 2 g peptone water, 38 g/L artificial sea salt dissolved in 1 L distilled water (pH 7)	Isolation studies
M1 Broth ⁸⁷	10 g soluble starch, 4 g yeast extract, 2 g peptone water, 38 g/L artificial sea salt dissolved in 1 L distilled water (pH 7)	Fermentation studies

2.1.3. Chemicals

The chemicals used in this study to conduct fermentation isolation and purification studies are listed in **Table 2.2**.

Table 2.2. Utilized chemicals

For fermentation studies	
Glycerol (Carlo Erba)	Peptone Water (Biolife)
Ethanol (EtOH) (Honeywell)	Artificial Sea Salt
D (+)-Glucose Monohydrate (Isolab)	Soluble Starch (Isolab)
D-Mannitol (Merck)	Soy Flour
Bacteriological Agar (Biolife)	Sodium Chloride (Isolab)
Yeast Extract (Biolife)	Kanamycin (Sigma-Aldrich)
Nystatin (Sigma-Aldrich)	Nalidixic acid (Sigma-Aldrich)
For Isolation Studies	
Chloroform (Honeywell)	Methanol (MeOH) (Honeywell)
Ethyl acetate EtOAc (Honeywell)	Acetone (Ace) (Honeywell)
Isopropyl alcohol (IPA) (Honeywell)	Sulfuric Acid (Merck)
<i>n</i> -Hexane (Honeywell)	<i>n</i> -Butanol (Honeywell)

2.1.4. Instruments

The equipment used in this study to conduct experiments, are listed in **Table 2.3**.

Table 2.3. Utilized equipment

Autoclave (Nüve)	LC/MS (Thermo Orbitrap Q-Exactive)
Nuclear Magnetic Resonance Spectrometer (Varian MERCURY plus-AS-400 400 MHz)	Rotary Evaporator (Heidolph)
Shaking Incubator (Nüve)	Vortex (Isolab)
Speedvac Concentrator (Thermo Scientific Savant SPD 121P)	Light Microscope (Olympus)
Convection Oven (JSR, JSOF-050)	-86 Freezer (Nüve)
Biosafety Cabinet (Level 2) (Nüve)	Static Incubator (Memert)
Ultra Centrifuge (Thermo Scientific)	Vacuum Pump (Isolab)
UV Lamp (Vilber Lourmat)	Orbital Shaker (Thermo Scientific)

2.2. Methods

2.2.1. Sample Collection

Samples were collected manually from Ilıca Bay Izmir/Turkey in the scope of preliminary studies of TÜBİTAK-1001 project (Grant no: 122R077). In total, five sediment samples were collected from the coast of the bay (38°12'28"K, 26°38'10"D). Samples were collected in sterile falcon tubes and preserved at 4 °C until they were taken to the laboratory. Environmental conditions of collected isolates were noted. Throughout the studies, aseptic conditions were maintained.

2.2.2. Isolation Studies of *Streptomyces* Species

Isolation studies started with homogenization of samples inside 0.9 % saline solution twice for 2 hours (h) at 28 °C and 150 rpm. Then the samples were diluted up to 10⁻². Afterward, 10⁻¹ and 10⁻² dilutions were inoculated onto agar plates in triplicates using

spread plate technique. M1 agar medium was used for isolation. It was prepared with antimicrobial agents, including Nystatin (50 µg/mL, antifungal) and Nalidixic acid (20 µg/mL, antibacterial), and without any supplementary agents. After inoculation processes, the Petri dishes were incubated at 28 °C for four weeks. They were examined weekly to observe newly formed colonies, and Actinobacteria suspected colonies were isolated using the streak plate technique to observe colony morphologies. SFM agar was used to check suspects of *Streptomyces* sp. as the medium leads them to sporulate quickly, which differentiates them from others.⁸⁶ Isolates were also investigated under a light microscope with 100x magnification to examine their filamentous structures. Then, they were all stored at -86 °C after 30 % glycerol spore stocks were prepared for future studies.

2.2.3. Analytical-Scale Fermentation

First, a proper nutrient medium for analytical-scale fermentation studies was determined. In the literature, Aksoy et al. (2014) used ten different media to be tested initially for Actinobacteria isolation from sediment samples. Among these, the four of them with the highest yields (M1, M6, MAIA, and MR2A) were selected for further isolation studies. Ultimately, it was statistically shown that M6 and M1 were the most effective for isolating active strains. Therefore, M6 and M1 were included in preparative-scale fermentation studies.⁸⁷ Based on these findings, the M1 medium, prepared with artificial sea salt, was chosen for fermentation studies in this thesis. Thus, analytical-scale fermentations were conducted by transferring each isolate into 50 mL of the M1 broth media in 250 mL Erlenmeyer flasks. These flasks were then incubated at 28 °C with shaking at 150 rpm for 7 days.

After incubation, fermentation broths were filtrated to remove bacterial biomass. Then, EtOAc was added to the broth (1:1, v/v), and liquid-liquid extraction was performed three times with fresh EtOAc using a separatory funnel. Organic phases were pooled and dried through a rotary evaporator, and EtOAc extracts were transferred in 4 mL amber vials.

Afterward, TLC was used to examine metabolite profiles of extracts using different mobile phase systems. TLC studies were conducted on plates with normal silica gel 60 F254 (105570, Merck Supelco) and coated with RP-18 F254 (105559, Merck

SupeIco). UV active molecules in extracts were detected at 254 and 365 nm before applying an indicator solution. As an indicator, 20 % aq. H₂SO₄ was sprayed onto plates and heated until spots were visible to the naked eye to visualize non-UV active compounds. Then, the plates were again visualized under 254 and 365 nm.

Mobile phases were used at various ratios, as:

CHCl₃:MeOH (98:2, 96:4, 94:6, 92:8, 90:10, 85:15), CHCl₃:MeOH:H₂O (70:30:3, 61:32:7), CHCl₃:IPA (94:6, 90:10), EtOAc:MeOH:H₂O (100:15:7.5), EtOAc:*n*-Hex:MeOH (90:5:6, 90:5:5), ACN :H₂O (40:60, 50:50, 60:40, 80:20), MeOH:H₂O (40:60, 50:50, 60:40, 80:20).

Ninhydrin reagent was utilized to detect amines, amino acids, and amino sugars. The procedure was done by spraying ninhydrin solution onto the surface of TLC plates and then exposing them to heat.

Then, the extracts were subjected to an antimicrobial activity screening.

2.2.3.1. Disc Diffusion Assay for Preliminary Screening

Antimicrobial activities of EtOAc extracts were tested via disc diffusion test, using *S. aureus*, *E. coli*, and *C. albicans*. EtOAc extracts were dissolved in 30:70 (EtOAc:MeOH) and loaded onto each blank disk (128 µg/disc), and then they were air-dried. Later, the pathogens were transferred to 0.9 % saline solution with sterile swabs to obtain 0.5 McFarland solution, and the solution was vortexed thoroughly to get a homogeneous solution.

Bacteria were taken with swabs and inoculated onto MHA plates using the spread plate technique, and yeast was inoculated onto MHA with 2 % D-glucose. Air-dried disks were put onto inoculated agar. Afterwards, they were incubated at 37 °C for 18-20 h.⁸⁸

Results were obtained by measuring the diameters of inhibition zones. Kanamycin was used as antibiotic control against the test bacteria while nystatin was used against the test yeast.

2.2.4. Further Studies with 35M1

Among others, an isolate, namely 35M1, was selected for further studies based on its antimicrobial activity, metabolite profile and extract yield.

2.2.4.1. Whole Genome Sequencing (WGS)

First, to isolate the DNA, the selected isolate (35M1) was sporulated on SFM agar for four days at 28 °C. Then, spores were inoculated into 50 mL M1 broth and incubated in the shaker at 28 °C for six days. Suspended colonies in broth were poured into a sterile falcon tube. Then, the sample was centrifugated at 6000 rpm for 5 minutes (min). The supernatant was removed, and the pellet was washed with 1x TE buffer (pH 8). Then, it was centrifugated again with the same conditions.

Later, the obtained pellet was suspended in 200 µL 1x TE buffer containing 25 % sucrose and 30 mg/mL lysozyme. After vortexing, the tube was incubated at 37 °C for 1 h. Subsequently, 370 µL 1x TE buffer with 1 mg/mL proteinase K and 30 µL SDS were added into the tube. Then, it was incubated again at the same conditions. Next, 100 µL 5 M NaCl and 30 µL solution (including 10 % cTAB and 0.7 M NaCl) were added into the same tube. Then, it was incubated for 10 min at 65 °C.

After that, DNA was precipitated with two volumes of ice-cold EtOH and 10 % (v/v) 3 M Sodium acetate. Later, the sample was incubated at -20 °C for 20 min. The centrifugation tube was placed at 14,000 g for 10 min at 4 °C before the pellet was washed with 70 % EtOH. The sample was air-dried and resuspended in 50 µl 1x TE buffer. Gel electrophoresis was performed to ensure dsDNA was isolated successfully.⁸⁹

Whole genome sequencing of 35M1 was done at Gen-Era Diagnostics Inc., Istanbul, Turkey.

BLAST (Basic Local Alignment Search Tool) tools of NCBI and DSMZ were used to analyze sequences, and BGCs were examined utilizing AntiSMASH.⁹⁰⁻⁹²

2.2.4.2. LC-MS/MS Studies

For LC-MS/MS studies, 5 mg of EtOAc extract was weighed and dissolved in 1 mL HPLC-graded MeOH (sample concentration:5000 ppm). Samples were filtered through 0.45 μm pores and transferred to the HPLC vial. Then, the vial was placed into the sample chamber of the Thermo Orbitrap Q-Exactive machine. Two μL samples were injected. Troyasil C18 (150 mm x3 mm, 3.5 μm) column was used. Mobile phases were ultrapure water (phase A) and MeOH (phase B) (**Table 2.4**), containing 1 % formic acid and 0.1 % ammonium formate. The mixtures were applied to gradient changes.

The flow rate and the column temperature were set to 0.35 mL/min and 35 $^{\circ}\text{C}$, respectively. ESI ion-sourced mass detector was used for detection. Scan range was set as m/z 150-2000 for MS. Parameters were set as follows: Gas flow: 45, supporting gas flow: 10, spray voltage: 3.8 kV, capillary temperature: 320 $^{\circ}\text{C}$, S-lens RF value: 50. Results were examined by utilizing Thermo-Scientific FreeStyle Version 1.8 SP2 QF1.

Later, molecular networking and dereplication studies were done using global natural product social molecular networking project (GNPS) database that had enabled comprehensive investigation of natural product metabolomics of the selected isolate.

Table 2.4. Chromatographic analysis method

Time (min)	Phase A (%)	Phase B (%)
0	53	47
35	5	95
58	5	95
62	53	47
70	53	47

2.2.4.3. Determination of the Growth Curve

Growth curve experiments were conducted using dry weight measurement. Fifty mL M1 broth was prepared as described in **Methods 2.1.2**. The isolate, 35M1, was inoculated into separate Erlenmeyer flasks (a total of 20), and two were kept as sterility control with no bacteria. Two Erlenmeyer flasks were retrieved at one-day intervals until the 10th day. Cells were filtered through filter paper (110 mm, Macherey-Nagel) to measure dry weight and washed with distilled water. The collected cells in filter paper were dried at 50 °C overnight. Afterward, they were weighed, and results were noted. Data was analyzed using GraphPad.

2.2.5. Preparative-Scale Fermentation

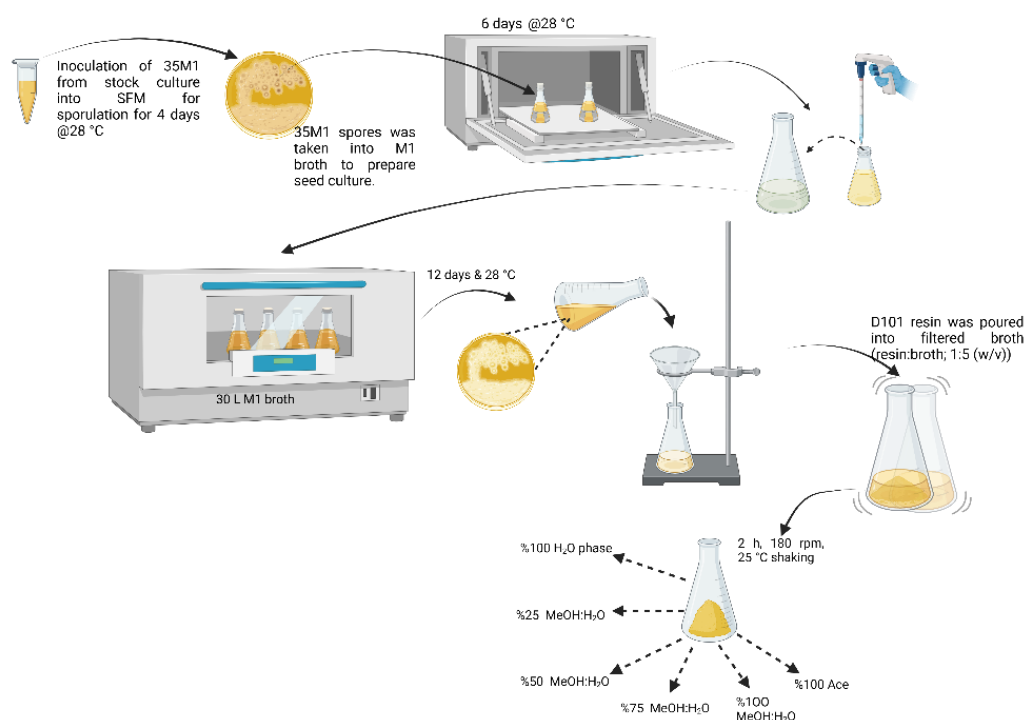


Figure 2.1. Overall preparative-scale fermentation and SPE processes

The 35M1 isolate was inoculated on SFM agar for four days at 28 °C as *Streptomyces* sp. sporulate well on this medium.⁸⁶ Afterward, the spore suspension was prepared in 1.5 L M1 broth and incubated at 28 °C, 150 rpm for six days. Then, the incubated spore culture was inoculated into 2 L of M1 broth in 5 L Erlenmeyer to have 5 % (v/v). Thirty liters of M1 broth was incubated for 12 days at 28 °C, 150 rpm. TLC analyses were performed on the 5th, 7th, 10th, and 12th days to monitor metabolite profiles. At the end of the 12th day, cultures were filtered to remove bacteria from the broth. Then, the purification studies were started with fractionation by D101 resin. Before use, D101 resin was soaked in EtOH and cleansed for 24 h. A gradient of MeOH:H₂O mixtures were used for solid-phase extraction (SPE) studies. D101 resin (1:5, w/v) was mixed with broth to have maximum adsorption of metabolites onto the resin, and this was achieved by shaking the solution for 2 h at 180 rpm. Later, resins were filtered to remove the broth, and the broth was labeled as water fraction. Desorption was conducted by adding MeOH:H₂O (1:3, v/v) mixture into the resin and was shaken at 100 rpm for 2 h. The eluent was labeled as a 25 % MeOH fraction. The fractionation was continued with 50 % and 75 % MeOH, and MeOH, shown in **Figures 2.1** and **2.2**. Then, at the end, the resin was washed with acetone (Ace). Each fraction was dried and weighed. TLC analysis was performed to examine the metabolite profiles of each fraction.

2.2.6. Bioactivity-Guided Isolation

In bioactivity-guided isolation studies, a disc diffusion assay was carried out for each chromatographic step to find fractions with antimicrobial activity (128 µg/disk). Active fractions were used for further chromatography steps (**Figures 2.3** and **2.4**).

The Ace fraction (4.9 g) was used for further studies (**Figure 2.2**). The Ace fraction was subjected to an RP-C18 silica gel (135 g) (**Figure 2.3**). Firstly, the fraction was dissolved in Ace:MeOH and mixed with seven g of RP-C18 to give a slurry. The viscous mixture was dried over Speedvac to afford the fraction adsorbed onto the resin. The column (3x37 cm , 261.53 cm³) was equilibrated with 600 mL of 40 % MeOH, and then dry loading was performed. Subsequently, the column was eluted with MeOH:H₂O mixtures (40:60→75:25, 4 L) to afford 33 main fractions. Upon antimicrobial screening,

the active fractions were selected, and the column chromatography studies were continued (*see Table 3.6*).



Figure 2.2. The evaporation process of D101-Ace fraction



Figure 2.3. Images of the fractionation step

After the overnight cooling step at 4 °C, the vial was centrifuged at 7000 rpm for 5 min. The supernatant was discarded, and precipitates were suspended in distilled water and centrifuged again. Then, the pellet was collected and dissolved in Ace, and TLC was performed to check its purity level. The precipitate was coded as **SG-01** (20 mg) and submitted to spectral analysis.

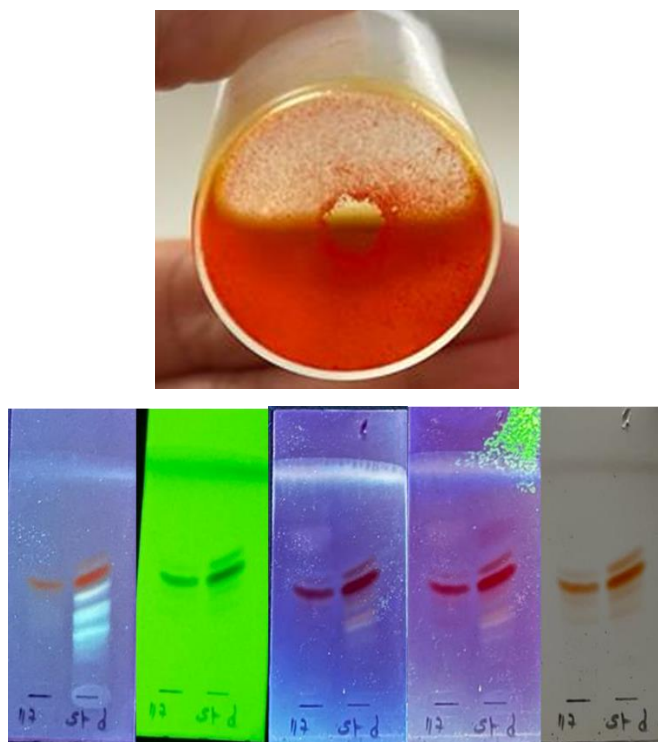


Figure 2.4. **SG-01** precipitate and TLC profile (left band belongs to precipitate, right bands belong to *ACT-RP211123-Fr108-119- Si071223-Fr28-108* subfraction, mobile phase: 90:10 (CHCl₃:MeOH)).

One of the active fractions, *RP2111-Fr32-54* (140.1 mg), was chromatographed over an RP-C18 column (2.4x17 cm, 30 g RP-C18) with MeOH:H₂O (50:50→62.5:37.5, total of 1.6 L) and 13 fractions were collected. Prep-RP-C18-TLC was done on fraction *RP1001-Fr45-49* (11.1 mg) with 80 % MeOH. As a result, **SG-04** (2.5 mg) and **SG-05** (2.6 mg) were obtained. Additionally, **SG-08** (0.8 mg) was isolated from the same TLC, but due to a lower amount, its spectral characterization was not pursued.

Another antimicrobial fraction *ACT-RP2111-Fr122-131* (211.3 mg) was chromatographed over silica gel 60 column (2.3x 28 cm, 40 g silica gel) with EtOAc:*n*-Hex:MeOH (80:20:1; 90:10:1; 90:5:5, total of 1.11 L). Then, a subfraction of the column *ACT2402Si-1801Si-Fr9-19* (51.7 mg) was submitted to a silica gel 60 column (2.4x26 cm, 40 g Silica gel) and eluted with CHCl₃:IPA (98:2→95:5, total of 1 L). To further purify compounds, *ACT3001Si-2402Si-Fr1-60* (44.4 mg) was submitted to a silica gel 60 column (2.4x18 cm, 40 g silica gel) and eluted with CHCl₃:IPA (98:2→97.75:2.25, total of 150 mL) to yield **SG-03** (10.3 mg).

The main fraction, *ACT2601Si-2111RP-Fr92-100* (40 mg), was submitted to a silica gel 60 column (2.4x33 cm, 40 g silica gel) and eluted with EtOAc:*n*-Hex:MeOH (90:5:5; 90:5:6, total of 750 mL) to give **SG-06** (5.5 mg) and **SG-02** (11.5 mg). The main fraction, *2111RP-Fr101-107*, was subjected to a Prep-TLC (silica gel 60) and developed with EtOAc:*n*-Hex:MeOH (90:5:6) solvent system to afford **SG-07** (2.7 mg).

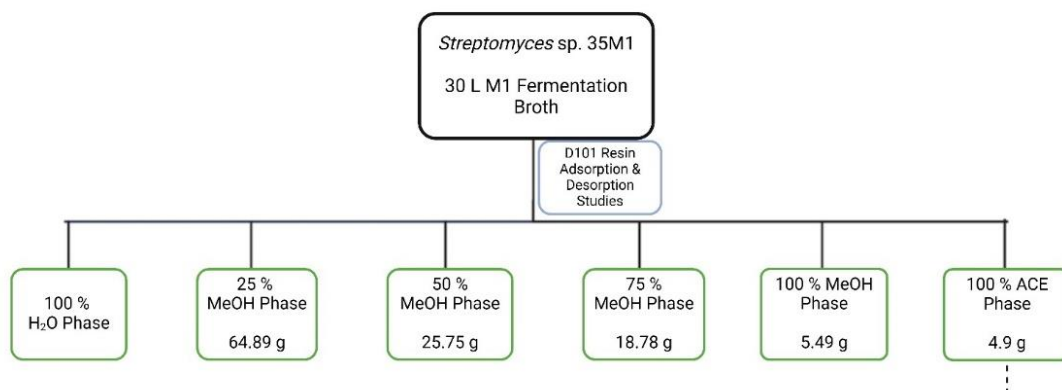


Figure 2.5. Isolation scheme (Part 1)

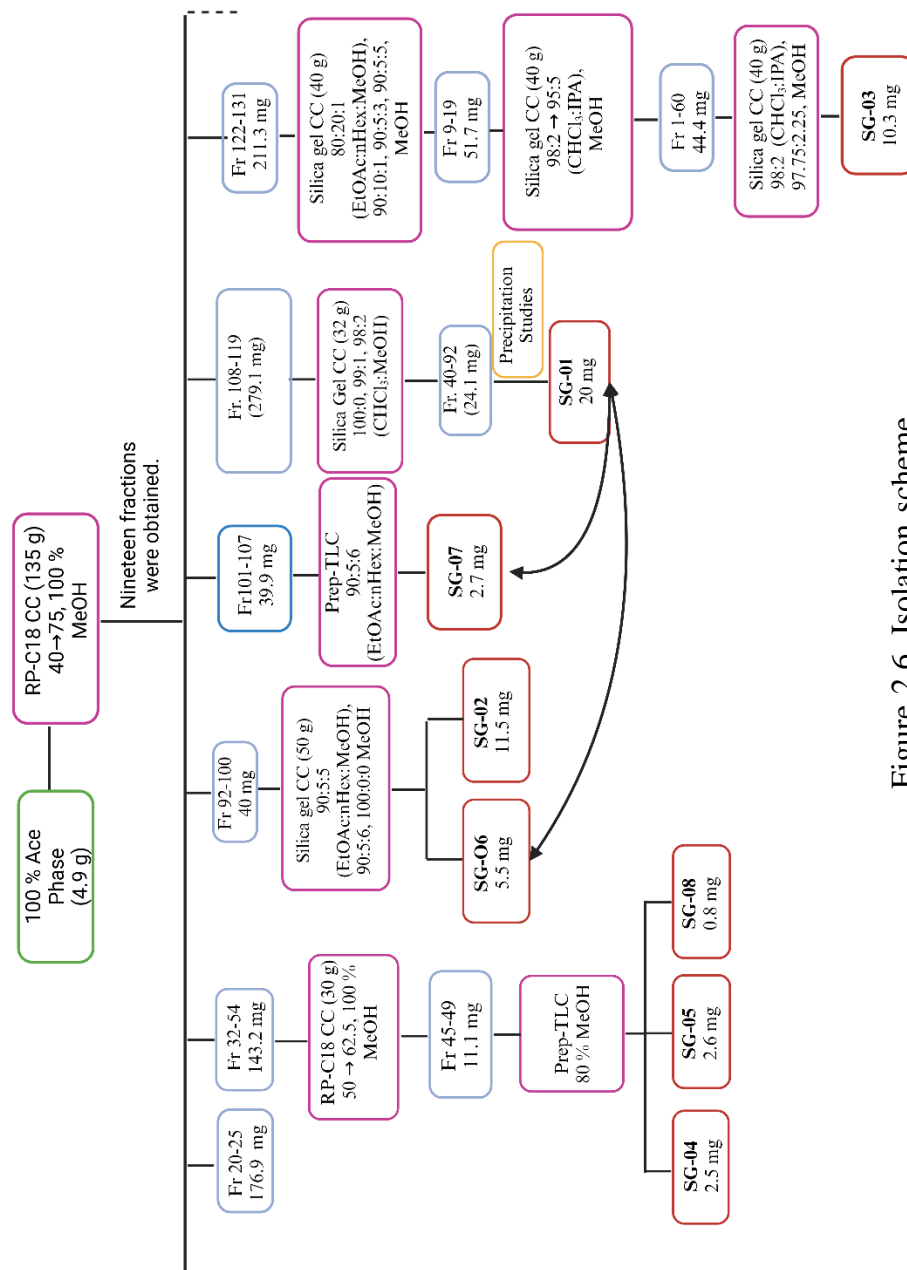


Figure 2.6. Isolation scheme

2.2.7. Bioactivity Analyses

2.2.7.1. MIC Test

Three different bacterial strains (*S. epidermidis*, MRSA and *L. monocytogenes*) were selected to conduct MIC studies. The pathogens were cultured on TSA plates at 37 °C for 24 h before testing, and colonies were picked to achieve a McFarland turbidity standard of 0.5 in 0.9 % saline solution. Afterward, a homogenous mixture was prepared by vortex. CLSI standards were applied for the preparation of antibiotic stock solutions, and the final concentration of DMSO in wells was kept below 2.5 %, which does not impact bacterial growth.^{93, 94} Dilutions in MHB were started from the highest concentration with a ½ concentration decrease at each step, in triplicates. Incubation conditions were set to 35 °C for 24 h. The highest concentrations were selected depending on the literature. MIC results were evaluated by comparing them with known antibiotics. For *C. albicans*, RPMI-1640 w/ 2 % glucose was used to determine MIC values of the compounds and incubation conditions were set to 37 °C for 24 h.¹⁶⁵

Control groups included:

- 1- A solution containing a sample and cell-free medium,
- 2- A solution containing DMSO (2.5 %) and medium without a sample as bacteria growth control (GC),
- 3- A solution without a sample and bacterium-free medium as sterility control (SC).

Five microliters of pathogens were added to each well. The final concentration inside the wells was set to 2.0-5.0x10⁵ CFU/mL. After the end of incubation, OD measurements were taken at 600 nm using a spectrophotometer.⁹⁵

2.2.7.2. Antibiofilm Tests

Antibiofilm studies in this thesis involve two parts. The first study included the biofilm inhibition effect. The second study involves the examination of biofilm

eradication properties of selected compounds. The control groups included were growth control wells and sterility control wells.

2.2.7.2.1. Biofilm Inhibition Assay

In the biofilm inhibition test, 10 % TSB + 0.1 % glucose were used as growth media. Stock solutions of pure compounds and antibiotics were serially diluted in Eppendorf tubes. The compounds were added into respective wells. Then, bacterial suspension was prepared to McFarland 0.5 standard (10^8 CFU/mL) and diluted to obtain $\sim 2.5 \times 10^5$ CFU/mL bacteria for each well. Then well plates were incubated at 35 °C for 18 h. At the end of the incubation period, OD₆₀₀ was recorded. After that, well plates were gently rinsed with distilled water three times to remove planktonic cells. Next, the plates were air-dried, and 100 μ L CV (Crystal Violet) solution was added to each well. They were placed in an orbital shaker and were allowed to shake at 100 rpm for 30 min at room temperature. Then, the CV was discarded and gently rinsed three times with distilled water. Rinsed plates were inverted onto dry paper towels and sharply tapped to remove water. After the air-drying process, crystal violet was solubilized in absolute EtOH, and plates were shaken at 100 rpm for 30 min at room temperature. Absorbance was recorded at 595 nm.⁹⁶

2.2.7.2.2. Biofilm Eradication Assay

Firstly, bacterial suspension was prepared by McFarland 0.5 standard ($\sim 10^8$ CFU/mL). Pure compounds and antibiotics were prepared as concentrated stock solutions. 100 μ L of 10 % TSB + 0.1 % glucose media were distributed into wells. Finally, 5 μ L diluted bacterial solutions were transferred into test wells. Thus, each well is set to have $\sim 2.5 \times 10^5$ CFU/mL concentration. The well plates were incubated at 35 °C for 24 h. At the end of the incubation period, OD₆₀₀ was recorded to check if all inoculated wells had similar growth. Afterward, well plates were gently rinsed three times with sterile growth media to remove planktonic cells. One plate was used for CV staining, and the

other was for TTC (2,3,5-Triphenyl-Tetrazolium Chloride). These two plates were replicates of each other at first. After all liquid remained in wells gently pipetted, the next step was taken. To the TTC plate, 2 μL of 5 % (w/v) TTC solution was added, and the final concentration of TTC in wells was set to 0.05 % (w/v). Wells had 100 μL final volume, including dilutions of compounds being tested. Control groups involved sterility controls and growth controls. Later, all plates were incubated for 18 h at 35 °C. After the incubation period, OD₆₀₀ was recorded. Then, the plates were rinsed with distilled water and inverted on dry paper to remove the remaining water. 200 μL CV solution was added to the CV plates and shaken at 100 rpm for 30 min at room temperature. At the same time, 200 μL of DMSO was added to each well of TTC staining plates to solubilize TTC dye and incubated for 30 min at 100 rpm. After 30 min, the crystal violet stain was discarded and rinsed with distilled water. Then 200 μL absolute EtOH was added to each well to solubilize CV. TTC plates were read at an absorbance of 500 nm (A_{500}), and CV plates were read at 595 nm (A_{595}) using a spectrophotometer.⁹⁶

2.2.7.3. Synergistic Activity Assay

In 2017, the World Health Organization (WHO) released a list of antibiotic-resistant priority pathogens that pose significant threats to human health and urgently require new antibiotics. Most pathogens on the WHO list are Gram-negative, more resistant than Gram-positive, due to their unique structure, leading to significant global morbidity and mortality.⁹⁷ For this reason, *E. coli* was selected to conduct synergistic activity tests.

The synergy studies were conducted using the checkerboard assay. Collismycins were not included here, as their isolated dry weights were not enough to conduct a synergism test. Thus, pure Actinomycin derivatives were combined with Ampicillin, Rifampicin and Nalidixic acid. Stock solutions of each drug were prepared, followed by serial dilutions of two-fold MIC to perform a Checkerboard test. MHB was used as the growth medium. From the antibiotic stock solution, 200 μL was added to the wells in Columns A-G, and a $\frac{1}{2}$ dilution was performed in each subsequent column, as described in Bellio et al. (2021).⁹⁸ Row 12 received two-fold the highest concentration. Then, test compounds were put into the rows 2-12. At the end of the dilution procedure, 5 μL diluted

bacterial solutions ($\sim 2\text{-}5 \times 10^5$ CFU/mL) were put into test wells. The microplates were placed in an incubator at 35 °C for 18 h. OD measurements were taken at 600 nm using a microplate reader.

The MIC was calculated for each combination from the obtained data (the lowest concentration reducing pathogen growth by more than 80 % was selected). Additionally, FICI values were calculated using the formula given in **Section 2.2.8**.⁹⁸

2.2.8. Data Analysis

For MIC and antibiofilm experiments:

Graphs were drawn, and p values were calculated by using GraphPad.

The average absorbance for all growth control wells within each microtiter plate was calculated for bacterial growth (600 nm) and CV-stained biomass (A_{595}). The average absorbance values of 100 % bacterial growth (GC_{OD600}) and biofilm (GC_{A595}) occurrence were used during calculations. The mean absorbance for all sterility control wells in each microtiter plate was computed for 0 % bacterial growth (SC_{OD600}), biofilm (SC_{A595}), and TTC (SC_{A500}) as the baseline.

The percentage of bacterial growth for each treatment condition was determined using the following equation: $\text{Bacterial growth (\%)} = 100 \times (\text{Sample}_{OD600} - SC_{OD600}) / (GC_{OD600} - SC_{OD600})$.

The percentage of biofilm growth for each treatment condition was computed using $\text{Biofilm occurrence (\%)} = 100 \times (\text{Sample}_{A595} - SC_{A595}) / (GC_{A595} - SC_{A595})$.

Lastly, the percentage of biofilm metabolism for each treatment condition was assessed with the formula: $\text{Biofilm metabolism (\%)} = 100 \times (\text{Sample}_{A500} - SC_{A500}) / (GC_{A500} - SC_{A500})$.⁹⁶

Sample absorbance values were only compared with the growth and sterility control samples within the same microtiter plate. Percentages of biofilm growth and metabolism were plotted as a function of concentration for each antibiofilm compound of interest to generate dose-effect curves.

For synergy experiments:

The Fractional Inhibitory Concentration Index (FICI) is calculated using the formula $FICI = (MIC_{AB}/MIC_A) + (MIC_{BA}/MIC_B)$, where MIC_{AB} represents the minimum

inhibitory concentration (MIC) of drug A when used in combination, MIC_A is the MIC of drug A when used alone, MIC_{BA} is the MIC of drug B in combination, and MIC_B is the MIC of drug B when used alone.

The FICI demonstrates that paired combinations of agents can have inhibitory effects greater than the sum of their individual effects (strong synergism; $FICI \leq 0.5$) or less than the sum of their individual effects (strong antagonism; $FICI > 4.0$).^{98-100, 162}

FICI, in theory, uses Loewe additivity, which does not include an "indifference" category since interactions are categorized as either additive or non-additive (synergistic or antagonistic). The term indifference was used instead of additivity only when one drug is inactive, as there is no effect from an inactive drug to add, leaving only the effect of the active drug according to the literature.¹⁰¹

CompuSyn was used to create combination index plots.

CHAPTER 3

RESULTS AND DISCUSSION

3.1. Isolation and Characterization of Isolates

Sediment samples were collected in gamma-sterilized 50 mL plastic Falcon tubes and transported to the laboratory as quickly as possible in a cold chain. In continuation, all sediment samples were used directly without pre-treatment. Nystatin (50 µg/mL) was added to the media to inhibit fungal growth, and Nalidixic acid (20 µg/mL) was used to suppress rapidly growing Gram-negative bacteria.¹⁰²

Despite the addition of Nalidixic acid and Nystatin to the isolation media in purification, bacterial and fungal contaminations in some plates could not be achieved, especially against *Bacillus* species. The slower growth of Actinobacteria compared to these organisms also contributes to contamination.

Consequently, several actinomycete colonies could not be retrieved from the isolation plates, and isolates that failed to grow successfully during passages for purification were disregarded.

Additionally, some isolates showed no growth during the purification stages and were also excluded from the study.

To avoid isolating identical strains, colonies grown on isolation plates were morphologically and microscopically evaluated, and those identified as different were used for further studies (**Figure 3.1**).

In the scope of this thesis, *Streptomyces* species were aimed to be isolated. For this purpose, characterization of the isolates was done based on colony morphologies (**Figure 3.2**) and microscopy images.

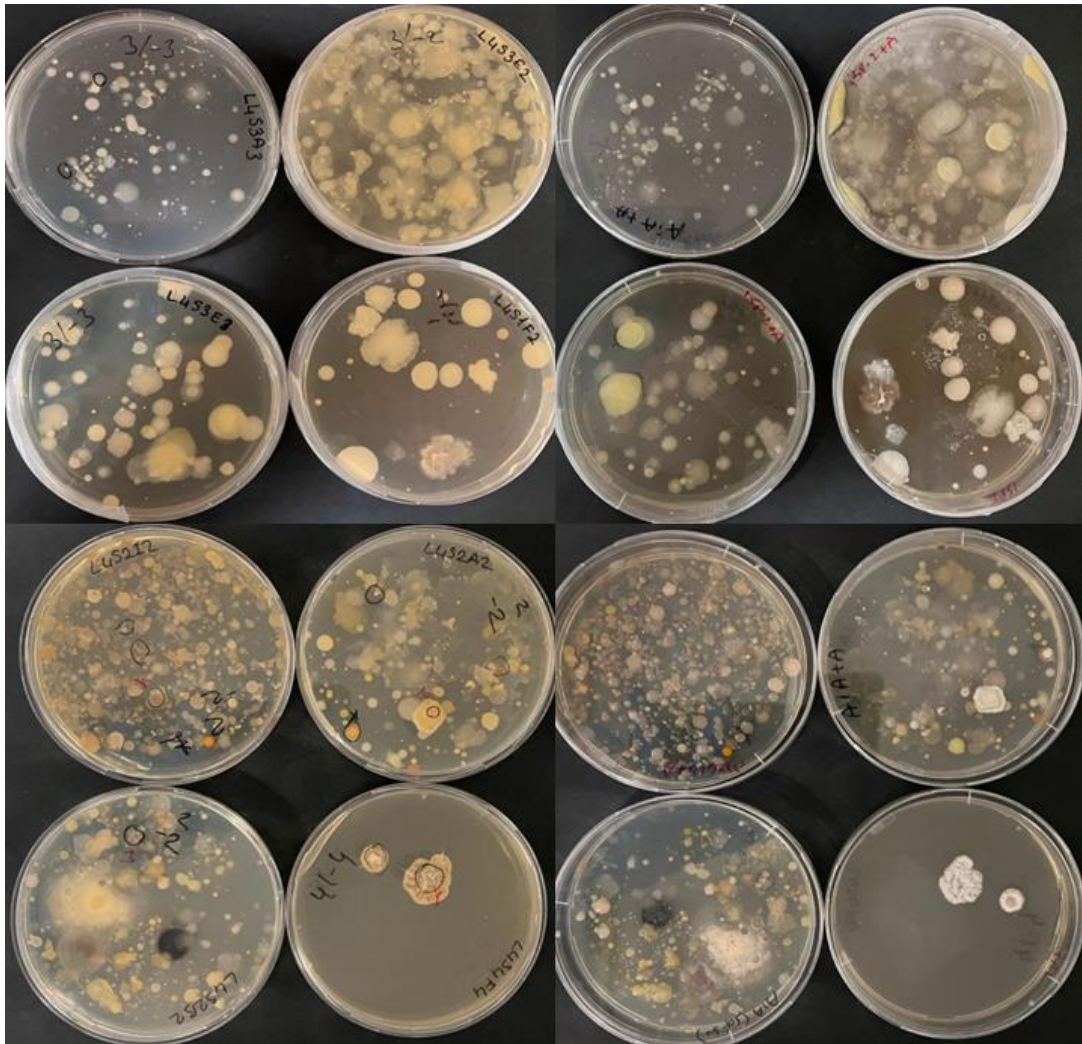


Figure 3.1. Examples of spread plate technique incubation results

In the case of colony morphologies, all selected colonies had chalky surfaces with aerial spores, and some produced diffusible pigments, as seen in the surrounding agar medium. According to the color classification system outlined in the Bergey's Manual of Determinative Bacteriology¹⁰³, and category IV of the Bergey's Manual of Systematic Bacteriology¹⁰⁴, the color of isolates was sorted into the subsequent categories as gray, white, red, yellow, green, blue, and black. White and brown were detected to be the most prevalent shades seen in this thesis. All of them had an earthy odor.



Figure 3.2. Examples of the isolated *Streptomyces* suspected cultures on SFM agar

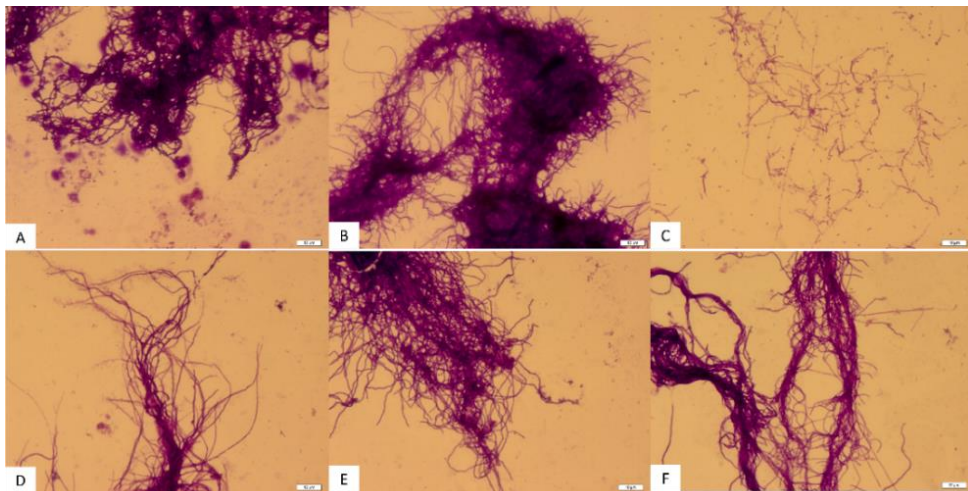


Figure 3.3. Microscope images of the selected isolates: A)3414, B)3121, C)35M1, D) 3515, E) 3311, F) 5-A-1 at 100x magnification.

Additional identification was based on the gram staining method as *Streptomyces* species are gram-positive. For this reason, samples were observed under a light microscope at 100x magnification. Specifically, those with spore chains in flexuous or straight forms were used as markers. According to the literature, multicellular and filamentous forms that produced branching vegetative hyphae were characteristics of these species.¹⁰⁵

After the microscope images were examined, some of them were suspected as *Streptomyces* sp., as shown in **Figure 3.3**. It was observed that all except C (35M1) had strong hairy filaments, and spores cannot be discriminated clearly. 35M1 was observed to have oval-shaped spores around tiny filaments.

3.2. Analytical-Scale Fermentation

One of the main goals of our study was to perform small-scale fermentations in liquid media using the twelve purified *Streptomyces* sp.

After incubation, broths were examined because *Streptomyces* sp., unlike many bacteria, do not cause cloudiness in the fermentation broth; instead, they grow in small pellets. Additionally, it was observed that *Streptomyces* sp., requiring a significant amount of O₂, grew along the walls of the Erlenmeyer flasks and formed chalky layers on the surface after sporulation. Samples showing cloudiness in the fermentation broth were presumed to be contaminated and were not included in further studies. Instead, the experiment was repeated. Thus, at the end of incubation, shown in **Figure 3.4**, contaminant-free fermentation broths proceeded to liquid-liquid extraction (LLE) studies. In LLE experiments, EtOAc was selected. After the extraction process, the extracts were chromatographed on silica plates to monitor their metabolite diversity. TLC profiles of the isolates are shown in **Figures 3.5** and **3.6**. Later, the extracts were taken into antimicrobial activity screening tests using the disc diffusion method.



Figure 3.4. Fermentation broths after the incubation

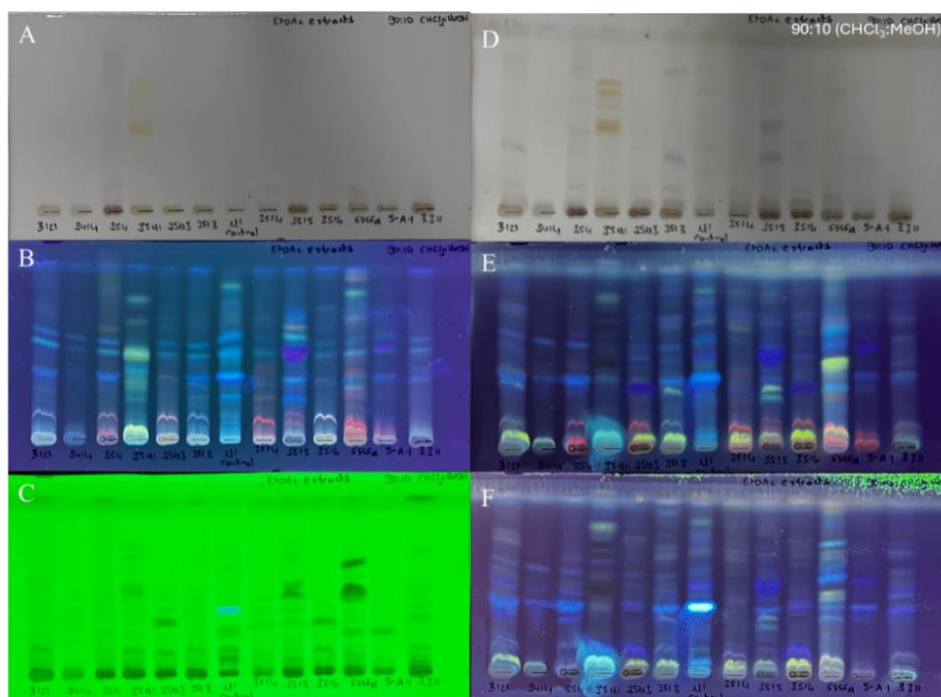


Figure 3.5. TLC profiles of the isolates with 90:10 (CHCl_3 :MeOH) system; Before H_2SO_4 treatment, A) under sunlight, B) under 364 nm, C) under 254 nm, After H_2SO_4 treatment, D) under sunlight, E) under 364 nm, F) under 254 nm.

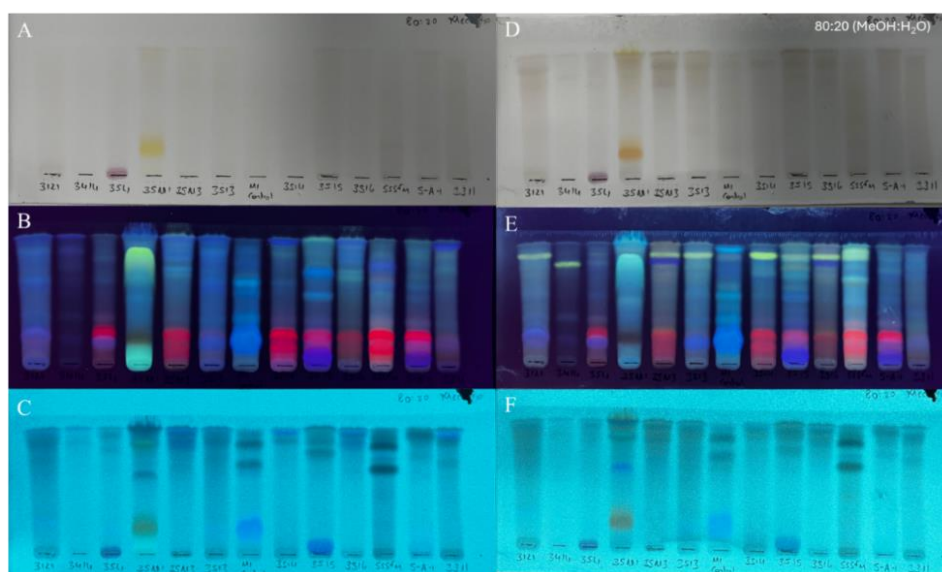


Figure 3.6. TLC profiles of the isolates with 80:20 (MeOH:H₂O) system; Before H₂SO₄ treatment, A) under sunlight, B) under 364 nm, C) under 254 nm, After H₂SO₄ treatment, D) under sunlight, E) under 364 nm, F) under 254 nm.

3.2.1. Antimicrobial Activity of Isolates

Out of 12 isolates, activity against at least one test pathogen was detected for eight extracts, representing 66 % overall, as shown in **Table 3.1**. Four out of them had > 20 mm zone diameter against *S. aureus*, showing high susceptibility. Against *C. albicans*, two isolates showed moderate activity while one with *E. coli* activity.

There are reasons why gram-negative bacteria have lower susceptibility to certain antibiotics compared to gram-positive bacteria.

One reason is their physiological differences. Gram-negative bacteria have an outer membrane (OM) that makes them resistant to various antibiotics such as β -lactams and quinolones. The OM is a complex structure consisting of phospholipids, lipopolysaccharides (LPS), lipoproteins, and β -barrel porins, which form a barrier to unknown compounds, including host defense molecules and antibiotics. The inner leaflet of the OM is composed of phospholipids, while the outer leaflet is densely packed with LPS, stabilized by Mg^{2+}/Ca^{2+} ions. ¹⁰⁶⁻¹⁰⁸

LPS contains the glucosamine-based glycolipid lipid A and tightly packed saturated fatty acid chains that maintain low membrane fluidity, restricting the permeation of hydrophobic compounds. The core and O-antigen oligosaccharides in the LPS of wild-type bacterial strains are crucial for microbial virulence, protecting bacteria from antibiotics and complement-mediated lysis. Additionally, β -barrel protein channels known as porins act as size exclusion channels, allowing small hydrophilic molecules like nutrients to diffuse into the periplasm while blocking large and/or hydrophobic molecules, including several antibiotics.¹⁰⁶⁻¹⁰⁸

Therefore, gram negatives are naturally resistant to certain antibiotics like one of the most prescribed drug classes, β -lactams. In addition, gram negatives can easily create resistance, making them hard to treat in the case of infections.¹⁰⁸

Table 3.1. Results of disc diffusion test together with dry weights of extracts from analytical-scale fermentation study

Isolate Codes / Test Organisms	Dry Weights (mg)	<i>S. aureus</i>	<i>E. coli</i>	<i>C. albicans</i>
3514	3.6	0 mm	0 mm	0 mm
3121	6.1	13 mm	0 mm	0 mm
3515	6.1	0 mm	0 mm	19 mm
3311	2.8	26 mm	0 mm	0 mm
3516	2.32	9 mm	0 mm	0 mm
3414	5.4	25 mm	12 mm	0 mm
354	7.6	9 mm	0 mm	0 mm

Cont. on next page

Table 3.1. (Cont.)

Isolate Codes / Test Organisms	Dry Weights (mg)	<i>S. aureus</i>	<i>E. coli</i>	<i>C. albicans</i>
35M1	9.2	26 mm	0 mm	14 mm
35M3	5.6	0 mm	0 mm	0 mm
55SFM	0.5	0 mm	0 mm	0 mm
5-A-1	2.9	0 mm	0 mm	0 mm
3513	2	27 mm	0 mm	0 mm
Kanamycin	ND	26 mm	24 mm	ND
Nystatin	ND	ND	ND	20 mm

ND: Not determined

3.2.2. Selection of an Isolate

For the selection of an organism for bioassay-guided isolation studies, we prioritized high antimicrobial activity, particularly against a greater number of test microorganisms, metabolite profiles on TLC, and yield of dry weights per volume of fermentation broth. Hence, isolates 3414 and 35M1, having activity against at least two pathogens, were candidates (**Table 3.1**). As 3414 had a 25 mm zone of inhibition against *S. aureus* and a 12 mm zone against *E. coli*, while 35M1 had 26 mm and 14 mm inhibition zones, respectively. Meanwhile, the TLC results were examined to see the richness of metabolite profiles. The isolate 35M1 exhibited a richer metabolite profile than 3414 (**Figures 3.5** and **3.6**). Another point taken into consideration was the yields of dry weight

per 50 mL fermentation broth. While the isolate 3414 afforded 5.4 mg, 35M1 yielded 9.2 mg dry weight.

Consequently, the isolate 35M1 was chosen for subsequent studies.

3.3. Successive Studies with 35M1

The colony morphology of 35M1 is shown in **Figure 3.7**.



Figure 3.7. The colony morphology of 35M1 on M1 agar

3.3.1. WGS Analysis

The whole genome sequence belonging to the *Streptomyces* sp. 35M1 has been deposited at DDBJ/ENA/GenBank under the accession JBCLWP000000000. The version described in this thesis is version JBCLWP010000000. NCBI Blast analysis was done on the isolate, and the best three results are shown in **Table 3.2**.

Due to the levels of genome coverage and percent identity, *Streptomyces* sp. 35M1 might be a novel strain, which will be investigated in further studies.

Table 3.2. NCBI Blast results.

Organism	Total Alignment Length	Organism Genome Size	Genome Coverage	Mean Similarity
<i>Streptomyces</i> sp. Tue6075 Complete Genome	5583842	7931832	0.70397	94.92 %
<i>Streptomyces globisporus</i> C-1027 Complete Genome	5791750	7608611	0.76121	93.91 %
<i>Streptomyces</i> sp. S063 Complete Genome	5742684	7614683	0.75416	93.57 %

Later, the data of genome sequence was uploaded to the Type (Strain) Genome Server (TYGS) for comprehensive genome-based taxonomic analysis, and the phylogeny tree obtained from the server is shown in **Figure 3.8**. This analysis incorporated recently introduced methodological updates and features.¹⁰⁹⁻¹¹¹

Delta (δ) statistics in a phylogeny tree allow phylogenetic accuracy assessment in terms of tree-likeness, so the lower the value, accuracy the higher.¹¹² The GDBP tree, based on the whole genome sequence, had a 0.159 δ value on average, showing high accuracy (*see Table 3.3*).

Table 3.3. DSMZ Type (Strain) Genome Server Results

<i>Streptomyces</i> sp. 35M1	DSMZ Type (Strain) Genome Server Results
Data Type	Whole Genome
Distance Formula	D5
Distance Algorithm	GreedyWithTrimming
Percent G + C	71.44-71.87
δ Statistics	0.128-0.195
Genome Size (bp)	7,329,962-8,848,949
Number of Proteins	6,689-7,800
SSU Lengths (bp)	801-1,516

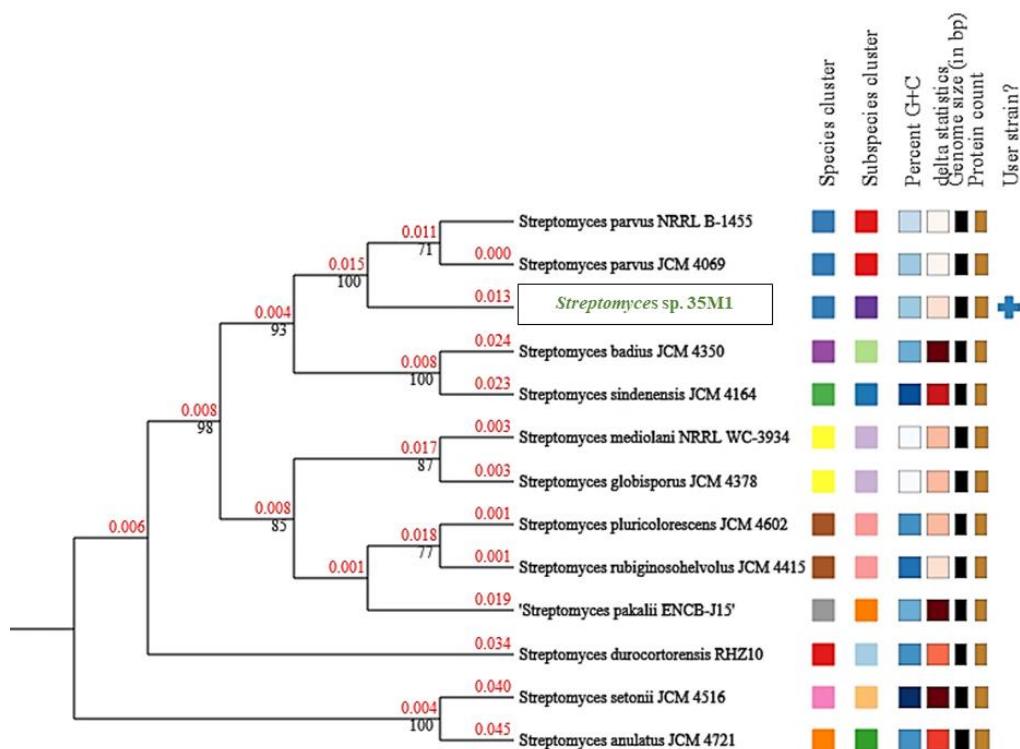


Figure 3.8. The phylogeny tree of 35M1. The tree was constructed using FastME 2.1.6.¹¹⁰ based on Genome BLAST Distance Phylogeny (GBDP) distances derived from genome sequences. Branch lengths are scaled according to the GBDP distance formula D5. Numbers above the branches represent GBDP pseudo-bootstrap support values greater than 60 % from 100 replications, with an average branch support of 83.8 %. The tree was rooted at the midpoint.¹¹¹

3.3.3.1. Analysis of Gene Clusters

BGCs of *Streptomyces* sp. 35M1 were also investigated in this thesis. For this purpose, the gene clusters responsible for secondary metabolite production were determined using AntiSMASH version 7.1.0.⁹²

The whole genome was uploaded to the system and results are given in **Table 3.4**. The genome of *Streptomyces* sp. 35M1 was found to contain genes involved in producing various secondary metabolites such as polyketides, non-ribosomal peptides, siderophores, and terpenes.

Above 70 % similarity, ActD (**1**) (**Figure 3.9**) was found to be produced by *Streptomyces* sp. 35M1, which was also confirmed by LC-MS/MS studies (*see Section 3.4.2*). NRPS pathway produces Actinomycin D, and as part of this thesis, we successfully isolated the compound.

AmfS was found to be coded in the genome with 100 % similarity. It is known as a class III lantipeptide and is a morphogen found in *Streptomyces* species. The Amf gene cluster acts as a positive regulator for initiating the formation of aerial mycelium.¹¹³

The Ravidomycin gene cluster was also found in the genome, which has a 74 % similarity. Its chemical structure is shown in **Figure 3.9 (2)**, produced from the T2PKS pathway. It is an aromatic ether member of phenols with tertiary amine and an acetate ester. It is known to have antibiotic and anticancer properties.¹¹⁴

A similarity of 74 % was found in the gene cluster producing ColA, which was also confirmed by an LC-MS analysis. ColA (**3**, **Figure 3.9**) is produced via NRPS and T1PKS pathways as a hybrid⁴⁴. As part of this thesis, we successfully isolated the compound.¹¹⁵

Streptomyces sp. 35M1 has 100 % potential to produce Geosmin (**6**, **Figure 3.9**). It is a natural bicyclic terpene known for its earthy odor.¹¹⁶

Ectoine (**8**, **Figure 3.9**), an extremolyte derived from bacteria, can protect the membrane and proteins from damage caused by harsh environmental conditions such as heat, UV light, high osmolarity, and dryness.¹¹⁷

Coelichelin (**9**, **Figure 3.9**) is a tetrapeptide hydroxamate siderophore derived from *Streptomyces coelicolor*. It functions as a siderophore.¹¹⁸

Deferoxamine B (DFOB) (**7**, **Figure 3.9**) is a naturally occurring siderophore initially identified in the soil bacterium *Streptomyces pilosus*. Typically, the primary role of siderophores like DFOB is to scavenge Fe(III) from the environment or the host.¹¹⁹ DFOB is marketed under Desferal as a medication that binds to iron and aluminum. It is specifically used for treating iron overdose, hemochromatosis, and aluminum toxicity in patients undergoing dialysis.¹²⁰

2-Methylisoborneol (MIB) (**11**, **Figure 3.9**) is an atypical monoterpene originating from the common monoterpene precursor geranyl pyrophosphate. MIB and the atypical sesquiterpene geosmin are responsible for most taste and odor issues in drinking water worldwide caused by biological factors.¹²¹

Overall, the prediction of some of the secondary metabolites potentially produced by *Streptomyces* sp. 35M1 were overlapped with dereplication results.

Table 3.4. AntiSmash results

Gene Region Type	Most Similar Known Cluster	Similarity
NRPS	Azotobactin D	16 %
NRPS	Actinomycin D (1)	71 %
Lantipeptide Class III	AmfS	100 %
Lantipeptide Class II	Chalcomycin A	9 %
T2PKS	Ravidomycin (2)	74 %
NRPS, T1PKS	Collismycin A (3)	74 %
Hydrogen cyanide	Aborycin	21 %
NRPS	Cinnaeptin	10 %
NRPS-like, T1PKS	Bafilomycin B1 (4)	100 %
T3PKS	Naringenin (5)	100 %
NRPS-like, T1PKS	Caniferolide A-D	10 %
Terpene	Geosmin (6)	100 %

Cont. on next page

Table 3.4. (Cont.)

Gene Region Type	Most Similar Known Cluster	Similarity
Butyrolactone	Coelimycin P1	16 %
Lasso peptide	SRO15-2005	100 %
T1PKS, NRPS-like	Rotihibin A	21 %
NI-siderophore	Deferoxamine B (7)	100 %
Terpene	Steffimycin D	19 %
Ectoine	Ectoine (8)	100 %
Terpene	Hopene	30 %
NRP-metallophore, NRPS	Coelichelin (9)	81 %
HR-T2PKS, RiPP-like, thioamide-NRP, NRPS	Colibrimycin	46 %
Terpene	Hopene	38 %
NRP-metallophore, NRPS	Griseobactin	100 %
Melanin	Melanin (10)	100 %
RiPP-like	Streptamidine	66 %

Cont. on next page

Table 3.4. (Cont.)

Gene Region Type	Most Similar Known Cluster	Similarity
NRPS, NRPS-like	Thiocoraline	21 %
Butyrolactone, ectoine	Showdomycin	47 %
RiPP- like	Tetronasin	3 %
NRPS-like	Nocathiacin	6 %
Terpene	2-methylisoborneol (11)	100 %
T1PKS, NRPS	10-epi-HSAF/10-epi-3-deOH-HSAF	100 %
NRPS, T1PKS	Paulomycin	5 %
NRPS-like, T1PKS	Quinolidomicin A	30 %
T1PKS	Stambomycin A-D	36 %
NI-siderophore	Kinamycin	13 %
T1PKS	Funisamine	20 %
NRPS	Rhizomide A-C (12-14)	100 %

Cont. on next page

Table 3.4. (Cont.)

Gene Region Type	Most Similar Known Cluster	Similarity
T3PKS	Alkylresorcinol	100 %
T1PKS	JBIR-100	33 %
T1PKS	Quinolidomicin A	15 %
T1PKS	Aculeximycin	23 %
T1PKS	Ebelactone A-B	60 %
NRPS	Virginiamycin S1	11 %

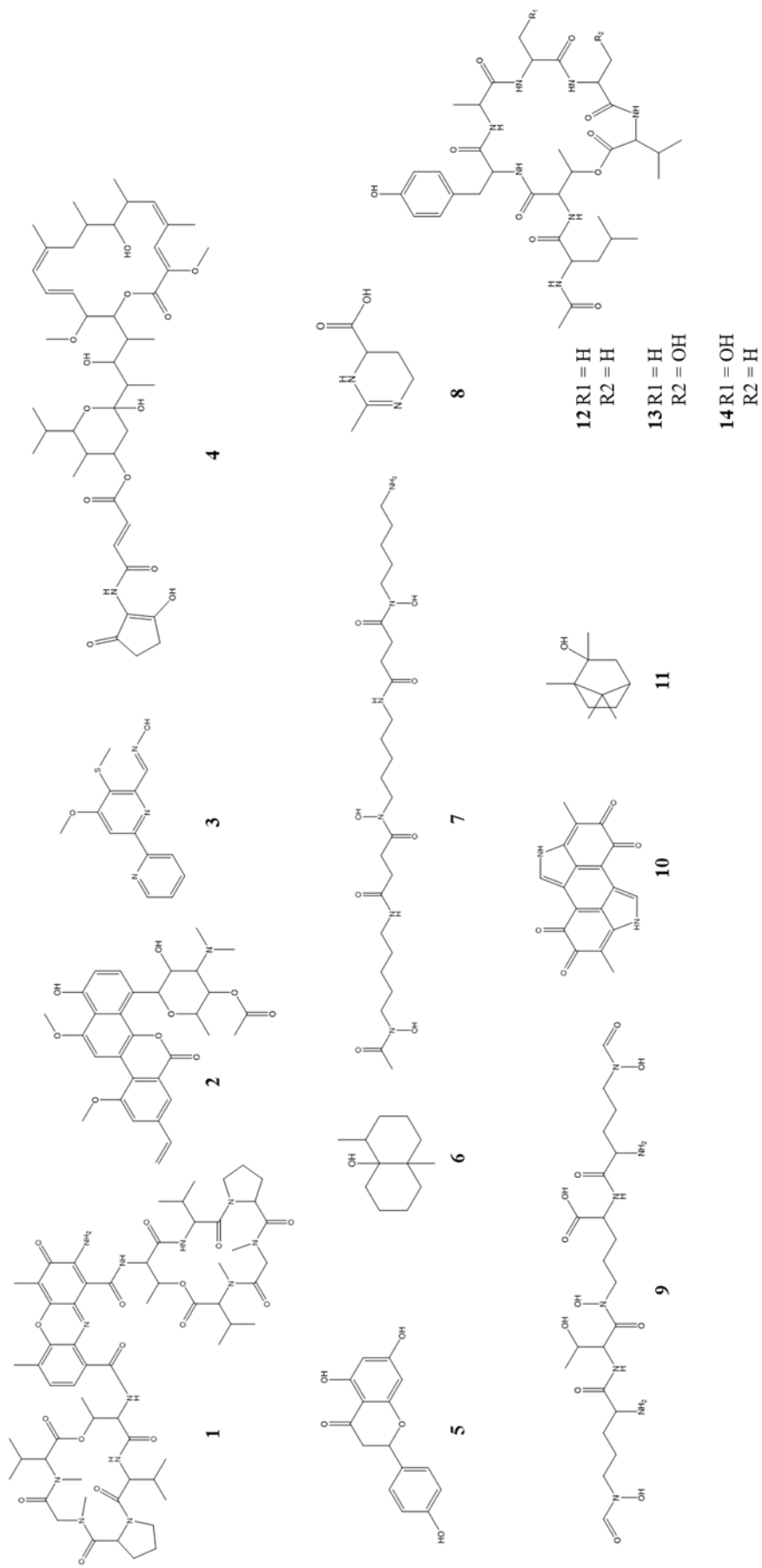


Figure 3.9. The chemical structures of selected compounds from AntiSmash results

3.3.2. Determination of Growth Curve

Determination of the growth curve is crucial to understanding when a microorganism enters its stationary phase, in which secondary metabolites are mainly synthesized. With respect to this, the incubation period for preparative-scale fermentation can be decided. As a result of the study, the highest dry-weight biomass (mg) was achieved during the incubation period of 24 to 48 h, indicating the occurrence of the exponential growth phase. However, after 48 h, the stationary phase began with no notable increase in biomass, as shown in **Figure 3.10**. After the growth curve was examined, it was concluded that the 35M1 isolate reached its stationary phase at 48 h. Additionally, the TLC profiles were examined, as shown in **Figure 3.12**.

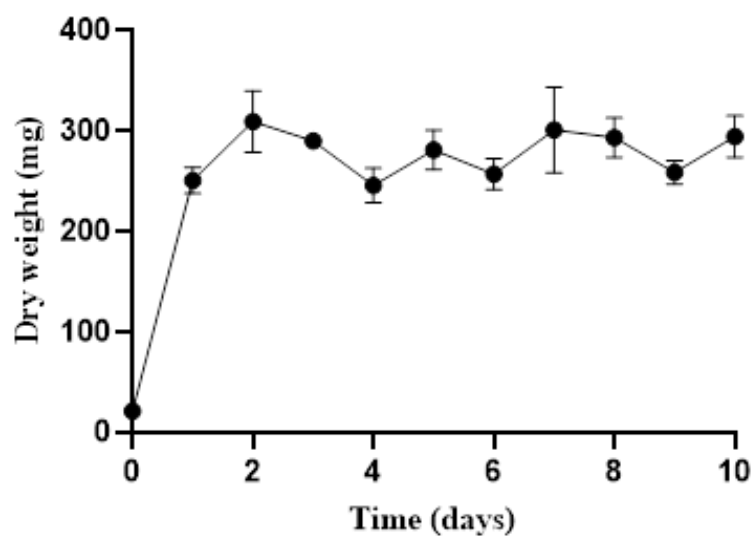


Figure 3.10. The growth curve of *Streptomyces* sp. 35M1. **p*-value (two-tailed): <0,0001

Afterward, EtOAc extraction was performed with the fermentation broths, and it was found that on the 6th day of incubation, there was the highest yield of extract as it reached 22 mg among the daily samples.

Later, a disc diffusion test was carried out with *Streptomyces* sp. 35M1 extracts of each day to understand at which incubation time point antimicrobial activity had its peak.

The test was performed on *S. aureus*, *C. albicans*, and *E. coli*, and the results are shown in **Figure 3.11**. There was no significant change in zone diameters against *S. aureus* from day 2 to day 10, as zones were about 26 mm. This shows that *Streptomyces* sp. 35M1 has produced the active compound/s starting from day 2.

Regarding *C. albicans*, the maximum activity was 12 mm zone on day 2. However, there was a slight decrease in zone diameters in the following days. For *E. coli*, the highest zone diameter reached was also 12 mm. Overall, gram-negative *E. coli* and yeast *C. albicans* had weak susceptibilities against the extract.

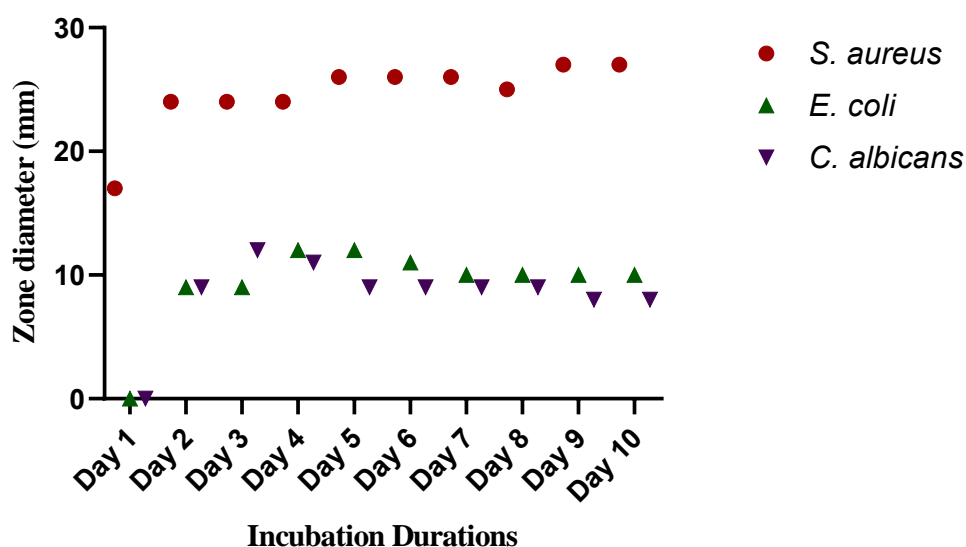


Figure 3.11. Antimicrobial disc diffusion results of *Streptomyces* sp. 35M1 extract concerning incubation times

With respect to **Figures 3.10- 3.12**, there was no significant difference between TLC metabolite profiles after day 2, which was also compatible with no significant change in bioactivity between days 2 and 10.

As a result, 8 days of incubation time for preparative-scale studies was decided (**Section 3.4**) because it corresponds to the mid-to-late stationary phase, during which secondary metabolite production peaked and bioactivity was stable.

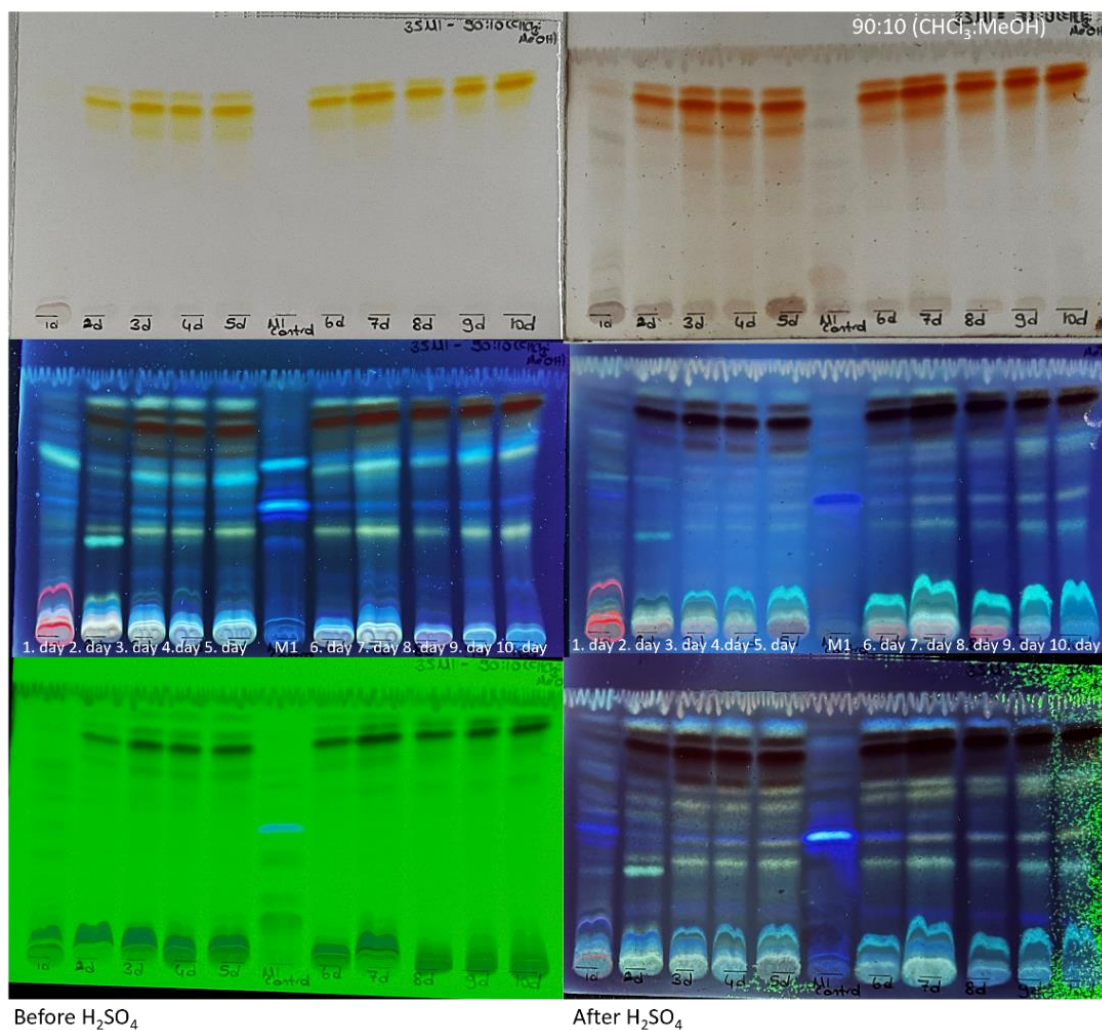


Figure 3.12. EtOAc extract TLC profiles of daily fermentation samples

3.4. Preparative-Scale Studies

Preparative-scale fermentation was conducted with *Streptomyces* sp. 35M1 at 30 L scale. As mentioned before, the M1 medium was used in preparative-scale studies relying on the literature⁸⁷ as a suitable medium for secondary metabolite production.

During the preparative-scale fermentation, samples from the broth were taken during the incubation period shown in **Figure 3.13**. Then, they were subjected to bioactivity and TLC studies to compare the data with analytical-scale results. When the TLC profile and bioactivities matched with day 8 of the analytical scale, the fermentation

was terminated by filtration. After filtration to remove bacterial biomass, SPE was performed for 30 L fermentation broth.

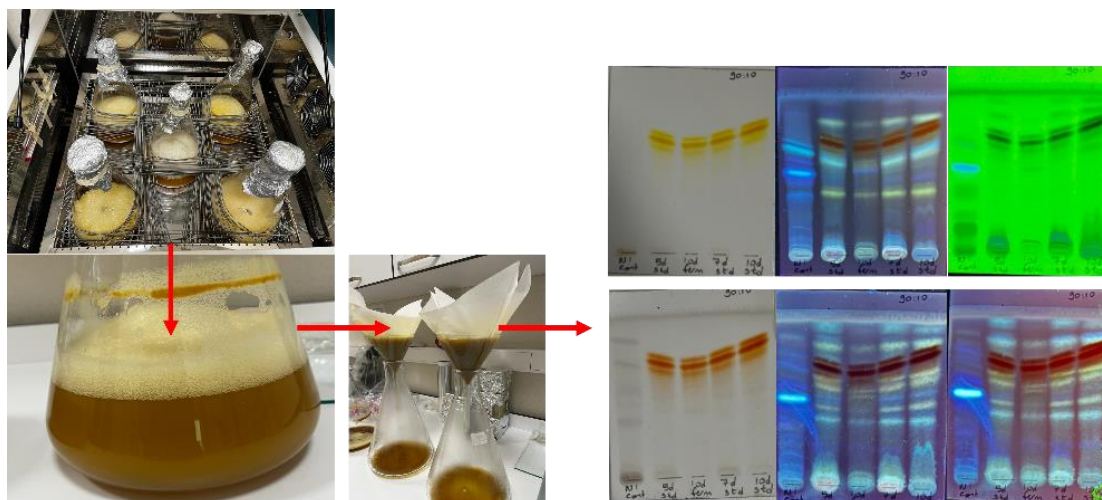


Figure 3.13. Depiction of the preparative-scale fermentation endpoint and TLC profiles of specific days for comparison with the analytical scale.

As mentioned, LLE was used for analytical-scale fermentation, but SPE was selected to extract secondary metabolites for the preparative-scale fermentation study. It is chosen because SPE has certain advantages over LLE for preparative-scale studies. SPE is simpler than LLE because separating a liquid from a solid is more manageable than separating two immiscible liquids which sometimes form stable emulsions difficult to break. Moreover, if the volume to be handled in the LLE process is high, SPE becomes a reasonable option. As well, the adsorbent in SPE provides a higher surface area, providing more efficient extraction. Therefore, SPE over LLE is more advantageous due to lower solvent usage, increased extraction efficiency, decreased evaporation volume, less complex extract profiles, higher selectivity, more straightforward automation, and avoidance of emulsion formation.¹²²

Consequently, SPE was preferred for preparative-scale studies, and D101, a cationic exchange resin with a matrix structure of crosslinked polystyrene, was chosen as the stationary phase. D101 is a reasonable choice used in natural product chemistry

studies, offering microporous adsorption, a cost-effective option, and easy preprocessing for preparative scale production.¹⁶³

Thus, D101 resin was used to fractionate fermentation broth with varied solvent mixtures (100 % H₂O, 25-100 % MeOH and 100 % Ace). Following evaporation of the fractions in the rotary evaporator, dry weights were determined as 64.89 g (25 % MeOH:H₂O), 25.75 g (50 %), 18.94 g (75 %), 5.49 g (100 % MeOH), and 4.9 g (100 % Ace), shown in **Figure 3.14**.

Table 3.5. Disc diffusion results of fractions from SPE. *Control 1 describes LLE extraction of fermentation broth with EtOAc.

Fractions from SPE	<i>S. aureus</i>	<i>E. coli</i>	<i>C. albicans</i>
100 % Ace	22 mm	0	11 mm
100 % MeOH	16 mm	0	0
75 % MeOH	9 mm	0	0
50 % MeOH	0	0	0
25 % MeOH	0	0	0
100 % H ₂ O	0	0	0
Kanamycin	20 mm	24 mm	32 mm
Control 1*	25 mm	0	13 mm

Later, disc diffusion assay and TLC analysis were performed on five main fractions. Ace fraction had the highest activities among other fractions as it had a 22 mm zone of inhibition against *S. aureus* while 0 mm and 11 mm against *E. coli* and *C. albicans*, as shown in **Table 3.5**.

MeOH:H₂O fractions showed lower activity. Water fraction exhibited no antimicrobial activity.



Figure 3.14. Depiction of dry forms of fractions from left to right 25 % MeOH:H₂O, 50 %, 75 %, 100 % MeOH and 100 % Ace.

Table 3.6. The zone of inhibition (mm) from disc diffusion tests of the main column (*ACT-RP2111*) fractions against *S. aureus*, *E. coli* and *C. albicans*. Standard: D101-Ace extract, Positive Control: Kanamycin for bacteria and Nystatin for yeast.

Fractions/ Pathogens	<i>S. aureus</i>	<i>E. coli</i>	<i>C. albicans</i>
Fr 1-5	0	0	0
Fr 6-11	0	0	0
Fr 12-19	0	0	0
Fr 20-25	12	0	0
Fr 26-31	0	0	0
Fr 32-54	11	13	13
Fr 55-67	0	0	0
Fr 68-74	0	0	0
Fr 75-88	15	0	11
Fr 89-91	23	0	15
Fr 92-100	26	0	0
Fr 101-107	30	0	0
Fr 108-119	30	12	14
Fr 120-121	30	12	14
Fr 122-131	31	12	14
Fr 132-144	24	0	0
Fr 145-149	16	0	0
Fr 150-155	8	0	0
Fr 156-159	8	0	0
Crude Ace Fr	25	0	9
Positive control	25	23	28

3.4.1. Structure Elucidation of Isolated Compounds

The chemical structures of the purified compounds were determined by spectral methods (1D- and 2D-NMR). Five molecules (**SG-01**, **SG-02**, **SG-03**, **SG-04**, and **SG-05**) were established interpreting their spectra as well as comparing their data with those of previously reported molecules.

3.4.1.1. SG-01

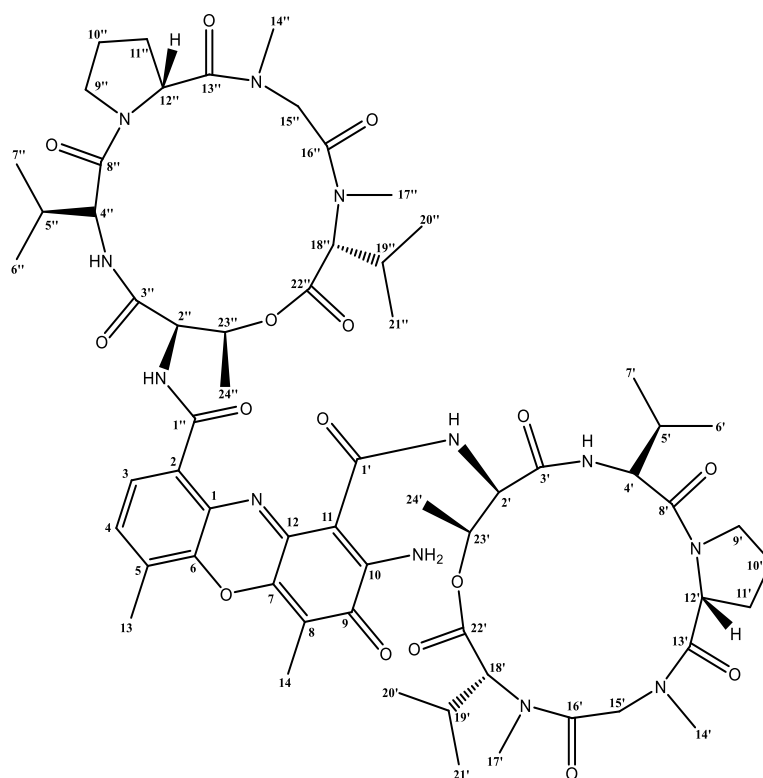


Figure 3.15. The chemical structure of **SG-01**.

The chemical structure of **SG-01** (Figure 3.15) was determined by interpreting ^1H , ^{13}C and 2D-NMR (COSY, HMQC, and HMBC) spectra (Figures 3.16-21, Table 3.7). These analyses revealed that **SG-01** was a chromopeptide from the Actinomycin group.

Spectral data comparison with the literature unambiguously established the structure as Actinomycin D (ActD).¹²⁴⁻¹²⁶

ActD is a natural chromopeptide that has two cyclic pentapeptide lactone rings and a heterocyclic chromophore. The heterocyclic component is a phenoxazine derivative with a quinonimine segment, which gives the compound its color and intercalative properties. It is the most thoroughly researched member of chromopeptide family originating from Actinobacteria and is notable for its antineoplastic properties. Its biological activity is linked to its ability to form intercalation complexes with DNA, inhibiting DNA-dependent RNA synthesis. For the DNA-Actinomycin complex to form, specific structural features of the Actinomycin molecule, such as the integrity of both lactone rings, are essential.^{31, 32, 125}

However, its use in patients is significantly restricted due to high systemic toxicity, which comes from a lack of metabolism, poor urinary and fecal elimination, and subsequent accumulation in the nucleated cells of host tissues.¹²⁷⁻¹²⁹

Table 3.7. ¹H and ¹³C NMR spectroscopic data of **SG-01** (ActD)^a (CDCl₃, ¹H: 400 MHz, ¹³C:100 MHz)

Position	δ_C (ppm)	δ_H (ppm), (J in Hz)
1	129.2 s	-
2	132.8 s	-
3	125.9 d	7.63 d (7.8)
4	130.4 d	7.36 d (7.8)
5	127.8 s	-
6	140.6 s	-
7	145.2 s	-
8	113.7 s	-
9	179.3 s	-
10	147.7 s	-
11	101.8 s	-
12	146.0 s	-
13	15.2 q	2.56 s
14	7.9 q	2.24 s

Cont. on next page

Table 3.7. (Cont.)

Position	δ_C (ppm)	δ_H (ppm), (J in Hz)
1'	166.4 s	-
NH-2'		7.14 d (6.9)
2'	55.4 d	4.49 dd (6.9, 2.5)
3'	168.6 s	-
NH-4'		8.15 d (6.0)
4'	59.0 d	3.53 dd (10.5, 6.0)
5'	31.7 d	2.20 ^b
6'	19.1 q	1.12 d (6.7)
7'	19.4 q	0.88 d (6.7)
8'	173.4 s	-
9'	47.5 t	3.96 td (10.6, 6.7); 3.71 ^b
10'	23.2 t	2.26 ^b ; 2.06 ^b
11'	31.1 t	2.66 ^b ; 1.78 ^b
12'	56.4 d	6.01 d (9.1)
13'	173.4 s	-
14'	35.0 q	2.87 s
15'	51.5 t	4.72 d (17.5); 3.63 d (17.5)
16'	166.5 s	-
17'	39.4 q	2.93 s
18'	71.6 d	2.66 ^b
19'	27.0 d	2.64 ^b
20'	19.2 q	0.73 d (6.7)
21'	21.7 q	0.94 d (6.7)
22'	167.7 s	-
23'	75.1 d	5.20 dd (6.3, 2.5)
24'	17.5 q	1.25 d (6.3)
1''	166.6 s	-
NH-2''		7.75 d (6.5)
2''	55.0 d	4.61 dd (6.5, 2.4)
3''	169.1 s	-
NH-4''		7.98 d (6.2)

Cont. on next page

Table 3.7 (Cont.)

4''	58.9 d	3.56 dd (10.5, 6.2)
5''	32.0 d	2.14 ^b
6''	19.2 q	1.11 d (6.7)
7''	19.4 q	0.90 d (6.7)
8''	173.9 s	-
9''	47.7 t	3.81 td (11.4, 7.0); 3.73 ^b
10''	23.0 t	2.26 ^b ; 2.08 ^b
11''	31.4 t	2.94 ^b ; 1.88 ^b
12''	56.6 d	5.94 d (9.1)
13''	173.5 s	-
14''	35.1 q	2.87 s
15''	51.5 t	4.81 d (17.5); 3.61 d (17.5)
16''	166.6 s	-
17''	39.3 q	2.90 s
18''	71.4 d	2.68 ^b
19''	27.1 d	2.62 ^b
20''	19.2 q	0.73 d (6.7)
21''	21.8 q	0.96 d (6.7)
22''	167.8 s	-
23''	75.2 d	5.16 dd (6.4, 2.4)
24''	17.9 q	1.24 d (6.4)

a) Assignments are confirmed by 2D-COSY, HSQC, HMBC experiments.

b) The signal pattern was unclear due to overlapping.

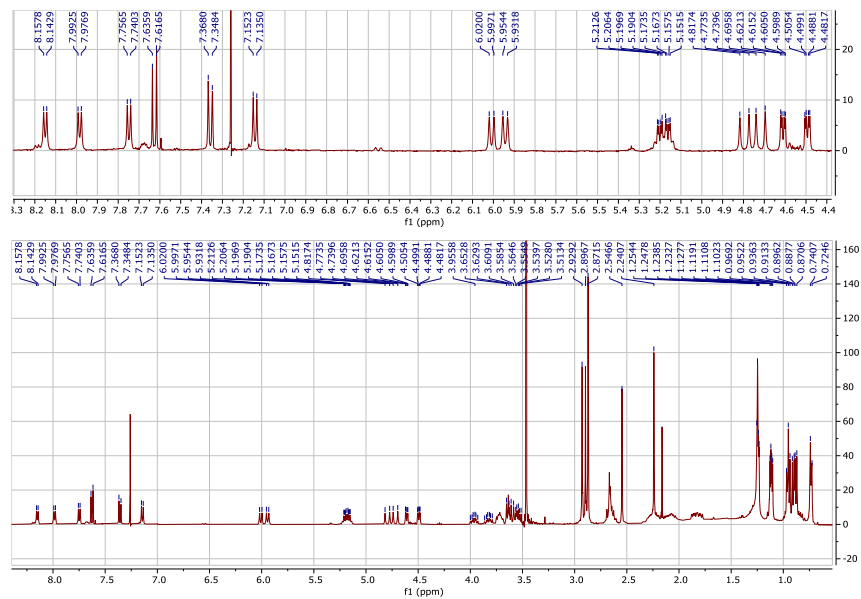


Figure 3.16. The ^1H NMR spectrum of **SG-01** (in CDCl_3 , ^1H : 400 MHz, ^{13}C :100 MHz).

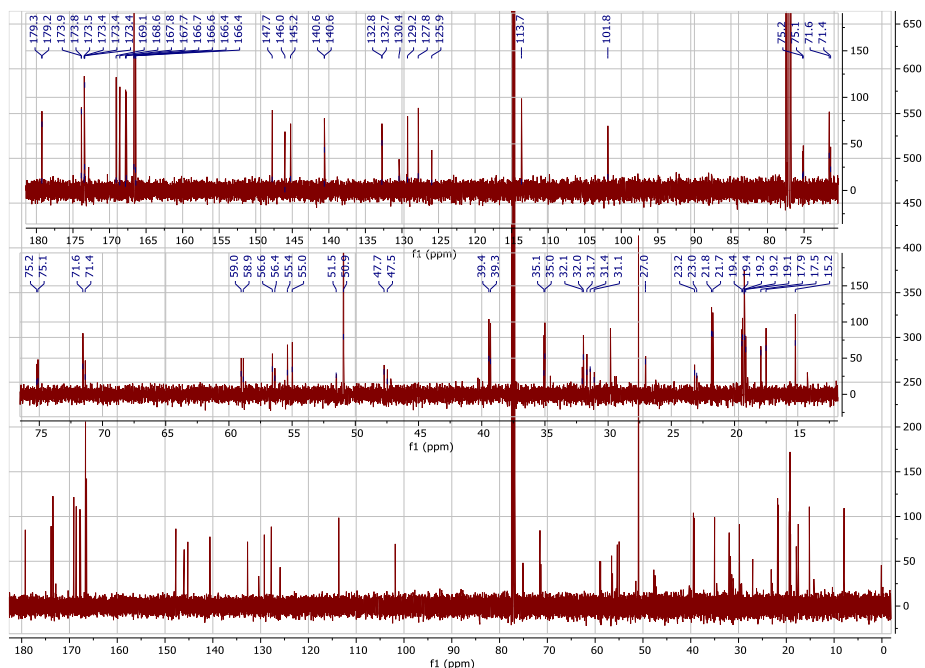


Figure 3.17. The ^{13}C NMR spectrum of **SG-01** (in CDCl_3 , ^1H : 400 MHz, ^{13}C :100 MHz).

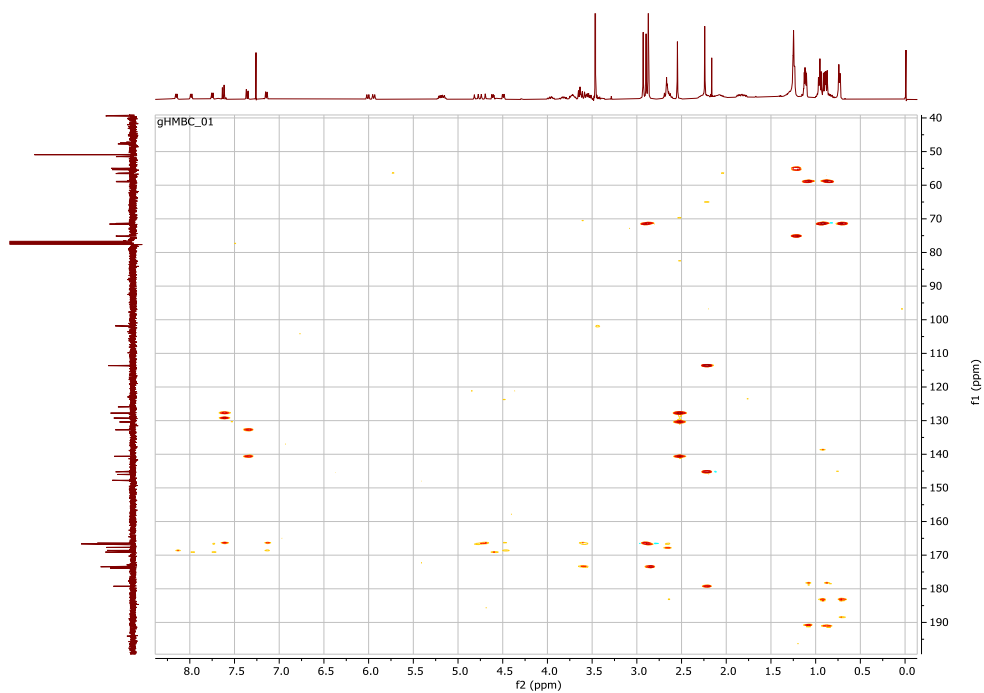


Figure 3.18. The HMBC spectrum of **SG-01** (in CDCl_3 , ^1H : 400 MHz, ^{13}C :100 MHz).

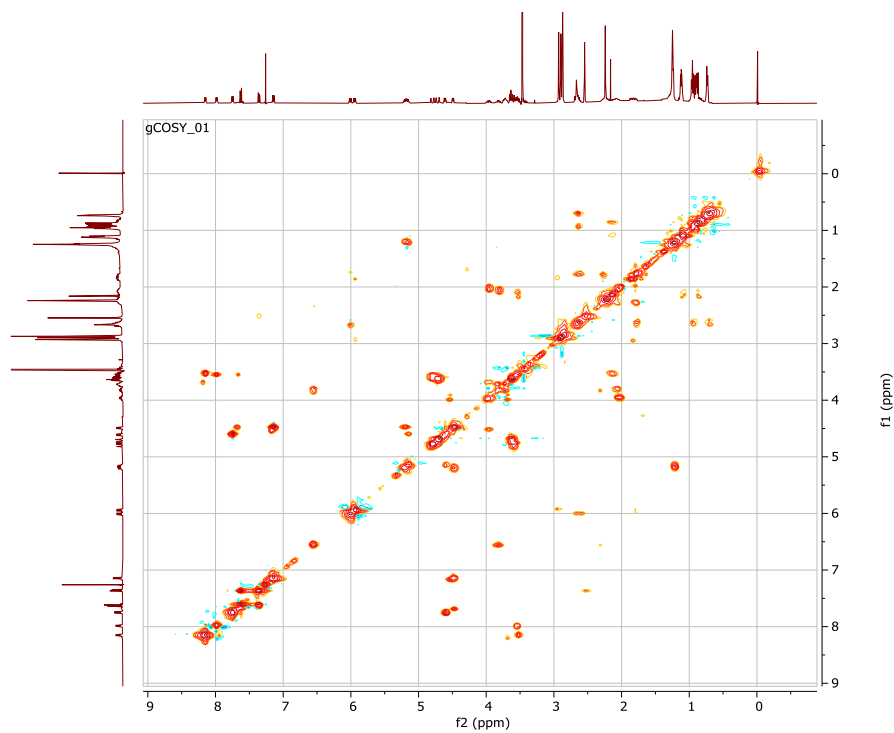


Figure 3.19. The COSY spectrum of **SG-01** (in CDCl_3 , ^1H : 400 MHz, ^{13}C :100 MHz).

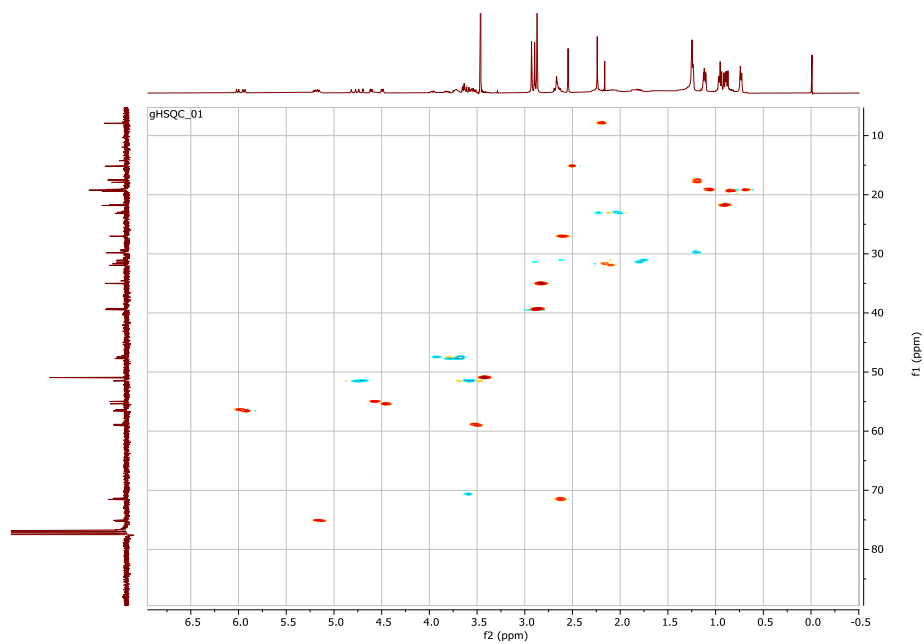


Figure 3.20. The HSQC spectrum of **SG-01** (in CDCl_3 , ^1H : 400 MHz, ^{13}C :100 MHz).

3.4.1.2. SG-02

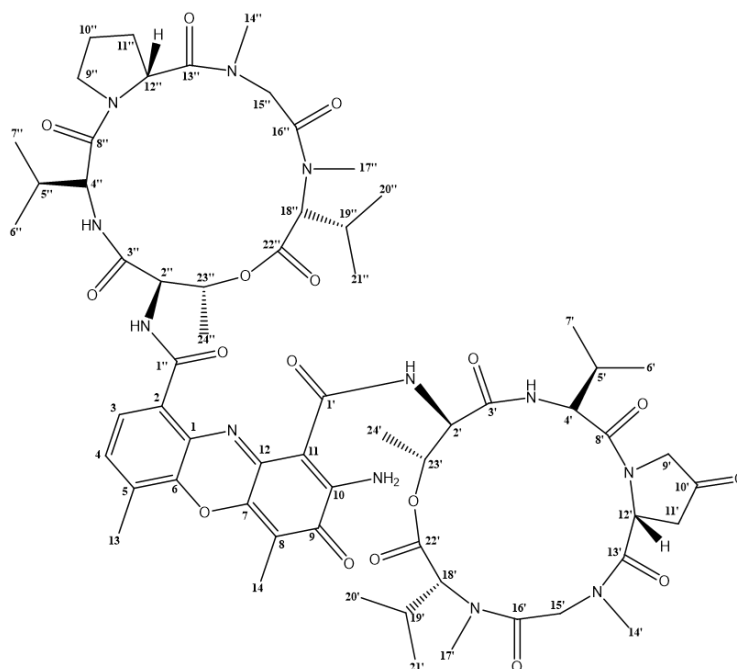


Figure 3.21. The chemical structure of **SG-02**.

The ^1H NMR spectrum of **SG-02** (**Figure 3.21**) revealed similar features of ActD, including a phenoxazine unit and two pentapeptide lactone rings (*see Table 3.8*). Consequently, the compound is identified as ActX2 based on the data reported previously.¹³⁰⁻¹³¹

Actinomycin X2 (synonym with Actinomycin V) was found to be produced by *Streptomyces antibioticus* and *Streptomyces heliomycini*.^{61, 131}

Table 3.8. ^1H spectroscopic data of **SG-02** (ActX2)^a (CDCl_3 , ^1H : 400 MHz)

Position	δ_{H} (ppm), (J in Hz)	Position	δ_{H} (ppm), (J in Hz)
1	-	4'	3.71 dd (10.0, 6.0)
2	-	5'	2.09 ^b
3	7.61 d (7.8)	6'	0.90 d (6.8)
4	7.36 d (7.8)	7'	1.15 d (6.8)
5	-	8'	-
6	-	9'	4.55 d (17.6); 3.88 d (17.6)
7	-	10'	-
8	-	11'	3.84 dd (17.5, 10.4); 2.33 d (17.5)
9	-	12'	6.56 d (10.4)
10	-	13'	-
11	-	14'	2.89 s
12	-	15'	4.63 d (17.5); 3.64 d (17.5)
13	2.55 s	16'	-
14	2.24 s	17'	2.93 s
1'	-	18'	2.68 ^b
NH-2'	7.67 d (6.7)	19'	2.68 ^b
2'	4.50 dd (6.7, 2.6)	20'	0.98 d (6.4)
3'	-	21'	0.74 d (6.4)
NH-4'	8.22 d (6.0)	22'	-

Cont. on next page

Table 3.8. (Cont.)

Position	δ_{H} (ppm), (J in Hz)	Position	δ_{H} (ppm), (J in Hz)
23'	5.24 dd (6.4, 2.6)	11''	2.76 m; 1.85 dd (11.9, 6.7)
24'	1.26 d (6.4)	12''	5.94 d (9.2)
1''	-	13''	-
NH-2''	7.18 d (7.2)	14''	2.88 s
2''	4.57 dd (7.2, 2.7)	15''	4.72 d (17.5); 3.64 d (17.5)
3''	-	16''	-
NH-4''	7.70 d (6.7)	17''	2.92 s
4''	3.58 dd (9.5, 6.7)	18''	2.68 ^b
5''	2.10 ^b	19''	2.68 ^b
6''	0.91 d (6.8)	20''	0.95 d (6.4)
7''	1.12 d (6.8)	21''	0.75 d (6.4)
8''	-	22''	-
9''	3.89 dd (9.8, 5.2); 3.74 d (9.8)	23''	5.16 dd (6.3, 2.7)
10''	2.24 ^b	24''	1.13 d (6.3)

a) Data were assigned by ¹H-NMR.

b) Overlapped signals.

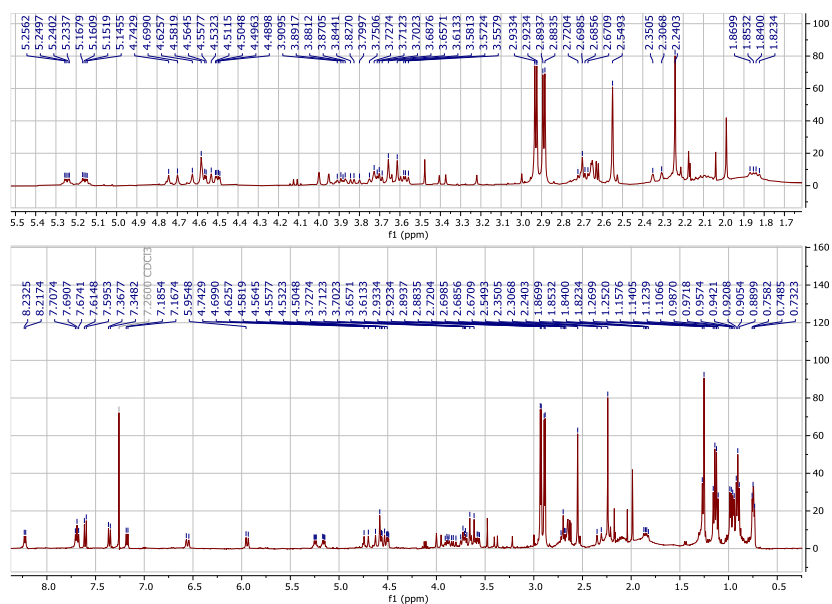


Figure 3.22. The ^1H NMR spectrum of **SG-02** (in CDCl_3 , ^1H : 400 MHz, ^{13}C :100 MHz).

3.4.1.3. SG-03

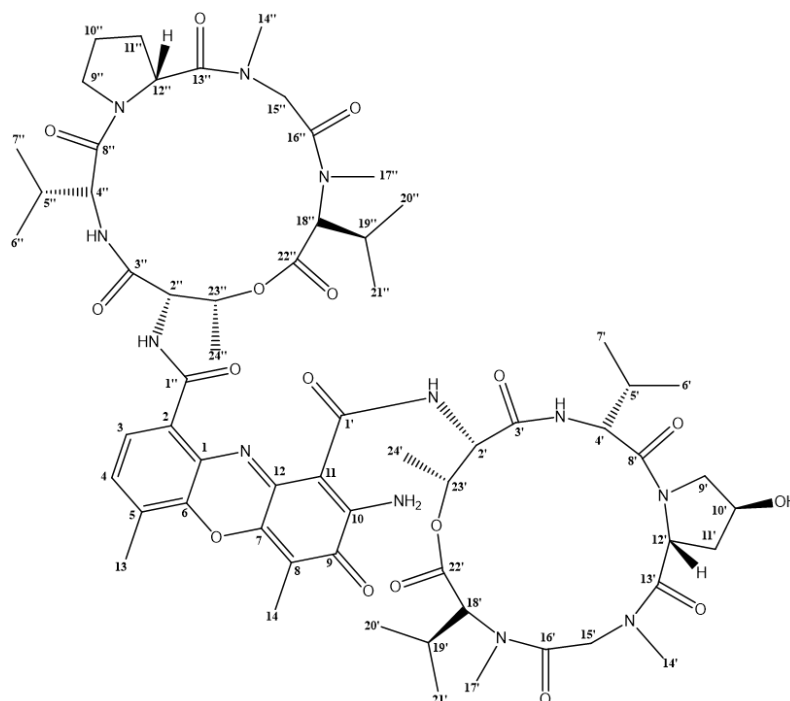


Figure 3.23. The chemical structure of **SG-03**.

The NMR spectroscopic data for **SG-03** (Table 3.9 and Figure 3.24) revealed typical features of an Actinomycin Xo β (ActXo β) molecule with respect to the literature.^{130, 131}

Table 3.9. ¹H NMR spectroscopic data of **SG-03** (ActXo β)^a (CDCl₃, ¹H: 400 MHz)

Position	δ_H (ppm), (J in Hz)	Position	δ_H (ppm), (J in Hz)
1	-	9'	3.57 ^b ; 3.09 m
2	-	10'	4.70 dd (6.8, 4.8)
3	7.66 d (7.8)	11'	4.15 dd (12.8, 4.8); 3.97 dd (12.8, 6.8)
4	7.36 d (7.8)	12'	6.07 dd (9.8, 3.2)
5	-	13'	-
6	-	14'	2.88 s
7	-	15'	4.55 d (17.5); 3.58 d (17.5)
8	-	16'	-
9	-	17'	2.93 s
10	-	18'	2.68 d (9.3)
11	-	19'	2.69 m
12	-	20'	0.95 d (6.6)
13	2.55 s	21'	0.75 d (6.3)
14	2.24 s	22'	-
1'	-	23'	5.24 dd (6.3, 2.5)
NH-2'	7.54 d (7.0)	24'	1.25 d (6.3)
2'	4.51 dd (7.0, 2.5)	1''	-
3'	-	NH-2''	7.49 d (6.5)
NH-4'	7.92 d (6.2)	2''	4.83 dd (6.5, 2.5)
4'	3.59 ^b	3''	-
5'	2.17 ^b	NH-4''	8.20 d (5.4)
6'	1.11 d (6.7)	4''	3.55 ^b
7'	0.88 d (6.6)	5''	2.13 ^b
8'	-	6''	1.14 d (6.7)

Cont. on next page

Table 3.9. (Cont.)

7''	0.97 d (6.6)	16''	-
8''	-	17''	2.95 s
9''	3.87 m; 3.75 m	18''	2.72 d (9.3)
10''	2.28 m; 2.08 m	19''	2.79 m
11''	2.78 m; 1.85 dd (12.1, 6.9)	20''	0.97 d (6.6)
12''	5.99 d (9.1)	21''	0.76 d (6.6)
13''	-	22''	-
14''	2.88 s	23''	5.26 dd (6.3, 2.5)
15''	4.73 d (17.5); 3.64 d (17.5)	24''	1.29 d (6.3)

a) Data were assigned by $^1\text{H-NMR}$.

b) The signal pattern was unclear due to overlapping.

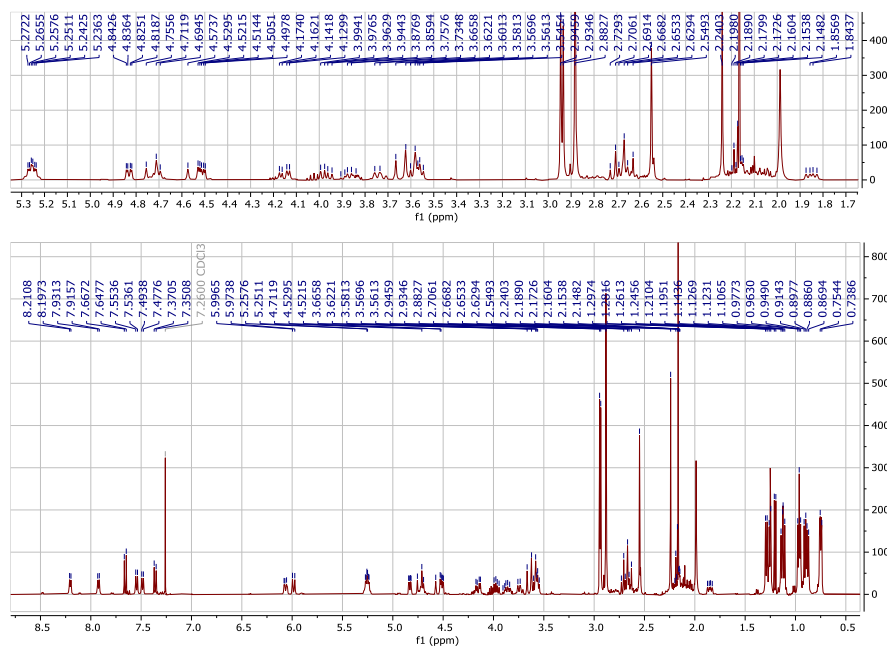


Figure 3.24. The $^1\text{H-NMR}$ spectrum of **SG-03** (in CDCl_3 , ^1H : 400 MHz, ^{13}C :100 MHz).

3.4.1.4. SG-04

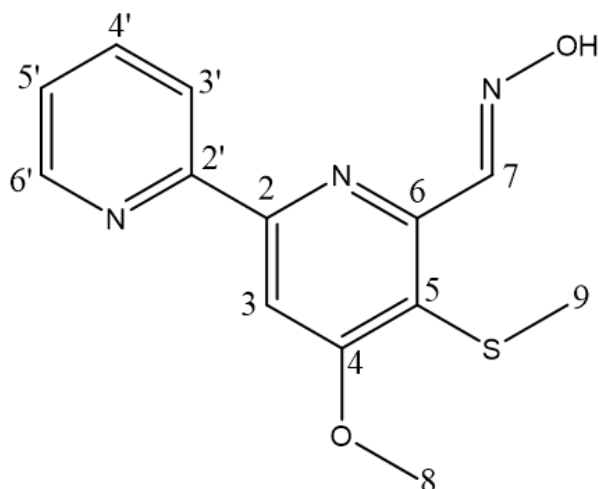


Figure 3.25. The chemical structure of **SG-04**.

The NMR spectroscopic data (*see Table 3.10*) for **SG-04** revealed typical features of Collismycin A molecule with respect to the literature.¹³²

ColA (**Figure 3.25**) is a natural product, characterized by a 2,2'-bipyridyl ring system. ColA has 4-O-methyl, 5-S-methyl, and 6-aldoxime groups in its structure. It is produced by hybrid PKS and NRPS pathways. The cell-permeable, intracellular Fe(II) chelator, 2,2'-bipyridine, is recognized for its ability to bind and sequester iron. The compound can exhibit antifungal, antibacterial, and cytotoxic activities and has the potential as a neuroprotectant by reducing oxidative stress in neurons.^{115, 133, 134}

Table 3.10. ¹H and ¹³C NMR spectroscopic data of **SG-04** (ColA)^a (d₆-DMSO, ¹H: 400 MHz, ¹³C:100 MHz)

Position	δ_{H} (ppm), (J in Hz)	Position	δ_{H} (ppm), (J in Hz)
1	-	9	2.34 s

Cont. on next page

Table 3.10. (Cont.)

2	-	N-OH	11.77 brs
3	8.02 s	1'	-
4	-	2'	-
5	-	3'	8.39 dd (7.9, 1.3)
6	-	4'	7.96 ddd (7.9, 7.5, 1.8)
7	8.73 s	5'	7.50 ddd (7.5, 4.9, 1.3)
8	4.06 s	6'	8.71 dd (4.9, 1.8)

a) Data were assigned by $^1\text{H-NMR}$.

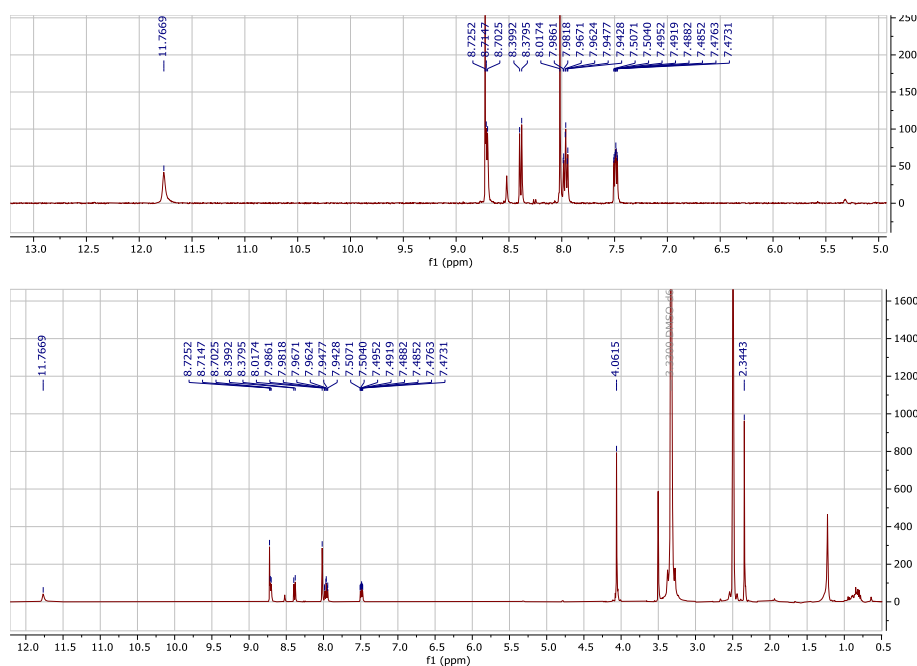


Figure 3.26. The ^1H NMR spectrum of **SG-04** (in CDCl_3 , ^1H : 400 MHz, ^{13}C :100 MHz).

3.4.1.5. SG-05

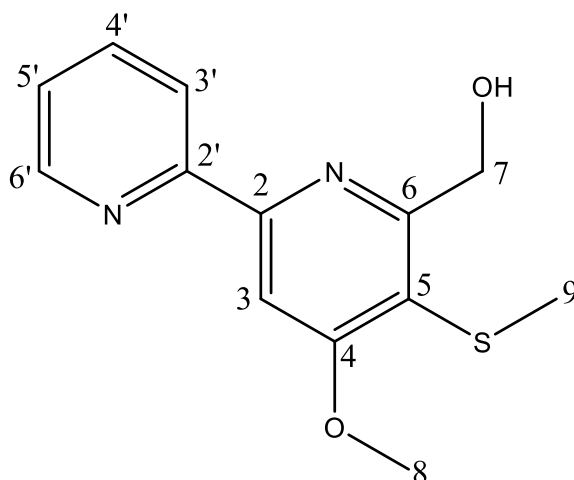


Figure 3.27. The chemical structure of **SG-05**.

The NMR spectroscopic data (*see Table 3.11*) for **SG-05** revealed typical features of Collismycin C molecule with respect to literature.¹³²

Compared with ColA, resonances corresponding to the aldoxime functional group are not observed in ColC. Additionally, ColC, like ColA, functions as an iron chelator. The antibiofilm activities of Collismycins are likely due to their ability to chelate iron in iron-limited environments.^{28, 133}

Table 3.11. ¹H and ¹³C NMR spectroscopic data of **SG-05** (ColC)^a (¹H: 400 MHz in d6-DMSO, ¹³C:100 MHz in CDCl₃)

Position	δ_C (ppm) ^b	δ_H (ppm), (J in Hz)
1	-	-
2	155.1 s	-
3	102.3 d	7.99 s
4	166.6 s	-

Cont. on next page

Table 3.11. (Cont.)

5	118.9 s	-
6	161.7 s	-
7	63.1 t	4.80 s, 4.78 s
8	56.2 q	4.05 s
9	17.3 q	2.33 s
OH		5.04 t (5.2)
1'	-	-
2'	154.6 s	-
3'	121.0 d	8.54 dd (8.0, 1.3)
4'	137.3 d	7.96 ddd (8.0, 7.5, 2.3)
5'	124.5 d	7.48 ddd (7.5, 4.9, 1.3)
6'	149.2 d	8.70 dd (4.9, 2.3)

a) Data were assigned by ^1H and ^{13}C NMR considering shifting values in literature.¹³²

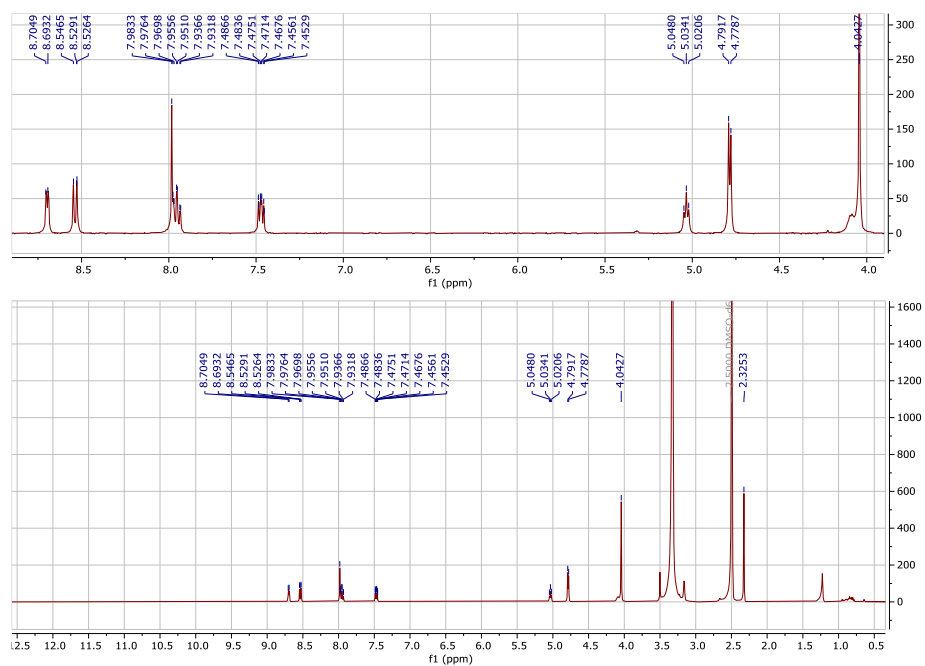


Figure 3.28. The ^1H NMR spectrum of **SG-05** (in CDCl_3 , ^1H : 400 MHz, ^{13}C : 100 MHz).

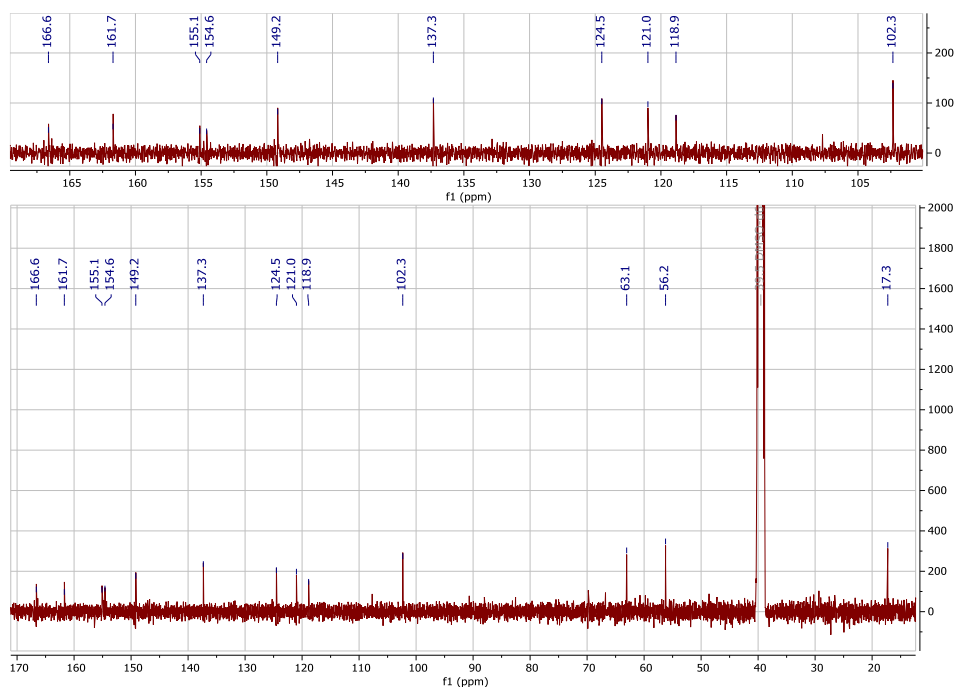


Figure 3.29. The ¹³C NMR spectrum of **SG-05** (in CDCl₃, ¹³C:100 MHz).

3.4.2. LC-MS/MS Analysis

Initially, the LC-MS/MS data of the extract of *Streptomyces* sp. 35M1 was analyzed on the heat map belonging to RT (retention time) mean vs parent masses (*see Figure 3.30*), plotted by Cytoscape Software. The extract was found to contain the compounds, predominantly having mass-to-charge ratios (m/z) between 200 and 400 with RT of 0-16.66 min. Additionally, another major group of compounds was detected at m/z around 1200-1400 with RT of 25-33.33 min. This data indicated that the majority of compounds produced by *Streptomyces* sp. 35M1 in M1 broth correspond to the mentioned parent masses.

The extensive investigation continued with matching the LC-MS/MS major ion peaks with the dereplication results from GNPS database (Global Natural Product Social Molecular Networking) and later comparing them with the NMR spectra of the purified compounds.

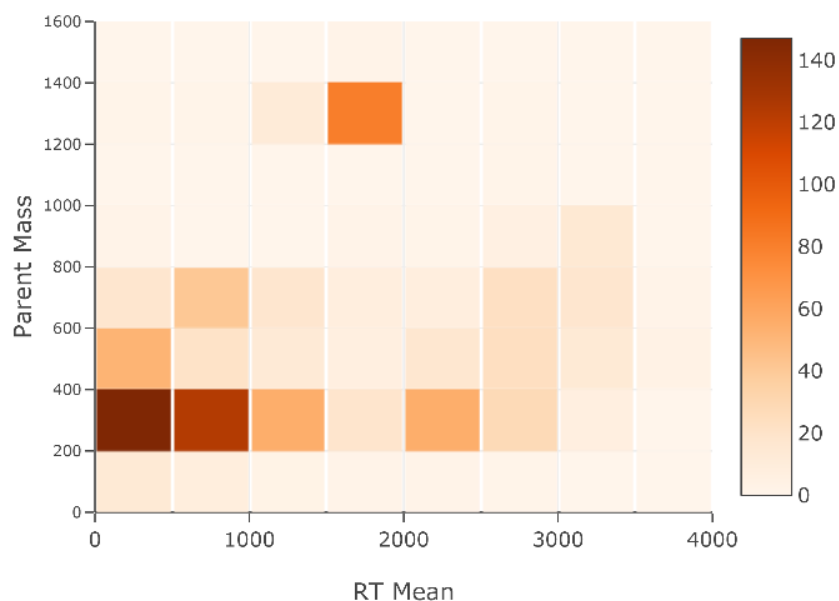


Figure 3.30. RT means vs Parent mass heat map, plotted by Cytoscape Software.

The full LC-MS/MS spectrum of 35M1 is given in **Figure 3.31**. A detailed examination of the spectrum indicated a major ion peak at m/z 1255.64 g/mol $[M+H]^+$ with 29.98 min RT and a monoisotopic mass of 1254.64 g/mol. The peak (**Figure 3.32**) was analyzed and identified by matching the mass spectra with the results of GNPS DereplicatorPlus. According to the analysis together with the NMR data, the presence of **SG-01** (ActD) was confirmed, unambiguously.¹³⁵

The full LC-MS/MS spectrum provided another major ion peak at m/z 1269.6156 $[M+H]^+$ with 29.83 min RT and a monoisotopic mass of 1268.6156 g/mol. This major ion was attributed to **SG-02** (**Figure 3.33**). The peak was identified via comparing the mass spectrum and the dereplication results together with 1D-NMR spectrum. Accordingly, **SG-02** (ActX2) presence was confirmed without ambiguity.¹³¹

Another major ion peak was investigated at m/z 1271.5922 g/mol $[M+H]^+$ with RT of 27.61 min. The peak was assessed together with dereplication results and 1D-NMR spectra. Consequently, **SG-03** (ActXO β) was proven to be found in the extract (**Figure 3.34**).¹³¹

In addition, the major ion peaks of the full spectrum at around 0 - 16.66 min RT were examined. Here, two major ion peaks at m/z 276.08 g/mol $[M+H]^+$ (**Figure 3.35**) with 4.23 min RT and at m/z 263.05 g/mol $[M+H]^+$ with 3.84 min RT (**Figure 3.36**) were

highlighted. Subsequently, the peaks and the dereplication results were compared with the obtained NMR spectra. Consequently, the presence of **SG-04** (ColA) and **SG-05** (ColC) in the extract was proven.

As a result of the dereplication study, approximately 800 different metabolites were detected in the extract. Among them, 21 different Actinomycin derivatives were found to be produced by *Streptomyces* sp. 35M1 in M1 broth (*see* Table **3.12**). Accordingly, three of these metabolites were purified and their structures were established thoroughly by interpreting their spectra (1D- and 2D-NMR) as mentioned before.

In addition, total of five compounds with m/z 663.569, 313.273, 269.21, 301.141 and 273.17 $[M+H]^+$, had no match in the GNPS database. Thus, they are suggested to be new chemical entities (*see* Table **3.13**). However, the purification studies were not afforded these compounds, probably due to the low quantity in the extract.

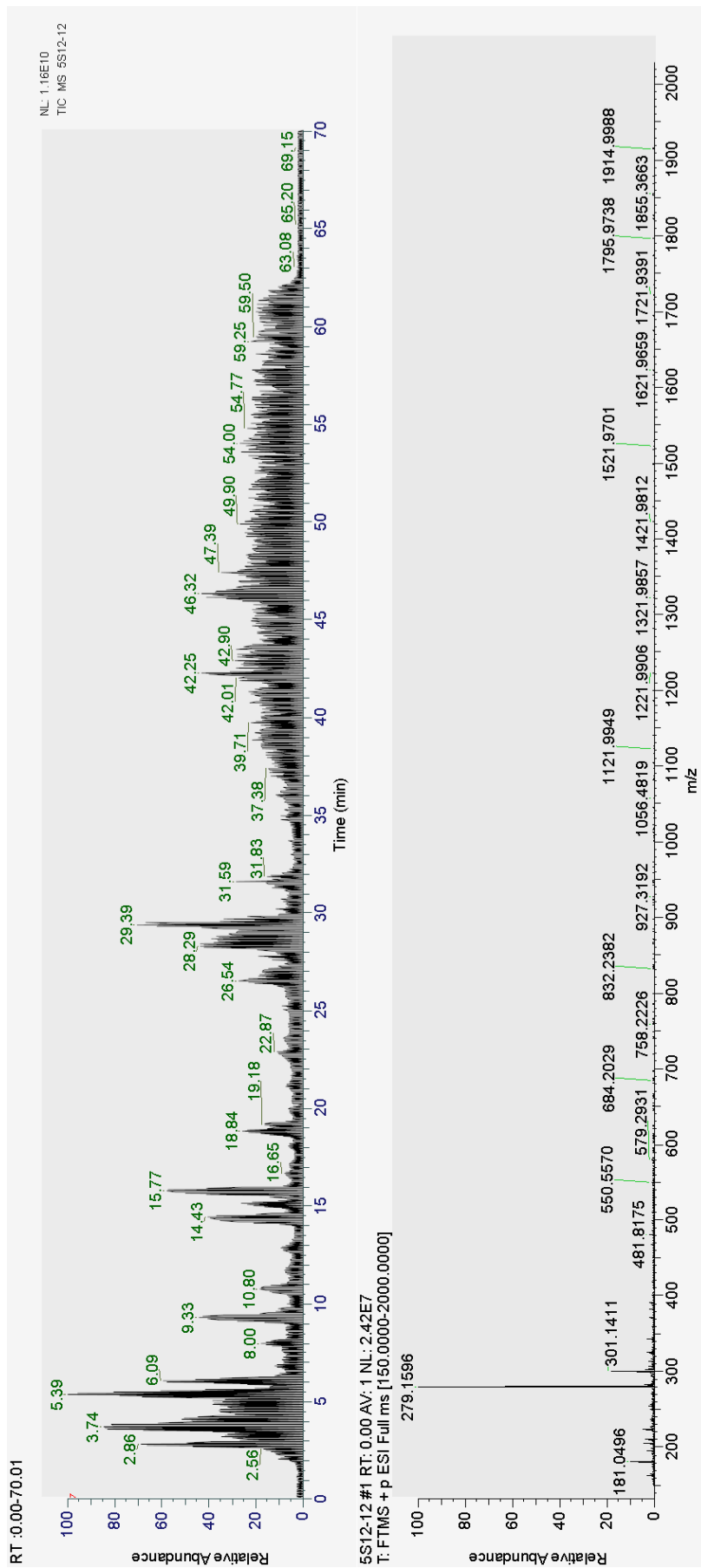


Figure 3.31. Full ESI-MS spectrum of 35MI extract

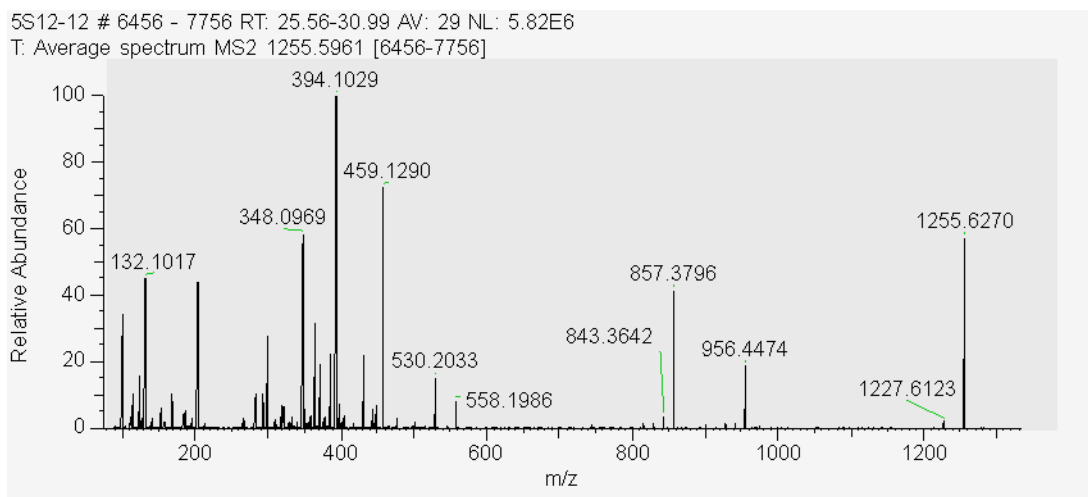


Figure 3.32. ESI-MS of m/z 1255.5961 peak (SG-01)

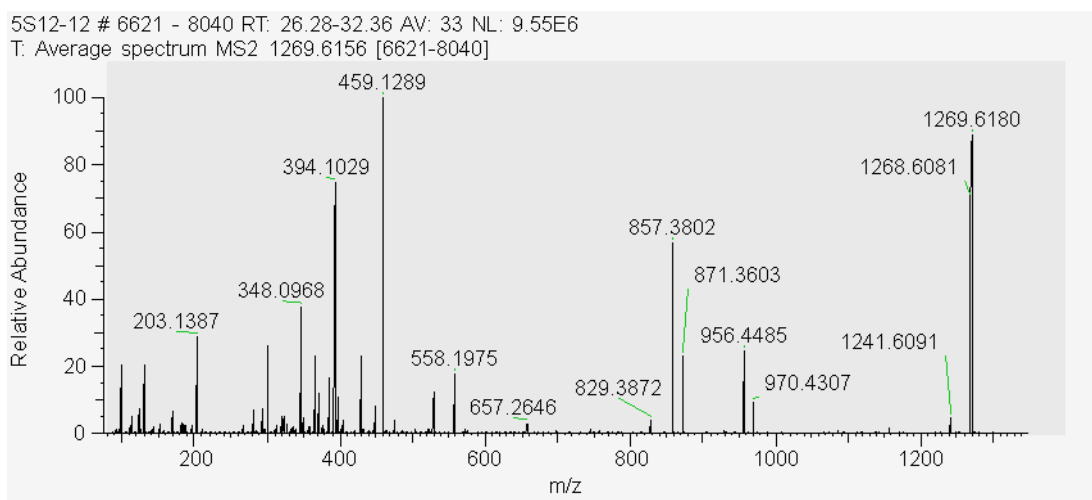


Figure 3.33. ESI-MS of m/z 1269.6156 peak (SG-02)

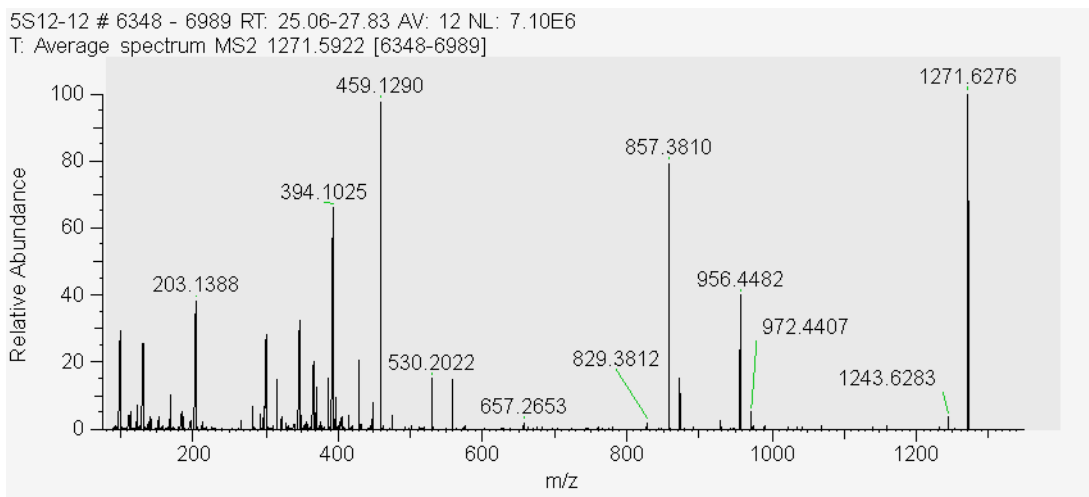


Figure 3.34. ESI-MS of m/z 1271.5922 peak (SG-03)

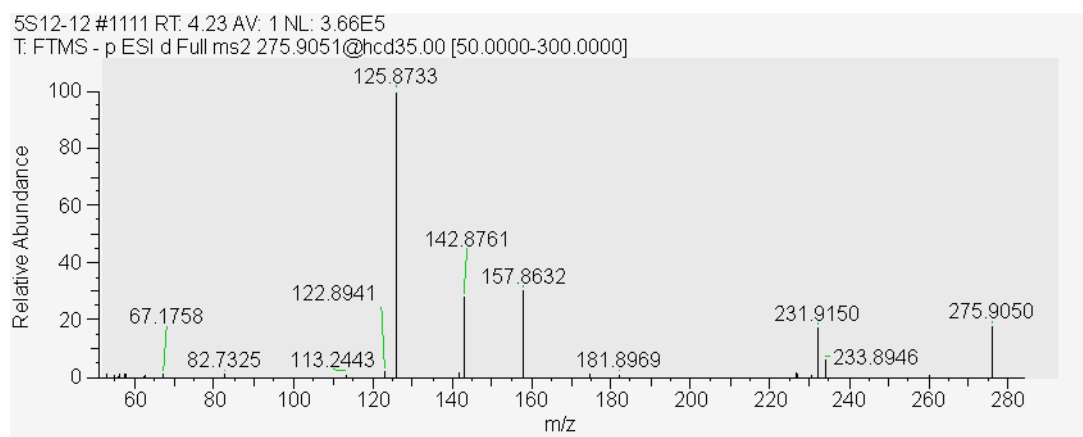


Figure 3.35. ESI-MS of m/z 276.08 peak (SG-04)

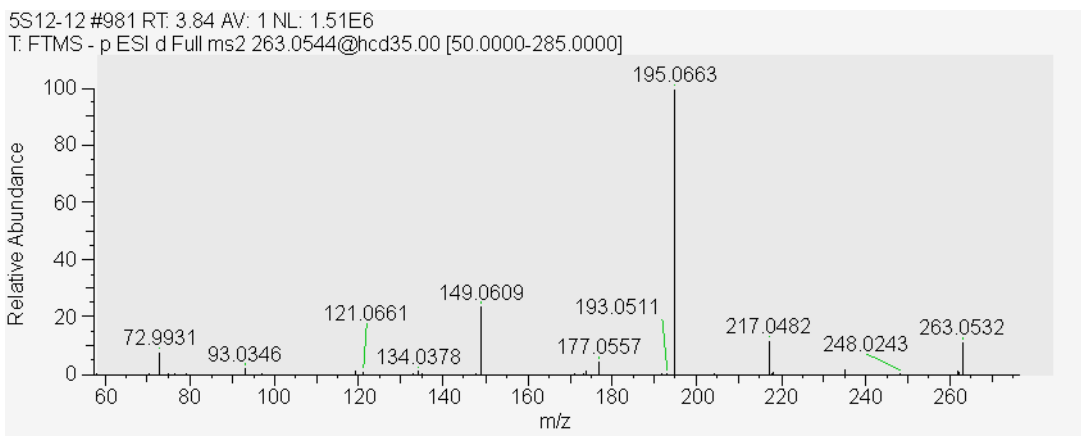


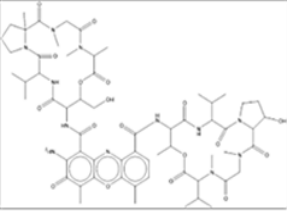
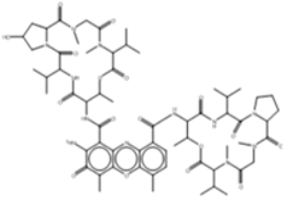
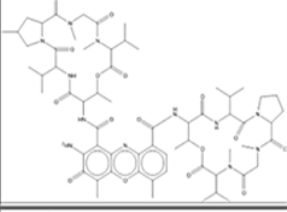
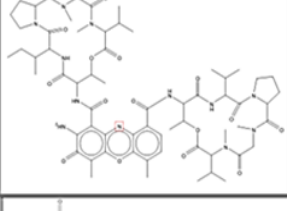
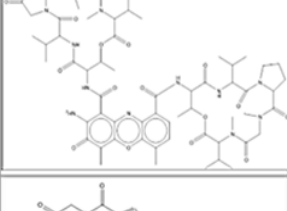
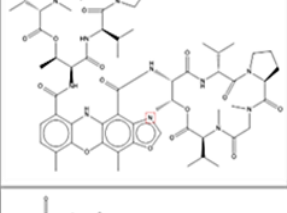
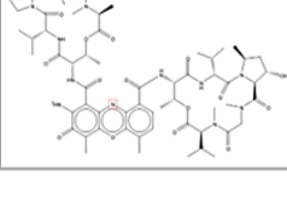
Figure 3.36. ESI-MS of m/z 263.05 peak (**SG-05**)

Table 3.12. GNPS metabolomics results related to Actinomycin derivatives

	Chemical Structure	Score	Peptide Mass	SpectrumMass	Retention	Common Name of the Compound
1		31	1284.64	643.326	1777.44	Actinomycin Pip 1 β
2		21	1284.6	1285.61	1618.93	Actinomycin Z2
3		35	1282.66	642.339	2007.82	Actinomycin Pip 2
4		31	1282.62	1283.63	1741.44	Actinomycin Pip 1 δ

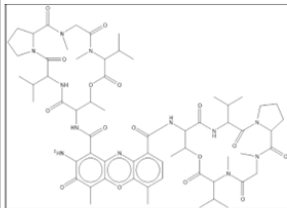
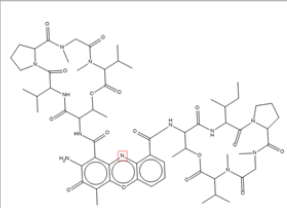
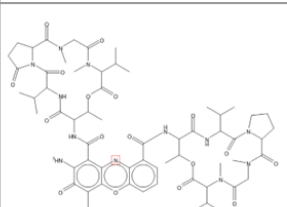
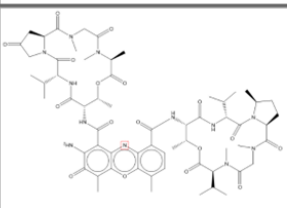
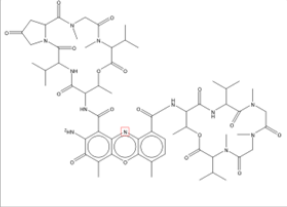
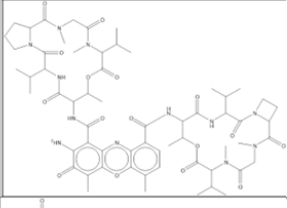
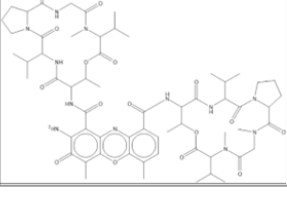
Cont. on next page

Table 3.12. (Cont.)

	Chemical Structure	Score	Peptide Mass	SpectrumMass	Retention	Common Name of the Compound
5		35	1272.6	637.309	1801.25	Actinomycin G3
6		53	1270.62	636.318	1650.94	Actinomycin Xoβ
7		49	1268.64	1269.65	1874.65	Actinomycin K1c
8		23	1268.64	635.326	1810.23	Actinomycin C2a
9		38	1268.61	1269.61	1789.83	Actinomycin X2
10		15	1266.63	1267.64	1837.74	Actinomycin D1
11		29	1256.61	629.31	1677.57	Actinomycin G4

Cont. on next page

Table 3.12. (Cont.)

	Chemical Structure	Score	Peptide Mass	SpectrumMass	Retention	Common Name of the Compound
12		44	1254.63	1255.64	1798.81	Actinomycin D
13		42	1254.63	628.322	1854.06	Aurantin II
14		29	1254.59	1255.6	1544.05	E'C-dimethyl-Actinomycin'
15		15	1254.59	1255.6	1700.72	Actinomycin Y9
16		31	1242.59	622.302	1520.76	Actinomycin X1a
17		48	1240.61	621.313	1742.71	Azetomycin I
18		41	1240.61	1241.61	1730.35	Actinomycin D0

Cont. on next page

Table 3.12. (Cont.)

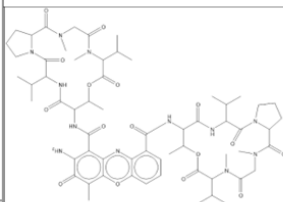
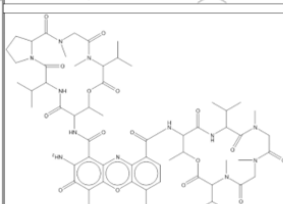
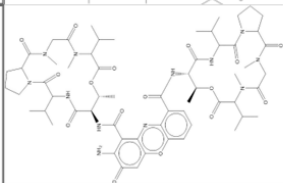
	Chemical Structure	Score	Peptide Mass	SpectrumMass	Retention	Common Name of the Compound
19		32	1240.61	1241.62	1654.59	Auranfin III
20		38	1228.61	615.313	1894.2	Actinomycin F9
21		33	1226.6	614.305	1678.81	1,8-DidesmethylActinomycin C1

Table 3.13. Five unknown compounds found by GNPS analysis.

LocalSpecIdx	Scan	LocalPeptideIdx	Chemical Structures	Name	Score	Peptide Mass	Spectrum Mass	Retention (min)	MassDiff	Adduct
7574	12054	377702	-	N/A	12	662,564	663,569	47,57	0,00225	M+H
5659	9341	383717	-	N/A	16	312,266	313,273	38,36	9,8E-06	M+H
4048	6510	458014	-	N/A	16	268,204	269,21	25,8	0,00112	M+H
1917	2811	416646	-	N/A	12	300,136	301,141	9,89	0,00185	M+H
762	1184	358927	-	N/A	13	272,162	273,17	4,45	-0,0005	M+H

3.5. Bioactivity Analyses

The antimicrobial, antibiofilm, and synergistic activities of the isolated metabolites were determined against *S. epidermidis*, *L. monocytogenes*, *E. coli*, MRSA and Fluconazole resistant *C. albicans*. Some of the bioactivity studies were performed with limited compounds due to insufficient amounts.

Additionally, in bioactivity studies involving crude extracts to compare with pure compounds, there were solubility problems at higher concentrations (256 µg/mL), so the data was not included.

3.5.1. MIC Test

MICs of the purified compounds against MRSA, *S. epidermidis*, *E. coli*, and *L. monocytogenes* and Fluconazole resistant *C. albicans* were determined using the microdilution method with 96-well microtiter plates.

Vancomycin was selected as a control for gram-positive bacteria because it inhibits peptidoglycan synthesis.¹³⁷ Since gram-negative organisms have OM, Vancomycin is less effective against them. Thus, Kanamycin was chosen as a control for gram-negative bacteria. MIC values were determined when 90 % bacterial growth was inhibited compared with growth control groups.⁹⁵

MIC values for ActD and ActX2 were 0.125 µg/mL against *S. epidermidis*, whereas Vancomycin had 1 µg/mL (**Table 3.14, Figure 3.37**). ActXOβ (MIC 0.5 µg/mL) showed 2-fold higher activity than Vancomycin. Although reaching a structure-activity relationship (SAR) by considering three compounds, the 4-fold difference activity difference between ActXOβ and the other Actinomycin derivatives is noteworthy. Thus, strain-specific SAR studies with more analogs are warranted to make final deductions. ColA and ColC had 16 µg/mL and 32 µg/mL MIC values against *S. epidermidis*, respectively.

Among tested compounds, the most potent ones against MRSA (**Figure 3.38**) were ActX2 and Vancomycin, with a MIC value of 0.125 µg/mL. ColA and ColC had 8 and 16 µg/mL MIC values, respectively. ActXOβ and ActD also showed significant activity with a 0.25 µg/mL MIC value.

In literature, one study showed that ActD had MIC value of 1 µg/mL against MRSA.¹⁶⁴ Chen et al. (2020) found that Actinomycin X2 and collismycin A had activity against MRSA ATCC 43300 with the MIC values of 0.25 and 8 µg/mL.¹³⁴ In another study, Actinomycin D was found to have 4 µg/mL while Actinomycin X2 had 3.5 µg/mL MIC value against MRSA.⁶¹

For *L. monocytogenes*, ActX2 had a MIC of 0.25 µg/mL. When compared with Vancomycin (0.5 µg/mL), it showed a 2-fold increase in activity. Interestingly, against *L. monocytogenes* (**Figure 3.39**), ActXOβ showed the lowest activity among Actinomycin derivatives.

The ActD is primarily bacteriostatic as it inhibits RNA synthesis and eventually suppresses protein synthesis.¹³¹ ColA had 16 µg/mL, whereas ColC had >32 µg/mL MIC values against *L. monocytogenes*.

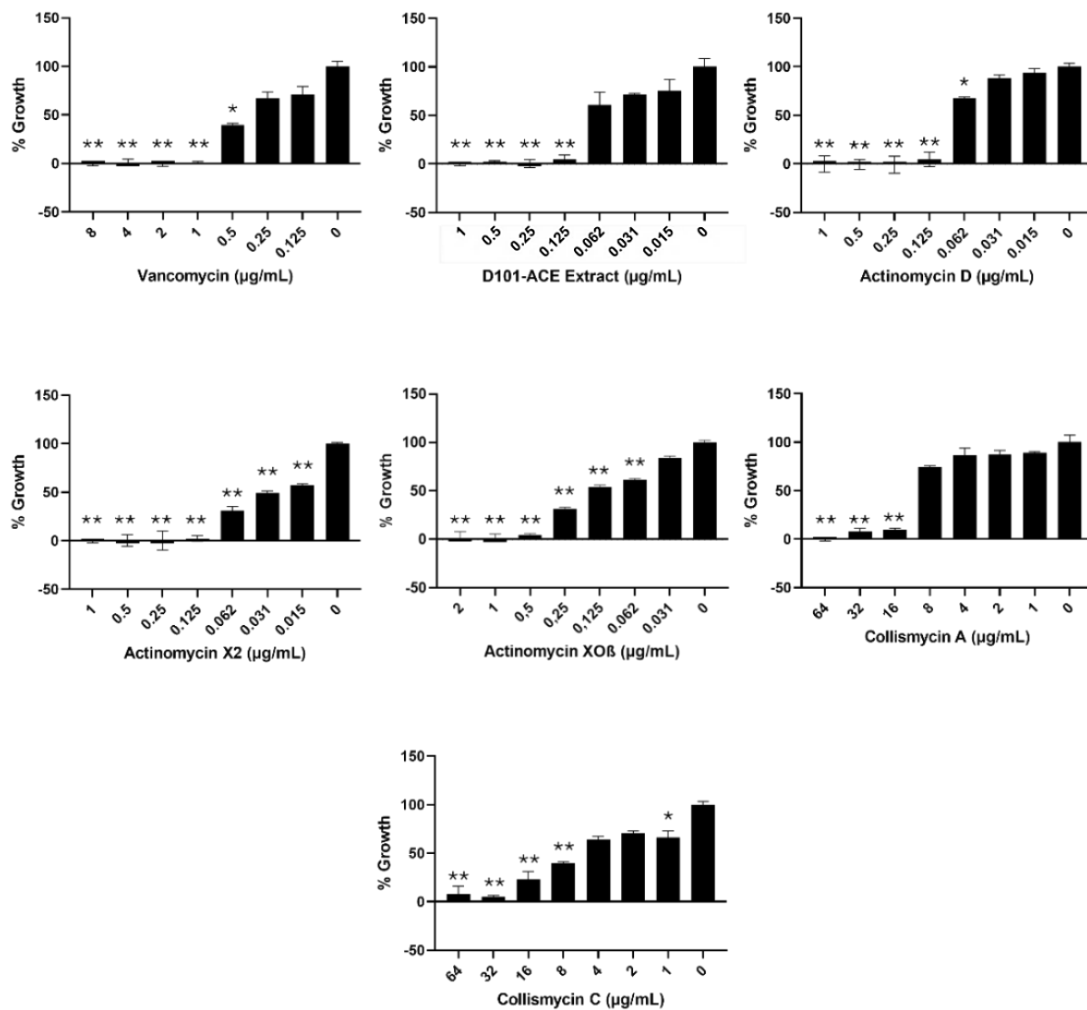


Figure 3.37. *S. epidermidis* growth percentages with respect to varied concentrations of agents. Statistical significance was determined utilizing one-way analysis of variance (one-way ANOVA). * $p < 0.005$, ** $p < 0.0001$ versus untreated growth controls.

In literature, the structure-activity relationship (SAR) of ActD was studied. It was shown that the lactone rings in ActD stabilize the peptide chains in a specific conformation, allowing the formation of four additional hydrogen bonds between phosphodiester oxygens and peptide-NH groups in DNA.¹²⁵

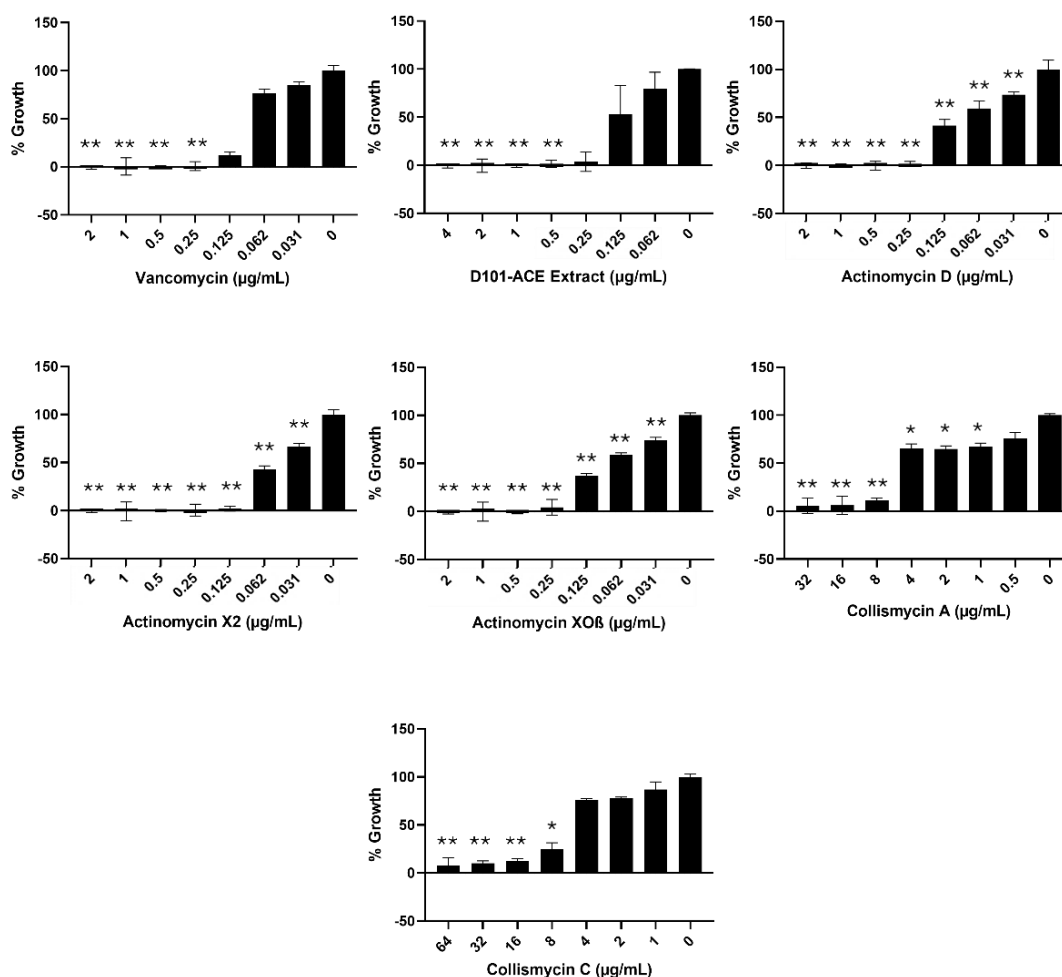


Figure 3.38. MRSA growth percentages with respect to varied concentrations of agents. Statistical significance was determined utilizing a one-way analysis of variance (one-way ANOVA). * $p < 0.005$, ** $p < 0.0001$ versus untreated growth controls.

Accordingly, the amino acid composition is crucial for the biological activity of Actinomycin derivatives. In literature, substituting proline with hydroxyproline altered the MIC values and concluded that changes in the peptide conformation can lead to variations in biological activity. When pipercolic acid was incorporated into the amino acid chains, it inhibited the growth of Gram-positive bacteria, not Gram-negative ones. Moreover, replacing both proline residues with pipercolic acid decreased the biological activity and DNA-binding capacity.^{125, 138-140}

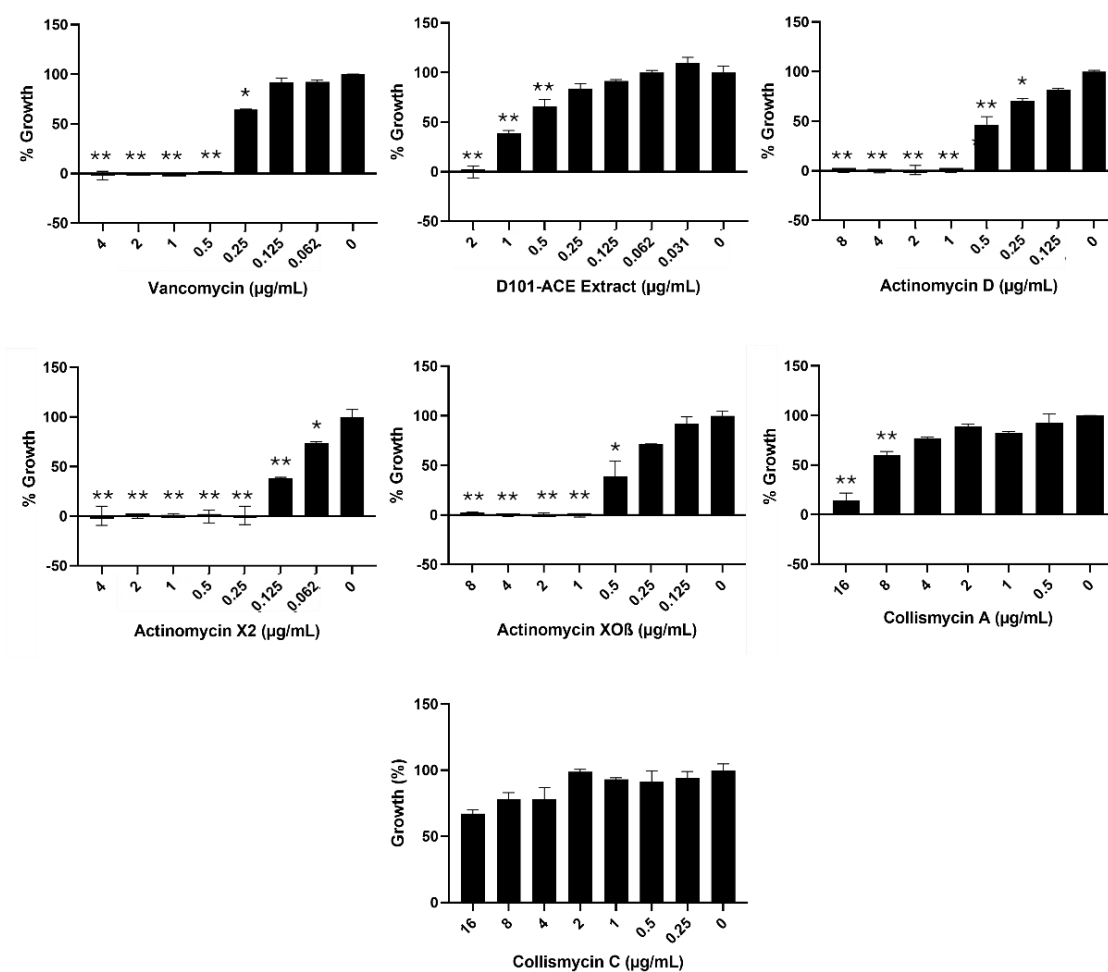


Figure 3.39. *L. monocytogenes* growth percentages with respect to varied concentrations of agents. Statistical significance was determined utilizing a one-way analysis of variance (one-way ANOVA). * $p < 0.005$, ** $p < 0.0001$ versus untreated growth controls.

Overall, ColA and ColC showed less activity than Actinomycin derivatives. The reason might be the nature of their action mechanism. The action mechanism of Collismycin lies in its ability to form complexes with Fe(II) and Fe(III) at a 2:1 ratio with a redox-inactive center.^{34, 141} When antimicrobial activities of ColA and ColC were compared against tested pathogens, ColA had lower MICs (ca. 2-fold). This suggests the importance of aldoxime functionality that is missing in ColC. Against clinical isolate fluconazole resistant *C. albicans*, all Actinomycin derivatives showed 64 µg/mL while ColC had >32 µg/mL MIC values. When compared with Fluconazole (8 µg/mL MIC value), ColA showed greatest activity against resistant *C. albicans*, having 1 µg/mL MIC value.

Additionally, Actinomycin derivatives were tested on *E. coli*, but the results were less prominent compared to other test pathogens.

Table 3.14. MIC values of isolated compounds and control groups against tested pathogens. FR: Fluconazole-resistant strain

MIC Values (µg/mL)	<i>S. epidermidis</i>	MRSA	<i>L. monocytogenes</i>	<i>E. coli</i>	<i>C. albicans</i> (FR)
ActD	0.125	0.25	1	256	64
ActX2	0.125	0.125	0.25	128	64
ActXOβ	0.5	0.25	2	>256	64
ColA	16	8	16	ND	1
ColC	32	16	>32	ND	>32
D101-Ace Extract	0.125	0.25	2	>256	4
Vancomycin	1	0.125	0.5	ND	ND
Kanamycin	ND	ND	ND	2	ND
Fluconazole	ND	ND	ND	ND	8

ND: Not determined

3.5.2. Antibiofilm Activity

Biofilm inhibition assay was done against *L. monocytogenes* and MRSA. As the two pathogens are gram-positive, 10 % TSB with 0.1 % (w/v) glucose was utilized as a medium because it is one of the media that propagate biofilm formation.⁹⁶

Results showed that the MBIC value of ActD for MRSA was 0.031 µg/mL, the same as Vancomycin. The second lowest MBIC was ActX2 with 0.125 µg/mL.

Against *L. monocytogenes*, Vancomycin had 0.062 µg/mL MBIC, while ActX2 had 0.125 µg/mL (see **Table 3.15**). ColA had an MBIC value of 32 µg/mL against MRSA and *L. monocytogenes*, while the MBIC of ColC was found to be > 32 µg/mL.

When the results of compounds against both pathogens were compared, ActX2 showed the same MBIC for both pathogens. However, for ActD, MBIC was 8-fold lower against MRSA than *L. monocytogenes*. ActXOβ showed 2-fold higher MBIC against *L. monocytogenes*. ColA had lower MBIC values than ColC against tested pathogens. Statistical significance was determined to be as $p < 0.0001$ versus untreated growth controls below MBIC values of compounds, demonstrated in **Figures 3.40** and **3.41**.

Table 3.15. MBIC values of isolated compounds and antibiotics

MBIC Values (µg/mL)	MRSA	<i>L. monocytogenes</i>
ActD	0.031	0.25
ActX2	0.125	0.125
ActXOβ	0.25	2
ColA	32	32
ColC	>32	>32
D101-Ace Extract	0.25	2
Vancomycin	0.031	0.062

In literature, it has been reported that several antibiotics at subinhibitory concentrations can promote biofilm formation¹⁴²⁻¹⁴⁴. Despite this, a study demonstrated that subinhibitory concentration of ActD inhibited biofilm formation in *S. epidermidis*. They showed that ActD decreased the production of EPS in *S. epidermidis*, leading to reduced cell surface hydrophobicity¹⁴⁵. Against *S. epidermidis*, the same results for ActD were obtained in this thesis as it had biofilm inhibition activity at concentrations less than its MIC. It was revealed for the first time that ActD and ActX2 had biofilm inhibition activity against *L. monocytogenes* at subinhibitory concentrations.

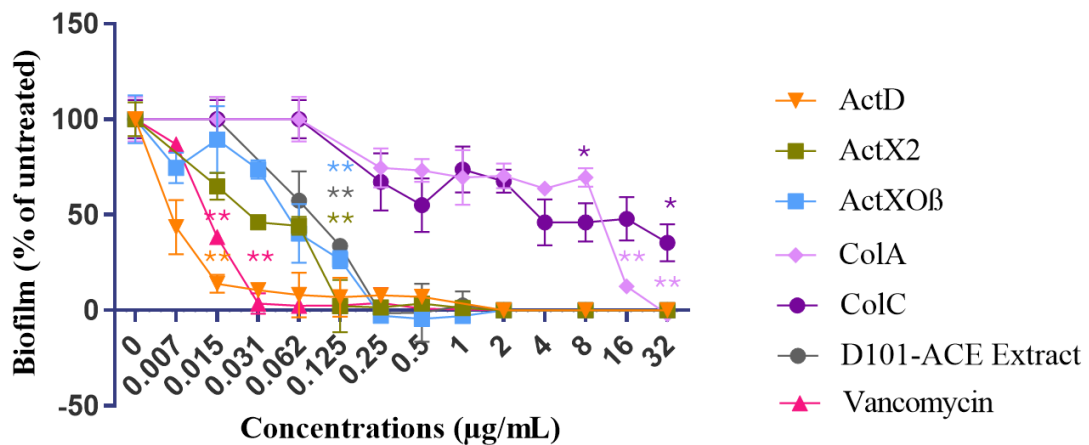


Figure 3.40. MRSA biofilm growth curve (%) with respect to varied concentrations of agents in 10 % TSB + 0.1 % glucose. Statistical significance was determined utilizing a one-way analysis of variance (one-way ANOVA). * $p < 0.005$, ** $p < 0.0001$ versus untreated growth controls.

In the biofilm eradication assay, only ActD was investigated further. As a result, concentration-effect curves were drawn, shown in **Figure 3.42** demonstrating the percentage of biofilm biomass and metabolism values. This dual plotting provided insights into the adhered biofilm biomass within the well and whether this biomass remains metabolically active.

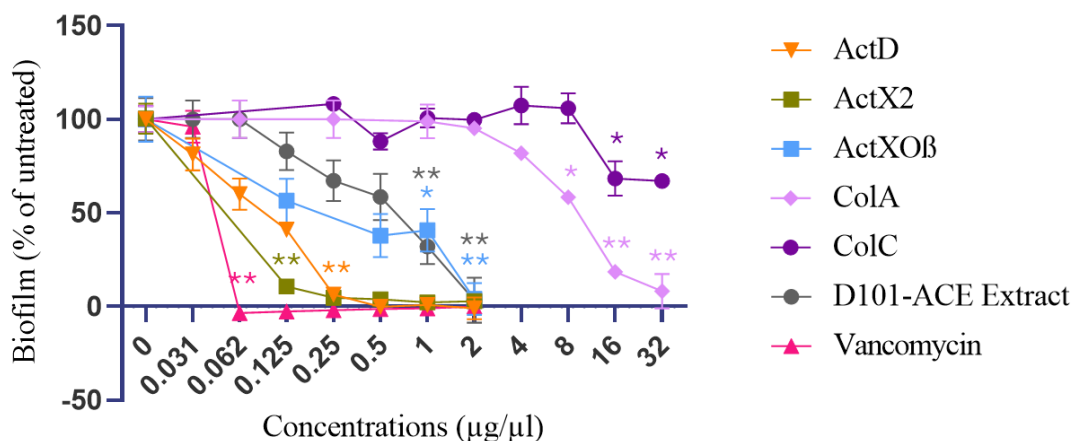


Figure 3.41. *L. monocytogenes* biofilm growth curve (%) with respect to varied concentrations of agents in 10 % TSB + 0.1 % glucose. Statistical significance was determined utilizing one-way analysis of variance (one-way ANOVA). * $p < 0.005$, ** $p < 0.0001$ versus untreated growth controls.

Our results demonstrated that ActD decreased 80 % of the preformed biofilm of *L. monocytogenes* while declining viability in the biofilm up to 60 % at 32 µg/mL. So, it could be stated that ActD has biofilm eradication capability against the pathogen. For *S. epidermidis*, there was about an 80 % decline in viability and a 50 % disruption in biofilm structure. Thus, the MBEC of ActD against *S. epidermidis* was 32 µg/mL in the case of viability given in **Figure 3.42**.

According to Clarke et al. (2023)¹⁴⁶, ActD isolated from *Streptomyces parvulus* could inhibit biofilm formation in *S. aureus* at subinhibitory concentrations. Biofilm biomass of MRSA decreased by about 60 %; however, viability decreased by about 50 %.

NaOCl was used as the control group since it is an effective antibiofilm agent in medical devices.¹⁴⁹ However, it cannot be used on the skin or implants, so the potential of our isolated compounds was investigated. The MBEC of NaOCl was determined to be 0.32 % (v/v).

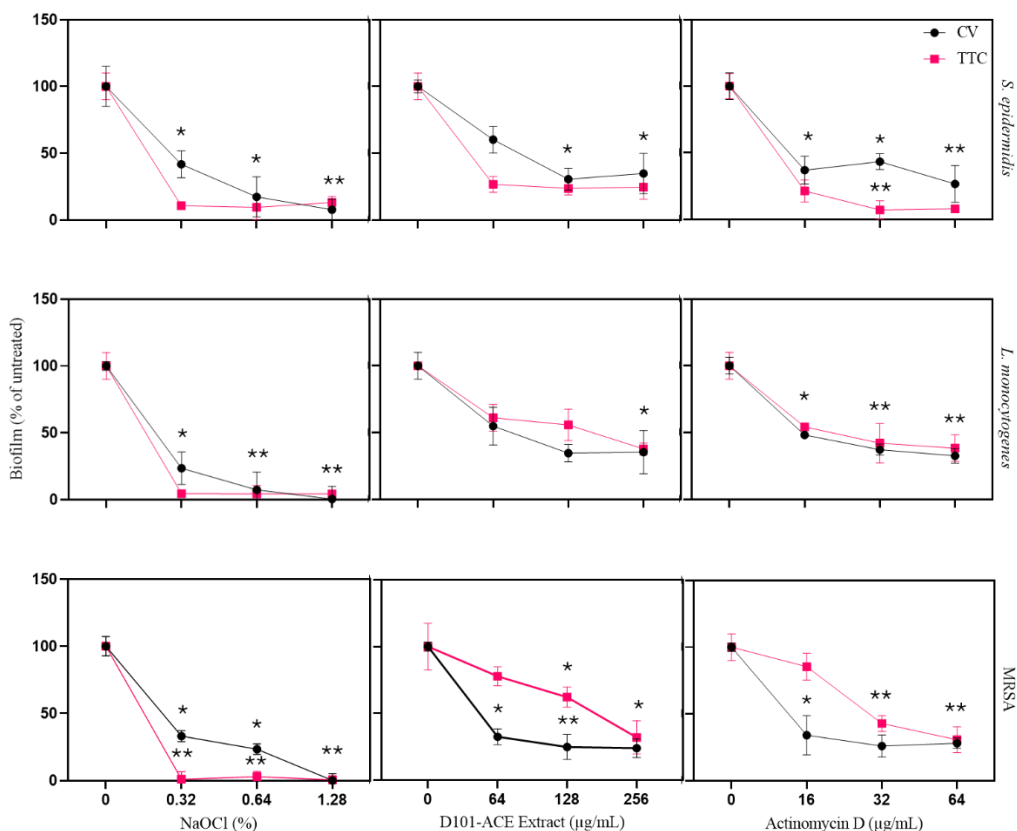


Figure 3.42. Biofilm eradication assay results as biofilm (%) vs concentration of compounds in 10 % TSB + 0.1 % glucose medium. Statistical significance was determined utilizing one-way analysis of variance (one-way ANOVA). * $p < 0.005$, ** $p < 0.0001$ versus untreated growth controls.

This distinction between biofilm biomass and viable bacteria remaining inside is crucial when evaluating compounds for antibiofilm activity against established biofilms, as a compound might inhibit cell growth within a biofilm without altering the biofilm structure or dispersing its cells. Thus, a compound can be considered effective against preformed biofilms if the treatment results in reduced CV staining (**Figure 3.43**), decreased TTC metabolism, or both.⁹⁶

When microscopy images of CV-stained wells were checked, it was seen that NaOCl eradicated biofilm on the surface completely compared to the growth control. Biofilm eradication property of D101-Ace extract showed at a concentration of 256 µg/mL, there were heterogeneously located big clumps in all three tested organisms, as seen in **Figure 3.43**. Such clumps were not observed in ActD-treated wells at 64 µg/mL

concentration, and there were stained dots that were rather distributed at the edges of the wells. ActD-treated wells showed biofilm eradication at the center of the wells.

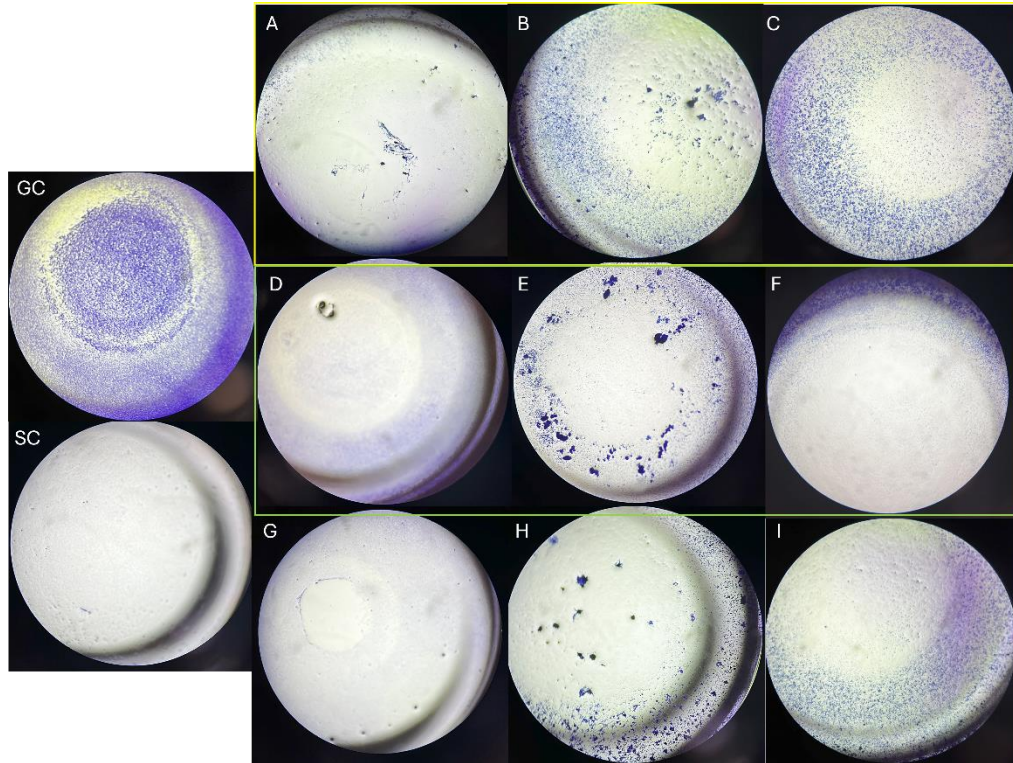


Figure 3.43. Images of wells belonging to biofilm eradication assay before the solubilization step of CV under a light microscope at 5x magnification. They represent the highest concentrations as NaOCl 1.28 % (v/v), D101-Ace Extract 256 $\mu\text{g}/\text{mL}$ and ActD 64 $\mu\text{g}/\text{mL}$. GC: Growth Control, SC: Sterility Control, A: NaOCl- *S. epidermidis*, B: D101-Ace Extract (256 $\mu\text{g}/\text{mL}$)-*S. epidermidis*, C: ActD-*S. epidermidis*, D: NaOCl- *L. monocytogenes*, E: D101-Ace Extract- *L. monocytogenes*, F: ActD- *L. monocytogenes*, G: NaOCl-MRSA, H: D101-Ace Extract- MRSA, I: ActD- MRSA.

One of the challenging points of using Actinomycin D as an antibiotic in clinics is that it has a low therapeutic window. Thus, with biofilm inhibition and eradication tests, we aimed to repurpose such a powerful antimicrobial agent to combat bacterial biofilms. In literature, some studies have investigated the effectiveness of known anticancer agents against biofilms for repurposing studies. Yuan et al. (2018) mentioned a repurposing

study on the anticancer drug Cisplatin and showed its efficacy against *P. aeruginosa* biofilms in a murine keratitis model. With topical application of Cisplatin on biofilm surfaces it was also found to decrease cytotoxicity in the host.¹⁴⁸ Similarly, another anticancer drug, 5-Fluorouracil, was re-used versus *E. coli* and displayed decreased biofilm formation in a dose-dependent manner.¹⁵⁰

Overall, for medical devices and implants, any remaining biofilm fragments are likely crucial in treatment failure, which makes complete eradication the goal of antimicrobial therapy.

3.5.3. Synergistic Activity

E. coli was selected for synergistic activity studies because treating them in clinics is much more difficult as it can easily develop resistance due to their OM nature mentioned before and can produce varied toxins causing serious infections. Thus, to treat *E. coli* infections, one of the most prescribed treatments is done by combination of Trimethoprim/Sulfamethoxazole. However, the combination has certain side effects as the dose increases, involving high potassium (hyperkalemia) and low sodium in the blood (hyponatremia).¹⁵¹ This situation prompted us to search for a potential combinatorial therapy to inhibit *E. coli* growth. As Collismycin derivatives were low in quantity, they were not included here. Thus, combination experiments of Actinomycin derivatives (ActD, ActX2, and ActXO β) with three commonly used antibiotics (Rifampicin, Ampicillin, and Nalidixic acid) were conducted while aiming to get increased activity with much fewer doses against *E. coli*.

Thus, 77 combinations of the selected compounds were tested in three replicates.⁹⁶ Dose-effect curves of single compounds are shown in **Figure 3.44**. The plots of growth percentages and doses are shown in **Figure 3.46**, together with the MIC values of each test compound. The highest concentrations were selected as 128 $\mu\text{g}/\text{mL}$ for Actinomycin derivatives, 16 $\mu\text{g}/\text{mL}$ for Ampicillin and Nalidixic acid, and 8 $\mu\text{g}/\text{mL}$ for Rifampicin. When the MIC exceeded 128 $\mu\text{g}/\text{mL}$, it was regarded to be 256 $\mu\text{g}/\text{mL}$ for calculating the FIC. As a result, the FIC was determined from the combination MICs of three replicates and reported as the average \pm standard error of the mean.

Of all the methods available to test interactions, the FICI approach is used most, but it is also particularly faced with reproducibility problems. For example, Rand et al. (1993)¹⁵² reported that 25 % of their replicate test sets yielded inconsistent FICI interpretations. Given the widely accepted standard in MIC testing, where a single result can vary within a three-dilution range (mode \pm 1 dilution), the potential for reproducibility errors in a MIC checkerboard is considerable.¹⁵³ Following recent recommendations to measure MIC on the same microarray plate, values between 0.5 and just under 1 were considered weakly synergistic (**Figure 3.46**).¹⁴⁵

Within this thesis using FICI, it has been found that ActD has synergistic activity with Nalidixic acid and Rifampicin, although no synergism was found with Ampicillin at the chosen concentrations. According to El-Naggar et al. (1998), ActX2 showed synergism (FICI 0.275) with Sulbactam/Ampicillin against *S. aureus*¹⁵⁴. We found that ActX2 with 64 μ g/mL concentration had a weak synergistic activity with 0.5 μ g/mL of Ampicillin. ActD and ActXOB had a weak antagonistic activity with Ampicillin. At the same time, ActXOB showed weak synergy at 128 μ g/mL and a weak antagonism at lower concentrations. Overall, results showed that ActD and ActX2 were found to have high synergistic activity with Nalidixic acid but not that strong with other tested antibiotics against *E. coli*. ActXOB demonstrated no synergy at all tested concentrations.

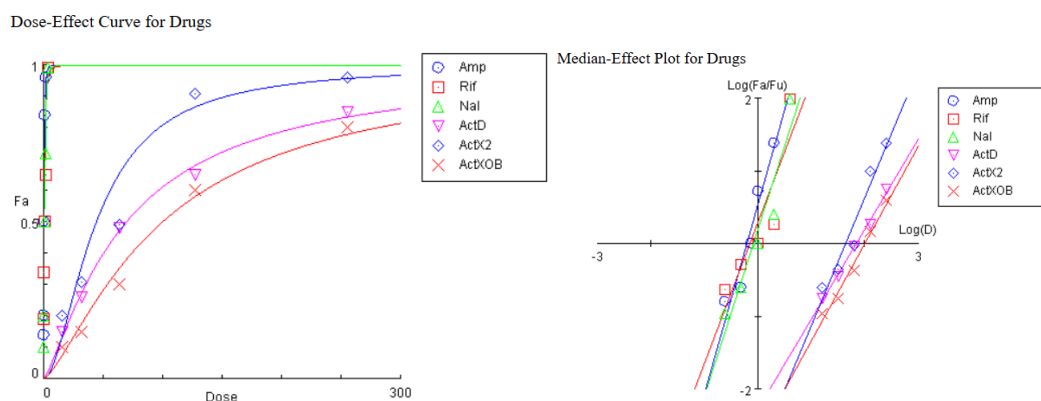


Figure 3.44. Dose-Effect curve and median-effect plot of single compounds, plotted using CompuSyn. Amp: Ampicillin, Rif: Rifampicin, Nal: Nalidixic acid

Results were also analyzed by the CompuSyn program (**Figure 3.45**), and with that combination, index plots were obtained. This method helps assess trends across different effect levels, such as the increasing synergy observed with higher effect levels at high concentrations and the more intricate trends seen at low concentrations, though it has certain limitations.

According to Zhao et al. (2004)¹⁵⁵, the combination index analysis is susceptible to minor variations in effect measurements at low and high concentrations. Additionally, it lacks a statistical assessment of synergy, additivity, or antagonism.¹⁵⁶

Here, a total of five different combinations were entered into the CompuSyn system, which were 1/4-, 1/2-, 1-, 2- and 4-folds of IC₅₀ values. In terms of that, ActD was found to have synergism with Nalidixic acid. ActX2 had a synergistic activity with all three tested antibiotics, as seen in **Figure 3.45**. Even though FICI did not have values >4 (antagonism), combination index plots showed antagonism at lower concentrations.

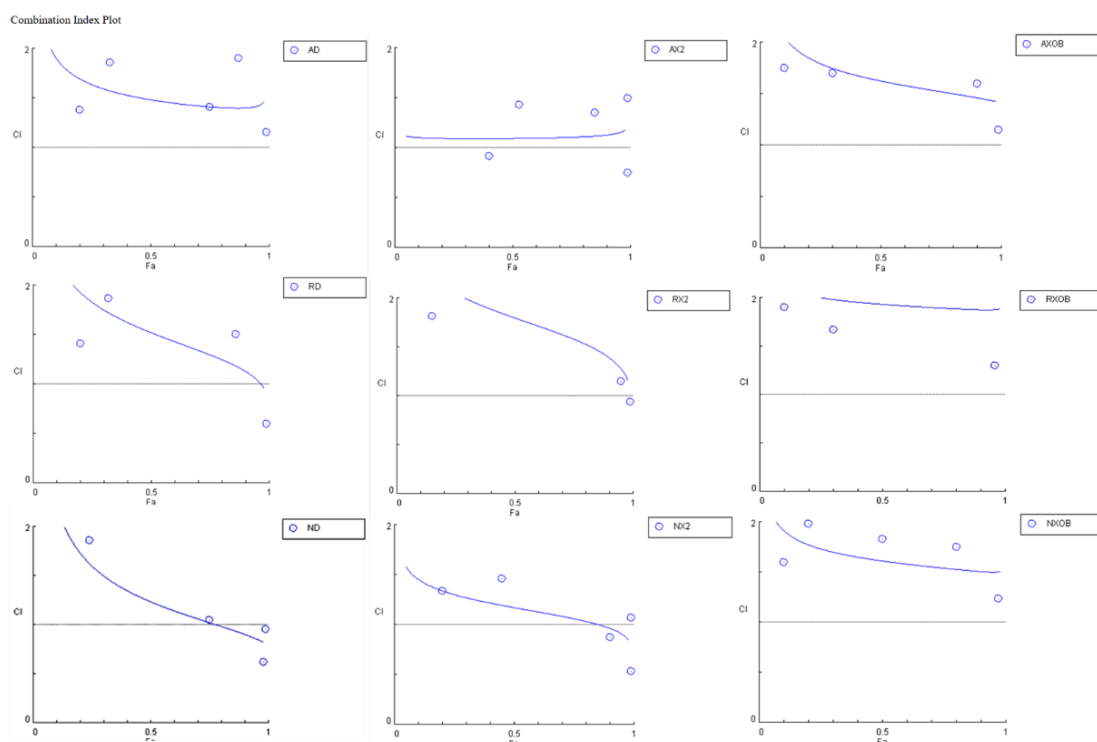


Figure 3.45. Combination index plots created with CompuSyn and AD: Amp-ActD, AX2: Amp-ActX2, AX0B: Amp-ActXO β , ND: Nalidixic acid-ActD, NX2: Nalidixic acid-ActX2, NX0B: Nalidixic acid-ActXO β , RD: Rifampicin-ActD, RX2: Rifampicin-ActX2, RX0B: Rifampicin-ActXO β .

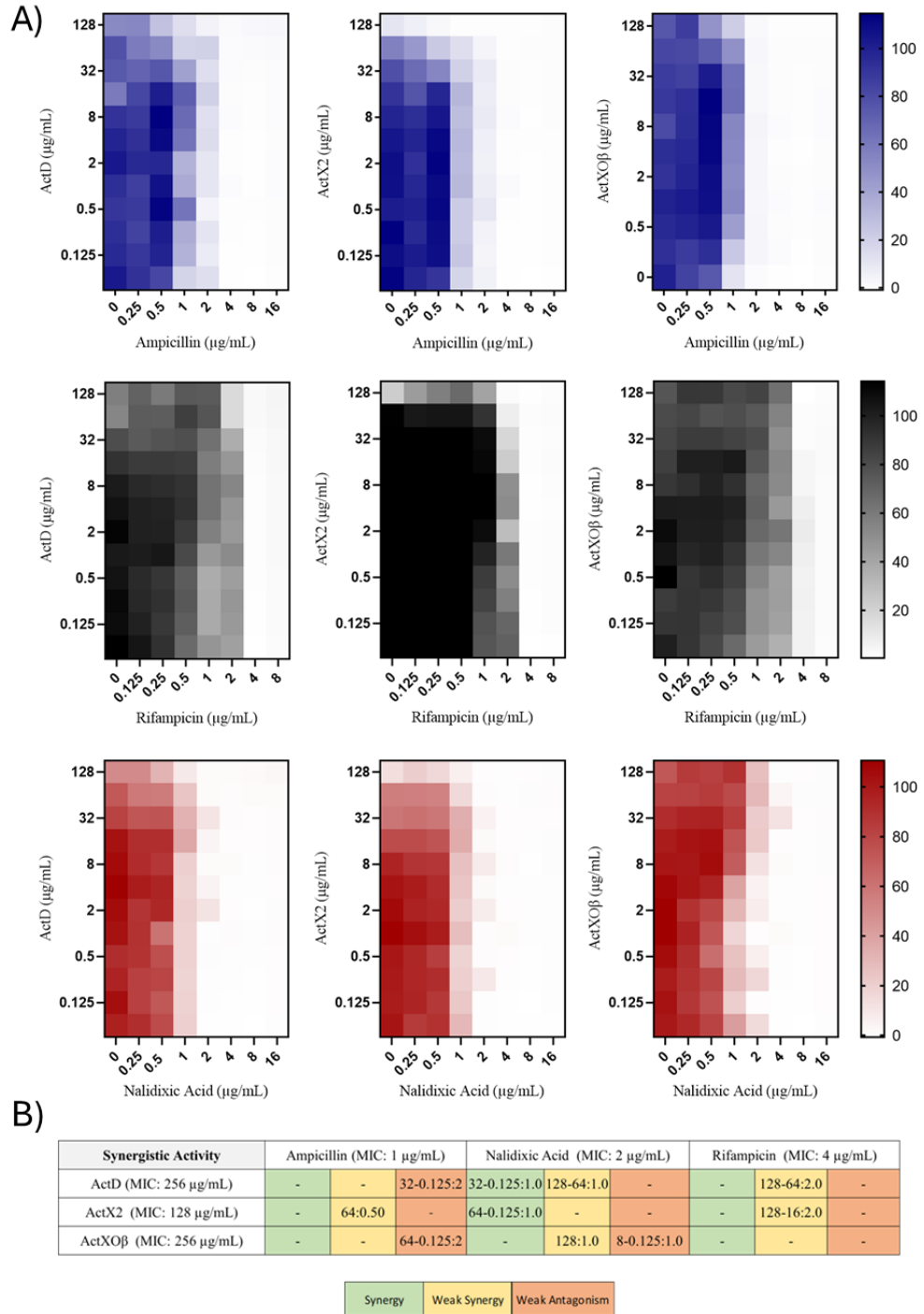


Figure 3.46. Synergy results obtained from growth percentages of *E. coli* with respect to combinations and FICI calculations; A) Heat map belonging to percent growth at 77 combinations, B) Synergism results with respect to FICI values.^{98-100, 162} Concentrations that are not written means indifference.

CHAPTER 4

CONCLUSION

Actinobacteria are widely known for their capacity for bioactive secondary metabolite production. Thus, there has been a focus on discovering new antimicrobial compounds from them. Despite the extensive research, the likelihood of finding new metabolites is decreased as many studies resulted in isolating previously identified compounds. Consequently, researchers have shifted their focus from terrestrial to marine environments, hypothesizing that microorganisms in high-stress conditions might produce distinctive secondary metabolites.^{9, 10}

Considering these, this thesis is focused on the isolation of Actinobacteria from coastal sediment samples collected from Ilica Bay of Izmir/Turkey.

Within this thesis, twelve isolates, likely *Streptomyces* sp., were obtained and morphologically characterized. Following analytical scale fermentation and EtOAc extraction, disk diffusion experiments on the extracts were performed. It was found that 66 % of the isolates had antimicrobial activity against at least one test organism (*S. aureus*, *E. coli* and *C. albicans*).

Notably, suspected *Streptomyces* sp. isolates 35M1 and 3414 demonstrated bioactivity against two of the test pathogens. As a result of TLC profiling and determination of dry weight yields, 35M1 was selected for further studies. Then, in order to identify 35M1, WGS studies were done. On the basis of NCBI and DSMZ BLAST results, the genome was deposited as *Streptomyces* sp. 35M1 in GenBank.

At the preparative scale, a 30 L fermentation experiment was performed in Erlenmeyer flasks, and the broth was processed by SPE using D101 resin. Ace fraction of the SPE (4.9 g) was found to have the highest activity against test organisms. Thus, bioactivity-guided isolation was started using this fraction. Then, by chromatographic techniques, five molecules were purified and then structurally characterized by spectral methods to be Actinomycin D, Actinomycin X2, Actinomycin XO β , Collismycin A, and Collismycin C. All the molecules displayed antimicrobial activity against MRSA, *S. epidermidis*, and *L. monocytogenes*. The most potent compound versus MRSA was

ActX2, with a MIC value of 0.125 µg/mL, matching that of Vancomycin. ActXOβ and ActD had MIC values of 0.25 µg/mL, while ColA and ColC had 8 and 16 µg/mL MIC against MRSA, respectively. Against *L. monocytogenes*, ActX2 had an MIC of 0.25 µg/mL, demonstrating twice the activity compared to Vancomycin. ActXOβ showed the lowest activity among the Actinomycin derivatives against *L. monocytogenes*. ColA had 16 µg/mL, and ColC had 32 µg/mL MIC values, while strong activity was found in ActD and ActX2 at 0.125 µg/mL concentration against *S. epidermidis*. Against clinical resistant *C. albicans*, Collismycin A was found to have 8-fold lower MIC value compared with fluconazole control.

As a result of biofilm inhibition tests, ActD (MBIC 0.25 µg/mL) and ActX2 (MBIC 0.125 µg/mL) exhibited higher activity than other isolated compounds while Vancomycin had an MBIC of 0.062 µg/mL against *L. monocytogenes*. ActD (MBIC 0.031 µg/mL), ActXOβ (MBIC 0.25 µg/mL), and ActX2 (MBIC 0.125 µg/mL) showed significant biofilm inhibition activity against MRSA.

As a result of biofilm eradication assays, ActD was found to reduce 80 % of the preformed biofilm formed by *L. monocytogenes* and decreased viability within the biofilm by up to 60 % at a concentration of 32 µg/mL. For *S. epidermidis*, biofilm viability decreased by approximately 80 %. The minimum concentration of ActD required to eradicate the biofilm (MBEC) against *S. epidermidis* was found to be 32 µg/mL. In the case of MRSA, biofilm mass decreased by approximately 60 %, and viability within the biofilm decreased by around 50 %.

Within the synergy studies, it was found that ActD exhibited synergistic activity with Nalidixic acid and Rifampicin but not with Ampicillin at the test concentrations. ActX2 at a 64 µg/mL concentration showed weak synergy with 0.5 µg/mL Ampicillin. ActD and ActXOβ displayed weak antagonistic activity with Ampicillin. Nalidixic acid showed synergism with ActD and ActX2 but not with ActXOβ. ActXOβ exhibited weak synergy at 128 µg/mL and weak antagonism at lower concentrations. ActD and ActX2 were synergistic with Nalidixic acid but not with other tested antibiotics against *E. coli*. ActXOβ did not demonstrate synergy at the test concentrations.

For future studies, the following needs to be taken into consideration.

Firstly, from *Streptomyces* sp. 35M1, isolation and purification of the other Actinomycin derivatives found in the dereplication study could be aimed. Since Dactinomycin exhibits high toxicity and therefore are not widely used in the chemotherapeutic treatment of antibacterial and antifungal diseases.

Thus, extensive studies needed to be performed to find its analogs which have enhanced its therapeutic index and increased bioactivity. In the case of the recently discovered Neo-actinomycin A-B, two new natural Actinomycins, have 5H-oxazolo[4,5-b]phenoxazine ring system, were found to have decreased the cytotoxicity.¹²⁸ Additionally, 7-bromo-actinomycin derivative demonstrated ~50 % greater antimicrobial activity when compared with Actinomycin D.¹⁶⁸

In addition to that, in literature, over 30 distinct naturally existing congeners of Actinomycin have been discovered with approximately 40 variations achieved through precursor-directed biosynthesis.^{128, 157, 158} Therefore, *Streptomyces* sp. 35M1 could be used in the precursor-directed biosynthesis studies to isolate distinct Actinomycin derivatives. An investigation revealed the identification of new Actinomycin analogs L1 and L2, isolated by introducing anthranilamide to *Streptomyces antibioticus* cultures.¹⁵⁸

Another point is that local drug delivery vehicles could be used for ActD and its derivatives to benefit from their antibiofilm activity. Thus, the ideal delivery system should ensure to have high effectiveness and minimize the biological toxicity of Actinomycins.¹⁵⁹⁻¹⁶¹

In conclusion, there is a lack of screening studies on marine-derived Actinobacteria from coastal areas of Turkey. Therefore, this study was one of the pioneer ones in our country, aimed to be a preliminary screening study for even more comprehensive research in the future. In addition, increased drug resistance coupled with reduced chance of discovering novel compounds lead researchers to focus on drug repurposing studies. The studies involve using an existing drug for a treatment that was not previously reported in the literature. This approach sometimes provides quicker solution to the strained healthcare system and increasing demands. Thus, studies on the repurposing of Actinomycin and Collismycin derivatives to target pathogens and their biofilms were conducted. With the data obtained, this thesis can assist further studies related to Actinomycin and Collismycin derivatives.

REFERENCES

1. Seyedsayamdost, M. R. Toward a global picture of bacterial secondary metabolism. *Journal of industrial microbiology & biotechnology*. **2019**, *46*(3-4), 301–311.
2. Netzker, T.; Flak, M.; Krespach, M. K.; Stroe, M. C.; Weber, J.; Schroeckh, V.; Brakhage, A. A. Microbial interactions trigger the production of antibiotics. *Current opinion in microbiology*. **2018**, *45*(1), 117-123.
3. Duffy, B.; Schouten, A.; Raaijmakers, J. M. Pathogen self-defense: mechanisms to counteract microbial antagonism. *Annual review of phyt pathology*. **2003**, *41*(1), 501–538.
4. Santamaria, G.; Liao, C.; Lindberg, C.; Chen, Y.; Wang, Z.; Rhee, K.; Pinto, F. R.; Yan, J.; Xavier, J. B. Evolution and regulation of microbial secondary metabolism. *eLife*. **2022**, *11*(1), 76119.
5. Monciardini, P.; Iorio, M.; Maffioli, S.; Sosio, M.; Donadio, S. Discovering new bioactive molecules from microbial sources. *Microbial biotechnology*. **2014**, *7*(3), 209–220.
6. Ribeiro da Cunha, B.; Fonseca, L. P.; Calado, C. R. C. Antibiotic Discovery: Where Have We Come from, Where Do We Go?. *Antibiotics*. **2019**, *8*(2), 45.
7. Srinivasan, R.; Kannappan, A.; Shi, C.; Lin, X. Marine Bacterial Secondary Metabolites: A Treasure House for Structurally Unique and Effective Antimicrobial Compounds. *Marine drugs*. **2021**, *19*(10), 530.
8. Liu M.; El-Hossary E.M.; Oelschlaeger T.A.; Donia M.S.; Quinn R.J.; Abdelmohsen U.R. Potential of marine natural products against drug-resistant bacterial infections. *Lancet Infect. Dis*. **2019**, *19*(7), 237-245.
9. Valliappan, K.; Sun, W.; Li, Z. Marine Actinobacteria associated with marine organisms and their potentials in producing pharmaceutical natural products. *Applied microbiology and biotechnology*. **2014**, *98*(17), 7365–7377.
10. Kothe, E. Special Focus: Actinobacteria. *Journal of basic microbiology*. **2018**, *58*(9), 719.
11. Barka, E. A.; Vatsa, P.; Sanchez, L.; Gaveau-Vaillant, N.; Jacquard, C.; Meier-Kolthoff, J. P.; Klenk, H. P.; Clément, C.; Ouhdouch, Y.; van Wezel, G. P. Taxonomy, Physiology, and Natural Products of Actinobacteria. *Microbiology and molecular biology reviews : MMBR*. **2015**, *80*(1), 1-43.

12. Bentley, S. D.; Chater, K. F.; Cerdeño-Tárraga, A. M.; Challis, G. L.; Thomson, N. R.; James, K. D.; Harris, D. E. et al. Complete genome sequence of the model actinomycete *Streptomyces coelicolor*. *Nature*. **2002**, *417*(6885), 141–147.
13. Belknap, K. C.; Park, C. J.; Barth, B. M.; Andam, C. P. Genome mining of biosynthetic and chemotherapeutic gene clusters in *Streptomyces* bacteria. *Scientific reports*. **2020**, *10*(1), 2003.
14. A Phase III Trial of With Marizomib in Patients with Newly Diagnosed Glioblastoma (MIRAGE). [Clinicaltrials.gov. https://clinicaltrials.gov/study/NCT03345095](https://clinicaltrials.gov/study/NCT03345095) (01 June 2024).
15. Chater, K. F. *Streptomyces* inside-out: a new perspective on the bacteria that provide us with antibiotics. *Biological sciences*. **2006**, *361*(1469), 761–768.
16. de Lima Procópio, R. E.; da Silva, I. R.; Martins, M. K.; de Azevedo, J. L.; de Araújo, J. M. Antibiotics produced by *Streptomyces*. *Braz J Infect Dis*. **2012**, *16*(5), 466-471.
17. Ruiz, P., Rodríguez-Cano, F.; Zerolo, F. J.; Casal, M. Investigation of the in vitro activity of streptomycin against *Mycobacterium tuberculosis*. *Microbial drug resistance* (Larchmont, N.Y.). **2002**, *8*(2), 147-149.
18. Mrugała, B.; Miłaczewska, A.; Porebski, P. J.; Niedzialkowska, E.; Guzik, M.; Minor, W.; Borowski, T. A study on the structure, mechanism, and biochemistry of kanamycin B dioxygenase (KanJ)-an enzyme with a broad range of substrates. *The FEBS journal*. **2021**, *288*(4), 1366-1386.
19. Wolfe, A.D.; Hahn, F.E. Erythromycin: Mode of action. *Science*. **1964**, *143*(3613), 1445-1446.
20. Asolkar, R. N.; Kirkland, T. N.; Jensen, P. R.; Fenical, W. Arenimycin, an antibiotic effective against Rifampicin- and methicillin-resistant *Staphylococcus aureus* from the marine actinomycete *Salinispora Arenicola*. *The Journal of antibiotics*. **2010**, *63*(1), 37-39.
21. Hohmann, C.; Schneider, K.; Bruntner, C.; Irran, E.; Nicholson, G.; Bull, A. T.; Jones, A. L. et al. Caboxamycin, a new antibiotic of the benzoxazole family produced by the deep-sea strain *Streptomyces* sp. NTK 937. *J Antibiot*. **2009**, *62*(2), 99-104.
22. Dijkmans, A. C.; Zacarías, N. V. O.; Burggraaf, J.; Mouton, J. W.; Wilms, E. B., van Nieuwkoop, C., Touw, D. J., Stevens, J., Kamerling, I. M. C. Fosfomycin: Pharmacological, Clinical and Future Perspectives. *Antibiotics*. **2017**, *6*(4), 24.

23. Hersperger, R.; Keller, T. H.; Ascomycin derivatives and their use as immunosuppressive agents. *Drugs of the Future*. **2000**, *25*(3), 269-275.
24. Li, J. M.; Lin, Z. B. Suppressive effect of kanglemycin C on T- and B-lymphocyte activation. *Zhongguo yao li xue bao Acta pharmacologica Sinica*. **1999**, *20*(6) , 546–550.
25. Jeon, C. W.; Kim, D. R.; Kwak, Y. S. Valinomycin, produced by *Streptomyces* sp. S8, a key antifungal metabolite in large patch disease suppressiveness. *World journal of microbiology & biotechnology*. **2019**, *35*(8), 128.
26. Argoudelis, A. D.; Bergy, M. E.; Pyke, T. R. Zorbamycin and related antibiotics. I. Production, isolation and characterization. *The Journal of antibiotics*. **1971**, *24*(8), 543-557.
27. Campbell, W. C.; Fisher, M. H.; Stapley, E. O.; Albers-Schönberg, G.; Jacob, T. A. Ivermectin: a potent new antiparasitic agent. *Science*. **1983**, *221*(4613), 823–828.
28. Lee, J. H.; Kim, E.; Choi, H.; Lee, J. Collismycin C from the Micronesian Marine Bacterium *Streptomyces* sp. MC025 Inhibits *Staphylococcus aureus* Biofilm Formation. *Mar Drugs*. **2017**, *15*(12), 387.
29. Heinstein, P.; Mechanism of action of granaticin: inhibition of ribosomal RNA maturation and cell cycle specificity. *J Pharm Sci*. **1982**, *71*(2), 197-200.
30. Koba, M.; Konopa, J. Aktynomycyna D i mechanizmy jej działania [Actinomycin D and its mechanisms of action]. *Postepy higieny i medycyny doswiadczalnej*. **2005**, *59*(1), 290-298.
31. Slotnick, I. J. Mechanism of action of Actinomycin D in Microbiological Systems. *Annals of the New York Academy of Sciences*. **1960**, *89*(2), 342-347.
32. Liu, X. F.; Xiang, L.; Zhou, Q.; Carralot, J. P.; Prunotto, M.; Niederfellner, G.; Pastan, I. Actinomycin D enhances killing of cancer cells by immunotoxin RG7787 through activation of the extrinsic pathway of apoptosis. *Proceedings of the National Academy of Sciences of the United States of America*. **2016**, *113*(38), 10666-10671.
33. Pang, B.; Liao, R.; Tang, Z.; Guo, S.; Wu, Z.; Liu, W. Caerulomycin and collismycin antibiotics share a trans-acting flavoprotein-dependent assembly line for 2,2'-bipyridine formation. *Nature communications*. **2021**, *12*(1), 3124.

34. Kawatani, M.; Muroi, M.; Wada, A.; Inoue, G.; Futamura, Y.; Aono, H.; Shimizu, K. et al. Proteomic profiling reveals that Collismycin A is an iron chelator. *Scientific reports*. **2016**, 6(1), 38385.
35. Tomat, E. Targeting iron to contrast cancer progression. *Current opinion in chemical biology*. **2023**, 74(1), 102315.
36. Guo, Q.; Li, L.; Hou, S.; Yuan, Z.; Li, C.; Zhang, W.; Zheng, L.; Li, X. The Role of Iron in Cancer Progression. *Frontiers in oncology*. **2021**, 11(1), 778492.
37. Frawley, E. R.; Fang, F. C. The ins and outs of bacterial iron metabolism. *Molecular microbiology*. **2014**, 93(4), 609-616
38. Dong, H.; Ming, D. A Comprehensive Self-Resistance Gene Database for Natural-Product Discovery with an Application to Marine Bacterial Genome Mining. *International journal of molecular sciences*. **2023**, 24(15), 12446.
39. Gokulan, K.; Khare, S.; Cerniglia, C. Metabolic pathways | production of secondary metabolites of bacteria. *Encyclopedia of Food Microbiology*. **2014**.
40. Dewick, P. D. Secondary Metabolism: The Building Blocks and Construction Mechanisms. *Medicinal Natural Products*. **2008**.
41. Komaki, H.; Sakurai, K.; Hosoyama, A.; Kimura, A.; Igarashi, Y.; Tamura, T. Diversity of nonribosomal peptide synthetase and polyketide synthase gene clusters among taxonomically close *Streptomyces* strains. *Scientific reports*. **2018**, 8(1), 6888.
42. Meier, J. L.; Burkart, M. D. Proteomic analysis of polyketide and nonribosomal peptide biosynthesis. *Current opinion in chemical biology*. **2011**, 15(1), 48-56.
43. Risdian, C.; Mozef, T.; Wink, J. Biosynthesis of polyketides in *Streptomyces*. *Microorganisms*. **2019**, 7(5), 124.
44. Staunton, J.; Weissman, K. J. Polyketide biosynthesis: A millennium review. *Nat. Prod. Rep.* **2001**, 18(1), 380-416.
45. Jiang, K.; Chen, X.; Zhang, W.; Guo, Y.; Liu, G. Nonribosomal antibacterial peptides isolated from *Streptomyces agglomeratus* 5-1-3 in the Qinghai-Tibet Plateau. *Microbial cell factories*. **2023**, 22(1), 5.
46. Dincer, S.; Takci, A. H. M., Ozdenefe, M. S. Nonribosomal Peptide Synthesis. *IntechOpen*. **2022**.

47. Wenzel, S. C.; Bode, H. B.; Kochems, I.; Müller, R. A type I/type III polyketide synthase hybrid biosynthetic pathway for the structurally unique ansa compound kendomycin. *ChemBioChem*. **2008**, *9*(1), 2711-2721.
48. West, A. K. R.; Bailey, C. B. Crosstalk between primary and secondary metabolism: Interconnected fatty acid and polyketide biosynthesis in prokaryotes. *Medicinal Chemistry Letters*. **2023**, *91*(1).
49. Revill, W. P.; Bibb, M. J.; Hopwood, D. A. Relationships between fatty acid and polyketide synthases from *Streptomyces coelicolor* A3(2): Characterization of the fatty acid synthase acyl carrier protein. *Journal of Bacteriology*. **1996**, *178*(19), 5660-5667.
50. Miao, V.; Coëffet-LeGal, M. F.; Brian, P.; Brost, R.; Penn, J.; Whiting, A.; Martin, S. et al. Daptomycin biosynthesis in *Streptomyces roseosporus*: cloning and analysis of the gene cluster and revision of peptide stereochemistry. *Microbiology*. **2005**, *151*(5), 1507-1523.
51. Doron, S.; Gorbach, S. L. Bacterial Infections: Overview. *International Encyclopedia of Public Health*. **2008**.
52. Otto, M. *Staphylococcus epidermidis*--the accidental pathogen. *Nature reviews. Microbiology*. **2009**, *7*(8), 555-567.
53. Vivant, A. L.; Garmyn, D.; Piveteau, P. *Listeria monocytogenes*, a down-to-earth pathogen. *Frontiers in cellular and infection microbiology*. **2013**, *3*(1), 87.
54. Kohanski, M. A.; Dwyer, D. J.; Collins, J. J. How antibiotics kill bacteria: From targets to networks, *Nature Reviews Microbiology*. **2010**, *8*(6), 423-435.
55. Cochrane, S. A.; Lohans, C. T. Breaking down the cell wall: Strategies for antibiotic discovery targeting bacterial transpeptidases. *Eur J Med Chem*. **2020**, *194*(1).
56. Knerr, P. J.; van der Donk, W. A. Discovery, biosynthesis, and engineering of lantipeptides. *Annu Rev Biochem*. **2012**, *81*(1), 479.
57. Nguyen, F.; Starosta, A. L.; Arenz, S.; Sohmen, D.; Dönhöfer, A.; Wilson, DN. Tetracycline antibiotics and resistance mechanisms. *Biol Chem*. **2014**, *395*(5), 559-575.
58. Farr, B.; Mandell, G. L. Rifampicin. *The Medical clinics of North America*. **1982**, *66*(1), 157-168.

59. Walsh, T. R.; Gales, A. C.; Laxminarayan, R.; Dodd, P. C. Antimicrobial Resistance: Addressing a Global Threat to Humanity. *PLoS medicine*. **2023**, *20*(7).
60. Vestergaard, M.; Frees, D.; Ingmer, H. Antibiotic Resistance and the MRSA Problem. *Microbiol Spectr*. **2019**, *7*(2).
61. Sharma, M.; Manhas, R. K. Purification and characterization of Actinomycins from *Streptomyces* strain M7 active against methicillin resistant *Staphylococcus aureus* and Vancomycin resistant *Enterococcus*. *BMC microbiology*. **2019**, *19*(1), 44.
62. Mah, T. F. Biofilm-specific antibiotic resistance. *Future microbiology*. **2012**, *7*(9), 1061-1072.
63. Tolker-Nielsen T. Biofilm Development. *Microbiol Spectr*. **2015**, *3*(2).
64. Sauer, K.; Stoodley, P.; Goeres, D. M.; Hall-Stoodley, L.; Burmølle, M.; Stewart, PS.; Bjarnsholt, T. The biofilm life cycle: expanding the conceptual model of biofilm formation. *Nat Rev Microbiol*. **2022**, *20*(10), 608-620.
65. Solanki, V.; Tiwari, M.; Tiwari, V. Host-Bacteria Interaction and Adhesion Study for Development of Therapeutics. *Int. J. Biol. Macromol*. **2018**, *112*(1), 54-64.
66. Solano, C.; Echeverz, M.; Lasa, I. Biofilm dispersion and quorum sensing. *Curr Opin Microbiol*. **2014**, *18*(1), 96-104
67. Miao, L.; Xu, J.; Yao, Z.; Jiang, Y.; Zhou, H.; Jiang, W.; Dong, K. The anti-quorum sensing activity and bioactive substance of a marine derived *Streptomyces*. *Biotechnol. Biotechnol*. **2017**, *31*(1), 1007-1015.
68. Conlon, B. P.; Rowe, S. E.; Lewis, K. Persister cells in biofilm associated infections. *Advances in experimental medicine and biology*. **2015**, *831*(1), 1-9.
69. Ramasubbu, N.; Thomas, L. M.; Rangunath, C.; Kaplan, J. B. Structural analysis of dispersin B, a biofilm-releasing glycoside hydrolase from the periodontopathogen *Actinobacillus actinomycetemcomitans*. *Journal of molecular biology*. **2005**, *349*(3), 475-486.
70. Sanchez, C. J.; Akers, K. S. J.; Romano, D. R.; Woodbury, R. L.; Hardy, S. K.; Murray, C. K.; Wenke, J. C. D-amino acids enhance the activity of antimicrobials against biofilms of clinical wound isolates of *Staphylococcus aureus* and *Pseudomonas aeruginosa*. *Antimicrobial agents and chemotherapy*. **2014**, *58*(8), 4353-4361.

71. Janež, N.; Škrlić, B.; Sterniša, M.; Klančnik, A.; Sabotič, J. The role of the *Listeria monocytogenes* surfactome in biofilm formation. *Microbial biotechnology*. **2021**, *14*(4), 1269-1281.
72. Nowak, J.; Cruz, C. D.; Palmer, J.; Fletcher, G. C.; Flint, S. Biofilm formation of the *L. monocytogenes* strain 15G01 is influenced by changes in environmental conditions. *Journal of microbiological methods*. **2015**, *119*(1), 189-195.
73. Lister, J. L.; Horswill, A. R. *Staphylococcus aureus* biofilms: recent developments in biofilm dispersal. *Frontiers in cellular and infection microbiology*. **2014**, *4*(1), 178.
74. Del Pozo, J. L. Biofilm-related disease. *Expert Rev Anti Infect Ther*. **2018**, *16*(1), 51-65.
75. Vasilchenko, A. S.; Julian, W. T.; Lapchinskaya, O. A.; Katrukha, G. S.; Sadykova, V. S.; Rogozhin, E. A. A Novel Peptide Antibiotic Produced by *Streptomyces roseoflavus* Strain INA-Ac-5812 With Directed Activity Against Gram-Positive Bacteria. *Frontiers in microbiology*. **2020**, *11*(1).
76. Jiménez, J. T.; Sturdíková, M.; Brezová, V.; Svajdlenka, E.; Novotová, M. Screening of mutant strain *Streptomyces mediolani* sp. AC37 for (-)-8-O-methyltetrangomycin production enhancement. *Journal of microbiology*. **2012**, *50*(6), 1014-1023.
77. Coates, A. R. M.; Hu, Y.; Holt, J.; Yeh, P. Antibiotic combination therapy against resistant bacterial infections: synergy, rejuvenation and resistance reduction. *Expert review of anti-infective therapy*. **2020**, *18*(1), 5-15.
78. Pletzer, D.; Hancock, R. E. Is synergy the key to treating high-density infections ?. *Future microbiology*. **2018**, *13*(1), 1629-1632.
79. Gustafsson, K.; Sykes, B. W.; Verwilghen, D.; Palmers, K.; Sullivan, S.; van Galen, G. Trimethoprim-sulfonamide: a valid antimicrobial treatment in foals?. *Journal of the American Veterinary Medical Association*. **2024**, *262*(6), 825-833.
80. Delgado, G.; Jr, Neuhauser, M. M.; Bearden, D. T.; Danziger, L. H. Quinupristin-dalfopristin: an overview. *Pharmacotherapy*. **2000**, *20*(12), 1469-1485.
81. Watanakunakorn, C.; Bakie, C. Synergism of Vancomycin-gentamicin and Vancomycin-streptomycin against *enterococci*. *Antimicrobial agents and chemotherapy*. **1973**, *4*(2), 120-124.

82. Ariza, J.; Gudiol, F.; Pallarés, R.; Rufí, G.; Fernández-Viladrich, P. Comparative trial of Rifampicin-doxycycline versus tetracycline-streptomycin in the therapy of human brucellosis. *Antimicrobial agents and chemotherapy*. **1985**, 28(4), 548-551.
83. Fernández-Hidalgo, N.; Almirante, B.; Gavalda, J.; Gurgui, M.; Peña, C.; de Alarcón, A.; Ruiz, J. et al. Ampicillin plus ceftriaxone is as effective as Ampicillin plus gentamicin for treating *enterococcus faecalis* infective endocarditis. *Clinical infectious diseases : an official publication of the Infectious Diseases Society of America*. **2013**, 56(9), 1261-1268.
84. Huttner, A.; Bielicki, J.; Clements, M. N.; Frimodt-Møller, N.; Muller, A. E.; Paccaud, J. P.; Mouton, J. W. Oral amoxicillin and amoxicillin-clavulanic acid: properties, indications and usage. *Clinical microbiology and infection :European Society of Clinical Microbiology and Infectious Diseases*. **2020**, 26(7), 871-879.
85. Bu, F.; Liu, M.; Xie, Z.; Chen, X.; Li, G.; Wang, X. Targeted Anti-Biofilm Therapy: Dissecting Targets in the Biofilm Life Cycle. *Pharmaceuticals*. **2022**, 15(10), 1253.
86. Shepherd, M. D.; Kharel, M. K.; Bosserman, M. A.; Rohr, J. Laboratory maintenance of *Streptomyces* species. *Current protocols in microbiology*. **2010**.
87. Aksoy, S. Denizel sediment örneklerinden biyoaktif metabolit üretici aktinomisetlerin kültürel ve moleküler yöntemlerle karakterizasyonu ve biyoaktif metabolitlerin saflaştırılması. Ege University. **2014**, PhD dissertation.
88. Bauer, A. W.; Kirby, W. M.; Sherris, J. C.; Turck, M. Antibiotic susceptibility testing by a standardized single disk method. *Technical bulletin of the Registry of Medical Technologists. American Society of Clinical Pathologists*. **1966**, 36(3), 49-52.
89. Wright, M. H.; Adelskov, J.; Greene, A. C. Bacterial DNA Extraction Using Individual Enzymes and Phenol/Chloroform Separation. *Journal of microbiology & biology education*. **2017**, 18(2).
90. National Center for Biotechnology Information (NCBI)[Internet]. Bethesda (MD): National Library of Medicine (US), *National Center for Biotechnology Information*; <https://www.ncbi.nlm.nih.gov/> (10 June 2024)
91. TYGS: A novel high-throughput platform for state-of-the-art genome-based taxonomy. ggdc.dsmz.de. (10 June 2024).

92. Blin, K.; Shaw, S.; Augustijn, H. E.; Reitz, Z. L.; Biermann, F.; Alanjary, M.; Fetter, A., et al. antiSMASH 7.0: new and improved predictions for detection, regulation, chemical structures and visualisation. *Nucleic acids research*. **2023**, *51*(1).
93. CLSI. Performance Standards for Antimicrobial Susceptibility Testing. 30th ed. CLSI supplement M100. Wayne, PA: *Clinical and Laboratory Standards Institute*; **2020**.
94. Alharthi, S.; Ziora, Z. M.; Moyle, P. M. Optimized protocols for assessing libraries of poorly soluble sortase A inhibitors for antibacterial activity against medically relevant bacteria, toxicity and enzyme inhibition. *Bioorganic & medicinal chemistry*. **2021**, *52*(1).
95. Wiegand, I.; Hilpert, K.; Hancock, R. E. Agar and broth dilution methods to determine the minimal inhibitory concentration (MIC) of antimicrobial substances. *Nature protocols*. **2008**, *3*(2).
96. Haney, E. F.; Trimble, M. J.; Hancock, R. E. W. Microtiter plate assays to assess antibiofilm activity against bacteria. *Nature protocols*. **2021**, *16*(5).
97. Breijyeh, Z.; Jubeh, B.; Karaman, R. Resistance of Gram-Negative Bacteria to Current Antibacterial Agents and Approaches to Resolve It. *Molecules*. **2020**, *25*(6).
98. Bellio, P.; Fagnani, L.; Nazzicone, L.; Celenza, G. New and simplified method for drug combination studies by checkerboard assay. *MethodsX*. **2021**, *8*(1).
99. Lee, H.; Yu, S.H.; Shim, J. E.; Yong, D. Use of a combined antibacterial synergy approach and the ANNOgesic tool to identify novel targets within the gene networks of multidrug-resistant *Klebsiella pneumoniae*. *mSystems*. **2024**, *9*(3).
100. Odds, F. C. Synergy, antagonism, and what the checkerboard puts between them. *The Journal of antimicrobial chemotherapy*. **2003**, *52*(1), 1.
101. Hall, M. J.; Middleton, R. F.; Westmacott, D. The fractional inhibitory concentration (FIC) index as a measure of synergy. *The Journal of antimicrobial chemotherapy*. **1983**, *11*(5), 427-433.
102. Ensign, J.C. Introduction to the Actinobacteria. *The Prokaryotes*, 2nd ed., **1992**.
103. Bergey, D. H.; Holt, J. G. Bergey's Manual of determinative bacteriology. *Baltimore: Williams & Wilkins*. **1993**.

104. Bergey, D. H.; Krieg, N. R.; Holt, J. G. Bergey's Manual of systematic bacteriology. *Baltimore, MD: Williams & Wilkins. 1984.*
105. Sharma, A. *Streptomyces. Encyclopedia of Food Microbiology. 1999.*
106. Wang, J.; Ma, W.; Wang, X. Insights into the structure of *Escherichia coli* outer membrane as the target for engineering microbial cell factories. *Microbial cell factories. 2021, 20(1), 73.*
107. Antonelli, G.; Cappelli, L.; Cinelli, P.; Cuffaro, R.; Manca, B.; Nicchi, S.; Tondi, S. et al. Strategies to Tackle Antimicrobial Resistance: The Example of *Escherichia coli* and *Pseudomonas aeruginosa*. *International journal of molecular sciences. 2021, 22(9), 4943.*
108. Scudamore, R. A.; Beveridge, T. J.; Goldner, M. Outer-membrane penetration barriers as components of intrinsic resistance to β -lactam and other antibiotics in *Escherichia coli* K-12. *Antimicrobial agents and chemotherapy. 1979, 15(2), 182-189.*
109. Farris J. S. Distance Data Revisited. *Cladistics : the international journal of the Willi Hennig Society. 1985, 1(1), 67-86.*
110. Meier-Kolthoff, J. P.; Göker, M. TYGS is an automated high-throughput platform for state-of-the-art genome-based taxonomy. *Nature communications. 2019, 10(1), 2182.*
111. Meier-Kolthoff, J. P.; Carbasse, J. S.; Peinado-Olarte, R. L.; Göker, M. TYGS and LPSN: a database tandem for fast and reliable genome-based classification and nomenclature of prokaryotes. *Nucleic acids research. 2022, 50(1), 801-807.*
112. Holland, B. R.; Huber, K. T.; Dress, A.; Moulton, V. Delta plots: a tool for analyzing phylogenetic distance data. *Molecular biology and evolution. 2002, 19(12), 2051-2059.*
113. Ueda, K.; Oinuma, K.; Ikeda, G.; Hosono, K.; Ohnishi, Y.; Horinouchi, S.; Beppu, T. AmfS, an extracellular peptidic morphogen in *Streptomyces griseus*. *Journal of bacteriology. 2002, 184(5), 1488-1492.*
114. Park, K. J.; Maier, S.; Zhang, C.; Dixon, S. A. H.; Rusch, D. B.; Pupo, M. T.; Angus, S. P.; Gerdt, J. P. Ravidomycin Analogs from *Streptomyces* sp. Exhibit Altered Antimicrobial and Cytotoxic Selectivity. *Journal of natural products. 2023, 86(8), 1968-1979.*
115. Garcia, I.; Vior, N. M.; González-Sabín, J.; Braña, A. F.; Rohr, J.; Moris, F.; Méndez, C.; Salas, J. A. Engineering the biosynthesis of the polyketide-

- nonribosomal peptide Collismycin A for generation of analogs with neuroprotective activity. *Chemistry & biology*. **2013**, 20(8), 1022-1032.
116. Zaroubi, L.; Ozugergin, I.; Mastronardi, K.; Imfeld, A.; Law, C.; Gélinas, Y.; Piekny, A.; Findlay, B. L. The Ubiquitous Soil Terpene Geosmin Acts as a Warning Chemical. *Applied and environmental microbiology*. **2022**, 88(7).
117. Bursy, J.; Kuhlmann, A. U.; Pittelkow, M.; Hartmann, H.; Jebbar, M.; Pierik, A. J.; Bremer, E. Synthesis and uptake of the compatible solutes ectoine and 5-hydroxyectoine by *Streptomyces coelicolor* A3(2) in response to salt and heat stresses. *Applied and environmental microbiology*. **2008**, 74(23), 7286-7296.
118. Challis, G. L.; Ravel, J. Coelichelin, a new peptide siderophore encoded by the *Streptomyces coelicolor* genome: structure prediction from the sequence of its non-ribosomal peptide synthetase. *FEMS microbiology letters*. **2000**, 187(2), 111-114.
119. Bellotti, D.; Remelli, M. Deferoxamine B: A Natural, Excellent and Versatile Metal Chelator. *Molecules*. **2021**, 26(11), 3255.
120. Velasquez, J. Deferoxamine. *StatPearls*. **2023**.
121. Abd El-Hack, M. E.; El-Saadony, M. T.; Elbestawy, A. R.; Ellakany, H. F.; Abaza, S. S.; Geneedy, A. M.; Salem, H. M. et al. Undesirable odour substances (geosmin and 2-methylisoborneol) in water environment: Sources, impacts and removal strategies. *Marine pollution bulletin*. **2022**, 178(1).
122. Ahadi, A.; Partoazar, A.; Abedi-Khorasgani, M. H.; Shetab-Boushehri, S. V. Comparison of liquid-liquid extraction-thin layer chromatography with solid-phase extraction-high-performance thin layer chromatography in detection of urinary morphine. *J Biomed Res*. **2011**, 25(5), 362-367.
123. Greco, W. R.; Bravo, G.; Parsons, J. C. The search for synergy: a critical review from a response surface perspective. *Pharmacological reviews*. **1995**, 47(2), 331-385.
124. Praveen, V.; Tripathi, C. K.; Bihari, V.; Srivastava, S. C. Production of Actinomycin-D by the mutant of a new isolate of *Streptomyces sindenensis*. *Brazilian journal of microbiology*. **2008**, 39(4), 689-692.
125. Koba, M. Zależność aktywności biologicznej aktynomycyn od ich budowy chemicznej na przykładzie modyfikacji struktury aktynomycyny D [Modifications of Actinomycin D structure as example of Actinomycins structure-activity relationship]. *Postępy higieny i medycyny doświadczalnej*. **2005**, 59(1), 276-282.

126. Toumatia, O.; Yekkour, A.; Goudjal, Y.; Riba, A.; Coppel, Y.; Mathieu, F.; Sabaou, N.; Zitouni, A. Antifungal properties of an actinomycin D-producing strain, *Streptomyces* sp. IA1, isolated from a Saharan soil. *Journal of basic microbiology*. **2015**, *55*(2), 221-228.
127. Sengupta, S. K.; Kelly, C.; Sehgal, R. K. Reverse and symmetrical analogues of Actinomycin D: metabolic activation and in vitro and in vivo tumor growth inhibitory activities. *Journal of medicinal chemistry*. **1985**, *28*(5), 620-628.
128. Wang, Q.; Zhang, Y.; Wang, M.; Tan, Y.; Hu, X.; He, H.; Xiao, C.; You, X.; Wang, Y.; Gan, M. Neo-Actinomycins A and B, natural Actinomycins bearing the 5H-oxazolo[4,5-b]phenoxazine chromophore, from the marine-derived *Streptomyces* sp. IMB094. *Scientific reports*. **2017**, *7*(1), 3591.
129. Julianti, E.; Abrian, I. A.; Wibowo, M. S.; Azhari, M.; Tsurayya, N.; Izzati, F.; Juansilfero, A. B.; Bayu, A.; Rahmawati, S. I.; Putra, M. Y. Secondary Metabolites from Marine-Derived Fungi and Actinobacteria as Potential Sources of Novel Colorectal Cancer Drugs. *Marine drugs*. **2022**, *20*(1), 67.
130. Qureshi, K. A.; Bholay, A. D.; Rai, P. K.; Mohammed, H. A.; Khan, R. A.; Azam, F.; Jaremko, M. et al. Isolation, characterization, anti-MRSA evaluation, and in-silico multi-target anti-microbial validations of Actinomycin X2 and Actinomycin D produced by novel *Streptomyces smyrnaeus* UKAQ_23. *Scientific reports*. **2021**, *11*(1), 14539.
131. Wang, D.; Wang, C.; Gui, P.; Liu, H.; Khalaf, S. M. H.; Elsayed, E. A.; Wadaan, M. A. M.; Hozzein, W. N.; Zhu, W. Identification, Bioactivity, and Productivity of Actinomycins from the Marine-Derived *Streptomyces heliomycini*. *Frontiers in microbiology*. **2017**, *8*(1), 1147.
132. Garcia, I.; Vior, N. M.; Braña, A. F.; González-Sabin, J.; Rohr, J.; Moris, F.; Méndez, C.; Salas, J. A. Elucidating the biosynthetic pathway for the polyketide-nonribosomal peptide Collismycin A: mechanism for formation of the 2,2'-bipyridyl ring. *Chemistry & biology*. **2012**, *19*(3), 399-413.
133. Lee, J. H.; Kim, E.; Choi, H.; Lee, J. Collismycin C from the Micronesian Marine Bacterium *Streptomyces* sp. MC025 Inhibits *Staphylococcus aureus* Biofilm Formation. *Marine drugs*. **2017**, *15*(12), 387.
134. Chen, Z.; Ou, P.; Liu, L.; Jin, X. Anti-MRSA Activity of Actinomycin X2 and Collismycin A Produced by *Streptomyces globisporus* WA5-2-37 From the Intestinal Tract of American Cockroach (*Periplaneta americana*). *Frontiers in microbiology*. **2020**, *11*(1), 555.
135. Rathod, B. B.; Korasapati, R.; Sripadi, P.; Reddy Shetty, P. Novel Actinomycin group compound from newly isolated *Streptomyces* sp. RAB12:

- isolation, characterization, and evaluation of antimicrobial potential. *Applied microbiology and biotechnology*. **2018**, *102*(3), 1241-1250.
136. Wang, M.; Carver, J. J.; Phelan, V. V.; Sanchez, L. M.; Garg, N.; Peng, Y.; Nguyen, D. D. et al. Sharing and community curation of mass spectrometry data with Global Natural Products Social Molecular Networking. *Nature biotechnology*. **2016**, *34*(8), 828-837.
 137. Levine, J. F. Vancomycin: a review. *The Medical clinics of North America*. **1987**, *71*(6), 1135-1145.
 138. Formica, J. V.; Apple, M. A. Production, isolation, and properties of azetomycins. *Antimicrobial agents and chemotherapy*. **1976**, *9*(2), 214-221.
 139. Sengupta, S. K.; Tinter, S. K.; Lazarus, H.; Brown, B. L.; & Modest, E. J. 7-substituted Actinomycin D analogs. Chemical and growth-inhibitory studies. *Journal of medicinal chemistry*. **1975**, *18*(12), 1175-1180.
 140. Formica, J. V.; Shatkin, A. J.; Katz, E. Actinomycin analogues containing pipercolic acid: relationship of structure to biological activity. *Journal of bacteriology*. **1968**, *95*(6), 2139-2150.
 141. Vior, N. M.; Olano, C.; García, I.; Méndez, C.; Salas, J. A. Collismycin A biosynthesis in *Streptomyces* sp. CS40 is regulated by iron levels through two pathway-specific regulators. *Microbiology*. **2014**, *160*(3), 467-478.
 142. Hoffman, L. R.; D'Argenio, D. A.; MacCoss, M. J.; Zhang, Z.; Jones, R. A.; Miller, S. I. Aminoglycoside antibiotics induce bacterial biofilm formation. *Nature*. **2005**, *436*(1), 1171-1175.
 143. Linares, J. F.; Gustafsson, I.; Baquero, F.; Martinez, J. L.; Antibiotics as intermicrobial signaling agents instead of weapons. *Proc Natl Acad Sci USA*. **2006**, *103*(1), 19484-19489.
 144. Kaplan, J. B.; Izano, E. A.; Gopal, P.; Karwacki, M. T.; Kim, S.; Bose, J. L.; Bayles, K. W.; Horswill, A. R. Low levels of β -lactam antibiotics induce extracellular DNA release and biofilm formation in *Staphylococcus aureus*. *mBio*. **2012**, *3*(1).
 145. Mu, Y. Q.; Xie, T. T.; Zeng, H.; Chen, W.; Wan, C. X.; Zhang, L. L. *Streptomyces*-derived Actinomycin D inhibits biofilm formation via downregulating ica locus and decreasing production of PIA in *Staphylococcus epidermidis*. *Journal of applied microbiology*. **2020**, *128*(4), 1201-1207.
 146. Lee, J. H.; Kim, Y. G.; Lee, K.; Kim, C. J.; Park, D. J.; Ju, Y.; Lee, J. C.; Wood, T. K.; Lee, J. *Streptomyces*-derived Actinomycin D inhibits biofilm

- formation by *Staphylococcus aureus* and its hemolytic activity. *Biofouling*. **2016**, 32(1), 45-46.
147. Clarke, M.; Hind, C. K.; Ferguson, P. M.; Manzo, G.; Mistry, B.; Yue, B.; Romanopulos, J. et al. Synergy between Winter Flounder antimicrobial peptides. *npj antimicrobials and resistance*. **2023**, 1(1), 8.
148. Yuan, M.; Chua, S. L.; Liu, Y.; Drautz-Moses, D. I.; Yam, J. K. H.; Aung, T. T.; Beuerman, R. W. et al. Repurposing the anticancer drug cisplatin with the aim of developing novel *Pseudomonas aeruginosa* infection control agents. *Beilstein journal of organic chemistry*. **2018**, 14(1), 3059-3069.
149. Röhner, E.; Jacob, B.; Böhle, S.; Rohe, S.; Löffler, B.; Matziolis, G.; Zippelius, T. Sodium hypochlorite is more effective than chlorhexidine for eradication of bacterial biofilm of staphylococci and *Pseudomonas aeruginosa*. *ESSKA*. **2020**, 28(12), 3912-3918.
150. Rangel-Vega, A.; Bernstein, L. R.; Mandujano-Tinoco, E. A.; García-Contreras, S. J.; García-Contreras, R. Drug repurposing as an alternative for the treatment of recalcitrant bacterial infections. *Frontiers in microbiology*. **2015**, 6(1), 282.
151. Masters, P. A.; O'Bryan, T. A.; Zurlo, J.; Miller, D. Q.; Joshi, N. Trimethoprim-sulfamethoxazole revisited. *Archives of internal medicine*. **2003**, 163(4), 402-410.
152. Rand, K. H.; Houck, H. J.; Brown, P.; Bennett, D. Reproducibility of the microdilution checkerboard method for antibiotic synergy. *Antimicrobial agents and chemotherapy*. **1993**, 37(3), 613-615.
153. Odds, F. C. Synergy, antagonism, and what the chequerboard puts between them. *The Journal of antimicrobial chemotherapy*. **2003**, 52(1), 1.
154. El-Naggar, Moustafa. Synergistic effect of Actinomycin X2 produced by *Streptomyces nasri* strain YG62 with other antibiotics. *Biomedical Letters*. **1998**, 58(1), 169-173.
155. Zhao, L.; Wientjes, M. G.; Au, J. L. Evaluation of combination chemotherapy: integration of nonlinear regression, curve shift, isobologram, and combination index analyses. *American Association for Cancer Research*. **2004**, 10(23), 7993-8004.
156. Zhao, L.; Au, J. L.; Wientjes, M. G. Comparison of methods for evaluating drug-drug interaction. *Frontiers in bioscience (Elite edition)*. **2010**, 2(1), 241-249.

157. Zhao, W.; Wang, G.; Guo, L.; Wang, J.; Jing, C.; Liu, B.; Zhao, F.; Zhang, S.; Xie, Z. Asp-containing actinomycin and tetracyclic chromophoric analogues from the *Streptomyces* Sp. strain S22. *Organic & biomolecular chemistry*. **2023**, *21*(8), 1737-1743.
158. Machushynets, N. V.; Elsayed, S. S.; Du, C.; Siegler, M. A.; de la Cruz, M., Genilloud, O.; Hankemeier, T.; van Wezel, G. P. Discovery of Actinomycin L, a new member of the Actinomycin family of antibiotics. *Scientific reports*. **2022**, *12*(1), 2813.
159. Wang, T.; Cornel, E. J.; Li, C.; Du, J. Drug delivery approaches for enhanced antibiofilm therapy. *Journal of controlled release : official journal of the Controlled Release Society*. **2023**, *353*(1), 350-365.
160. Hanssen, A. D. Local antibiotic delivery vehicles in the treatment of musculoskeletal infection. *Clinical orthopedics and related research*. **2005**, *437*(1), 91-96.
161. Hsieh, P. H.; Chang, Y. H.; Chen, S. H. et al. High concentration and bioactivity of Vancomycin and aztreonam eluted from Simplex cement spacers in two-stage revision of infected hip implants: a study of 46 patients at an average follow-up of 107 days. *J Orthop Res*. **2006**, *24*(1), 1615-1621.
162. Tang, J.; Wennerberg, K.; Aittokallio, T. What is synergy?. *Frontiers in pharmacology*. **2015**, *6*(1), 181.
163. Liu, Z.; Wang, J.; Gao, W.; Man, S.; Wang, Y.; Liu, C. Preparative separation and purification of steroidal saponins in *Paris polyphylla* var. *yunnanensis* by macroporous adsorption resins. *Pharmaceutical biology*. **2013**, *51*(7), 899-905.
164. Xia, X.; Liu, J.; Huang, L.; Zhang, X.; Deng, Y.; Li, F.; Liu, Z.; Huang, R. Molecular Details of Actinomycin D-Treated MRSA Revealed via High-Dimensional Data. *Marine drugs*. **2022**, *20*(2), 114.
165. de-Souza-Silva, C. M.; Guilhelmelli, F.; Zamith-Miranda, D.; de Oliveira, M. A.; Nosanchuk, J. D.; Silva-Pereira, I.; Albuquerque, P. Broth Microdilution In Vitro Screening: An Easy and Fast Method to Detect New Antifungal Compounds. *Journal of visualized experiments : JoVE*. **2018**, *132*(1), 57127.
166. Macias-Paz, I. U.; Pérez-Hernández, S.; Tavera-Tapia, A.; Luna-Arias, J. P.; Guerra-Cárdenas, J. E.; Reyna-Beltrán, E. *Candida albicans* the main opportunistic pathogenic fungus in humans. *Revista Argentina de microbiologia*, **2023**, *55*(2), 189-198.

167. Huang, K.; Zhang, B.; Shen, Z. Y.; Cai, X.; Liu, Z. Q.; Zheng, Y. G. Enhanced amphotericin B production by genetically engineered *Streptomyces nodosus*. *Microbiological research*. **2021**, 242(1), 126623.
168. Brockmann, H.; Ammann, J.; Müller, W. 7-Chlor- und 7-Brom-Actinomycine [7-chlor and 7-brom-actinomycin]. *Tetrahedron letters*. **1966**, 30(1), 3595-3597.